

Mechanistic Aspects of C–H Activation by Pt Complexes

Martin Lersch and Mats Tilset*

Department of Chemistry, University of Oslo, P.O. Box 1033 Blindern, N-0315 Oslo, Norway

Received November 15, 2004

Contents

1. Introduction	2471	6.5. Stoichiometric Arene C–H Activation at Cationic Pt(II) N ₂ Complexes	2497
2. Mechanistic Fundamentals	2474	6.6. Regioselectivities in Aromatic Activation	2501
2.1. Classification of C–H Activation Reactions	2474	6.7. Catalytic C–H Activation and Functionalization at Cationic Pt(II) N ₂ Complexes	2503
2.2. C–H Bond Cleavage Event: Oxidative Addition vs σ -Bond Metathesis and Electrophilic Activation	2474	6.8. Reactions at Pt Complexes with Neutral Acyclic N ₃ Ligands	2504
2.3. Hydrocarbon Coordination	2475	6.9. Reactions at Neutral Cyclic N ₃ Ligands	2507
2.4. σ Complexes of Alkanes and Arenes	2475	7. Reactions at Pt Complexes with Anionic Donor Ligands	2510
2.5. Principle of Microscopic Reversibility	2476	7.1. Anionic vs Neutral Ligands	2510
2.6. Kinetic Isotope Effects	2477	7.2. Reactions at Tp Complexes of Pt (Tp = Hydridotris(pyrazolyl)borate)	2510
3. Shilov-type Chemistry	2478	7.2.1. TpPtMeH ₂ and Tp'PtMeH ₂	2511
3.1. C–H Activation by Pt(II)	2479	7.2.2. TpPtMe ₂ H and Tp'PtMe ₂ H	2512
3.2. Mechanism of Multiple H/D Exchange	2480	7.2.3. Tp'Pt(Ar) ₂ H ₂	2515
3.3. H/D Exchange—1,2 Shift in Ethane	2481	7.2.4. Tp'PtAr ₂ H	2517
3.4. Computational Studies of the Shilov System	2481	7.3. Reactions at a fac-Chelating Sulfonated Di(pyridyl) System	2517
3.5. C–H Activation by Pt(IV)	2482	7.4. Reactions at Pt Diketiminato Complexes	2518
4. "Catalytica" System for Catalytic Methane Functionalization	2482	7.5. Reactions at a N ₃ Pincer Amido Pt Complex	2519
5. Reactions at Pt Complexes with Phosphine Ligands	2484	7.6. Reactions at 2-(<i>N</i> -Arylimino)pyrrolide Pt Complexes	2520
5.1. C–C and C–X Reductive Elimination from Octahedral Pt(IV) Complexes	2484	8. Examples of Applications in Synthesis	2520
5.2. C–H Reductive Elimination from Pt(II)	2484	9. Summary and Outlook	2522
5.3. C–H Activation at Pt(0) Complexes	2485	10. Abbreviations	2523
5.4. Protonation of Pt(II) and Reductive Elimination from Pt(IV) Complexes with Labile Anionic Donors	2486	11. Acknowledgment	2523
5.5. C–H Reductive Elimination from Pt(IV) Complexes without Labile Anionic Ligands	2489	12. References	2523
5.6. C–H Activations at Cationic Pt(II) Phosphine Complexes	2491		
5.7. C–H Activation at Zwitterionic Pt(II) Complexes	2492		
6. Reactions at Pt Complexes with Neutral Nitrogen Donor Ligands	2493		
6.1. Protonation of Pt(II) Alkyl Complexes and Reductive Elimination from Pt(IV) Hydridoalkyl Complexes with Neutral N ₂ Ligands	2493		
6.2. Protonation of Pt(II) Aryl Complexes and Reductive Elimination from Pt(IV) Hydridoaryl Complexes with Neutral N ₂ Ligands	2496		
6.3. Stoichiometric Methane C–H Activation at Cationic Pt(II) Complexes with Neutral N ₂ Ligands	2496		
6.4. Computational Studies of Stoichiometric Methane C–H Activation at Cationic Pt(II) Complexes with Neutral N ₂ Ligands	2496		

1. Introduction

Hydrocarbons are readily available from inexpensive petrochemical and natural gas feedstock and have been utilized as raw materials for the production of materials and energy for many decades. Nevertheless, efficient, selective, and direct functionalization of hydrocarbons under mild conditions remains a most difficult challenge to chemists even today.^{1–3} If successful, such new processes may give rise to cleaner and more efficient alternatives to existing technology. Taking into consideration that natural gas remains the most important source of hydrogen today⁴ (and probably will remain so until sufficiently efficient water-splitting technologies become available), insight into the nature of C–H bond activation may have implications even for important aspects of the technology that is needed for the proposed and intensely discussed hydrogen-based energy economy of the future.

* To whom correspondence should be addressed. Phone: +47 22855502. Fax: +47 22855441. E-mail: mats.tilset@kjemi.uio.no.



Martin Lersch was born in Frankfurt am Main in 1976. He attends the University of Oslo, where he received his M.Sc. degree in Organic Chemistry in 2001. He is currently in the process of finalizing his Ph.D. degree in the group of Professor Mats Tilset. His work has focused on the mechanism of platinum-mediated C–H activation. Besides his research he holds a strong interest in molecular gastronomy.



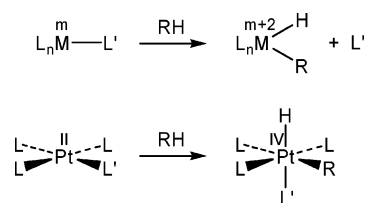
Mats Tilset was born in Oslo in 1956. He received his undergraduate Siv.Ing. degree at the Norwegian Institute of Technology, Trondheim, in 1980, and his Ph.D. degree at the University of California, Berkeley, in 1985, under the supervision of Professor K. Peter C. Vollhardt. This was followed by a postdoctoral stint in Trondheim with Professor Vernon D. Parker. He has been affiliated with the University of Oslo since 1989, as a full professor since 1993. His current research interests include metal-mediated C–H activation, reaction mechanisms, electron-transfer processes, and catalysis. Besides his research he holds a strong interest in practical gastronomy.

Hydrocarbon functionalization (eq 1) by default must involve the cleavage of at least one C–H bond.

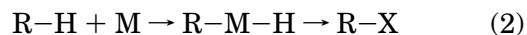


C–H bonds are very strong bonds and difficult to cleave directly, whether heterolytically or homolytically. For example, the estimated pK_a of methane is as high as ca. 48,⁵ and the homolytic bond dissociation enthalpy of methane at 25 °C is 440 kJ/mol.⁶ Homolytic pathways for activation and functionalization of alkanes will suffer from the fact that C–H bonds in viable products are weaker than those in the parent hydrocarbons, and as a result, the desired high selectivity will be impossible to achieve at high conversion.³ To circumvent the selectivity problem the use of transition-metal complexes has been promoted as an alternative. Chemo- and regioselectivities can, in principle, be achieved by tweaking the properties of the metal complex through choice of metal and by ligand design.

Scheme 1



A typical mechanism for the metal-complex-mediated C–H functionalization might involve the two steps depicted in eq 2—oxidative addition followed by functionalization of the metal alkyl moiety. If the overall reaction is to operate at a high rate, it is required that the energetic cost of cleaving the C–H bond (440 kJ/mol in methane, ca. 420 kJ/mol for other primary C–H bonds, and even lower for secondary and tertiary) is largely, if not completely, compensated for by the formation of strong M–H and M–C bonds in the intermediate R–M–H species.

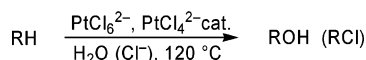


In addition, the unfavorable entropy of the oxidative addition contributes another ca. 42 kJ/mol that must be overcome.⁷ Accordingly, stoichiometric metal complex C–H activation is usually achieved at third-row and second-row transition-metal complexes that offer relatively strong bonds to their ligands. Pt–H bond enthalpies of about 306–314 kJ/mol have been reported in neutral square-planar Pt(II) complexes,^{8–11} and these rank among the strongest M–H bonds known. Analogously, Pt–CH₃ bond energies of 251–268 kJ/mol have been estimated in similar systems.^{8,9} Although experimental estimates for Pt–C bond strengths in octahedral Pt(IV) complexes are significantly lower, ca. 126–155 kJ/mol,^{12,13} the possible formation of relatively strong Pt–H and Pt–C bonds bodes well for the use of Pt complexes in C–H activation and functionalization.

It is a common feature of many C–H activating systems that they proceed by initial loss of a ligand L' to generate a vacant coordination site that facilitates the oxidative addition. For the most widely investigated systems the ligand L' remains unbonded in the final oxidative addition product, and this contributes unfavorably to the overall energetics of the reaction. In contrast, for oxidative additions at square-planar, 16-electron Pt(II) complexes, which encompasses a large part of the work to be presented in this review, the Pt(IV) oxidative addition product will be octahedral, 18-electron species in which the ligand L' (or a new ligand) remains bonded at the metal (Scheme 1). This might contribute to make thermal reactions at Pt(II) thermodynamically more favorable.

It has been demonstrated during the last couple of decades that organotransition-metal complexes are indeed capable of inserting into alkane C–H bonds^{14–16} with a definitive predominance of second- and third-row transition metals, and numerous excellent reviews have appeared.^{1,17–23} These reactions usually occur under relatively mild conditions. In general, significant regioselectivities are observed with a preference for reaction at the terminal C–H bonds

Scheme 2



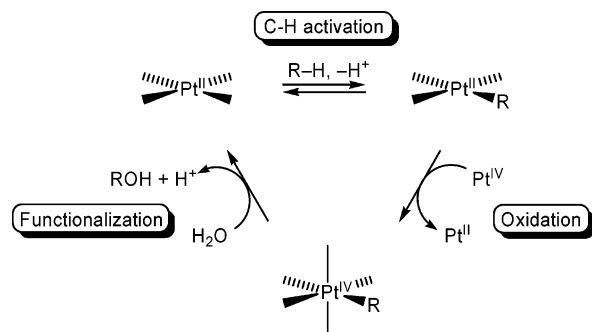
of alkanes, i.e., at the stronger bonds. Aromatic hydrocarbons, with C–H bond strengths even greater than those of alkanes, usually react at greater rates than alkanes. Desirable chemoselectivities are also often seen, implying that, in principle, reactions with alkane substrates can favorably compete with product degradation in catalytic systems.

It turns out that strong indications that Pt complexes should be viable in C–H activation chemistry were abundant prior to the seminal discoveries of the early 1980s.^{14–16} In fact, Pt-based catalysts are among the relatively few true catalytic systems that not only activate but also functionalize hydrocarbons. This chemistry is commonly referred to as “Shilov chemistry”. During the 1950s and early 1960s heterogeneous platinum systems were studied for use as catalysts to incorporate D into hydrocarbons.^{24–26} Looking for homogeneous equivalents of these systems, Garnett and Hodges demonstrated that aqueous Pt(II) salts catalyzed H/D exchange in aromatic hydrocarbons during the 1960s,²⁷ and these results were presented at the Fourth International Congress on Catalysis in Moscow in 1968.²⁸ Shilov and co-workers²⁹ write about the choice of the aqueous Pt(II) system that “the system was chosen because of its known activity in the deuterium–hydrogen exchange of aromatic molecules”, referring to the work of Garnett, Hodges, and Sollich-Baumgartner.²⁸ Thus, the Shilov group established in 1969 that Pt(II) salts in aqueous acid media were capable of catalyzing H/D exchange in alkanes.²⁹ The exchange of D for H is tell-tale proof that C–H activation has occurred and is frequently used experimentally as a diagnostic. The Shilov group further developed a catalytic system in which methane was converted to methanol and chloromethane (Scheme 2).

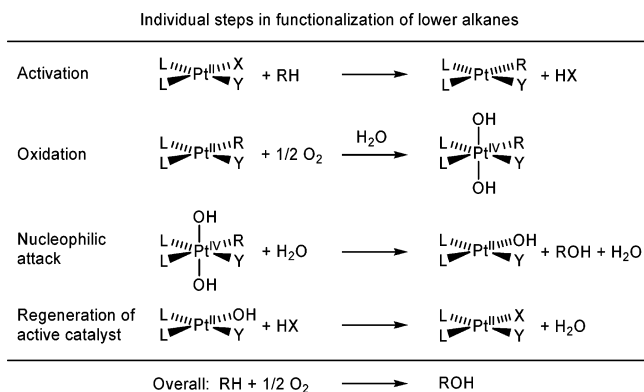
Here, the Pt(II) salt comprises the catalyst but stoichiometric amounts of an oxidant, Pt(IV), are required for catalytic action to occur. The inefficiency of the process has precluded its further use, but the Shilov system serves as a landmark proof-of-principle system. Homogeneous Pt(II)-mediated C–H activation did perhaps not receive the deserved attention at that time. However, beginning in the 1990s this chemistry has experienced a renaissance and the “Shilov chemistry” has been important for inspiring new research in this area. It is now clear that this chemistry is not only workable: Even mechanistic implications and conclusions drawn from the early experiments of Shilov, Garnett, and their co-workers are valid today. This is an impressive fact given the state of mechanistic understanding that was established in those relatively early years of organotransition-metal chemistry.

The Shilov catalytic system is believed to operate by the three individual reaction steps depicted in Scheme 3. It is important to note that each individual step in Scheme 3 may require several elementary reactions. Thus, a plethora of mechanistic possibili-

Scheme 3

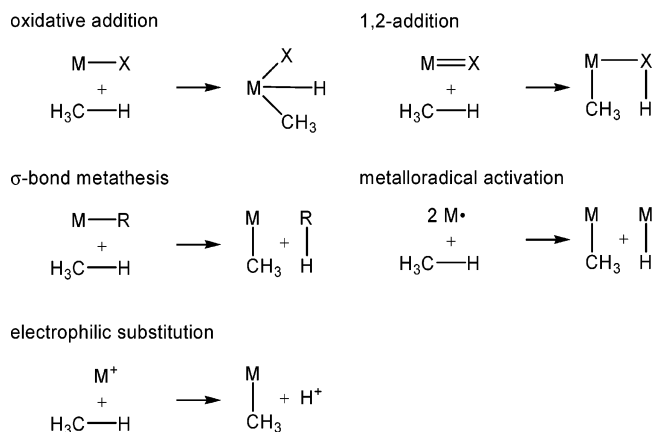


Scheme 4



ties is available to each; the actual operating mechanisms may be highly dependent on the exact nature of the Pt complexes, identity of hydrocarbon, solvent, and operating conditions. The first step is the actual activation step in which the C–H bond is broken. *This is the step on which this review will focus.* The second step is an oxidation step. With Pt(IV) as the oxidant, this is believed to proceed via an electron-transfer mechanism in the Shilov system. This opens the way for possible use of alternative (and cheaper!) oxidants. The search for such alternatives has been met with moderate success, in particular with Wacker-type oxidation systems O_2/Cu .³⁰ The third step is the actual functionalization of the hydrocarbyl fragment and liberation of the functionalized product. In the Shilov system this step is believed to proceed by nucleophilic attack by water at the Pt–C bond³¹ and this closes the catalytic cycle.

Much work aimed at understanding and improving the Shilov catalytic system has been done by the use of Pt complexes bearing a variety of ligand systems. Through these studies it has been established that many elementary steps that altogether constitute the oxidation of alkanes to alcohols using O_2 as the ultimate oxidizing agent are already in place, as shown in Scheme 4 and summarized by Labinger and Bercaw.¹ (It should be noted that although C–O bond formation from Pt(IV) has been demonstrated,^{31,32} none of these reactions involve the Pt(IV) dihydroxy alkyl species that are shown in Scheme 4.) It is now a great challenge to find a system in which all reactions operate efficiently in concert under conditions that are not detrimental to some of the steps. For example, organometallic complexes are often air and/or moisture sensitive; yet in Scheme 4, O_2 and H_2O are both required as reactants.

Scheme 5

The primary focus of this review will be on the C–H bond activation step in the Shilov cycle, although the oxidation and functionalization will be briefly discussed when deemed contextually appropriate. The discussion will be limited to the mechanistic behavior of molecular entities that exist in solution—significant contributions from studies of small Pt-based ions in the gas phase, primarily by mass spectrometry,^{33,34} and of hydrocarbon reactions at Pt metal surfaces are outside the scope of this review. We also decided not to include the ubiquitous aromatic cyclometalation reactions that are frequently observed in Pt(II) chemistry.³⁵ This review covers the literature published up to and including 2004.

2. Mechanistic Fundamentals

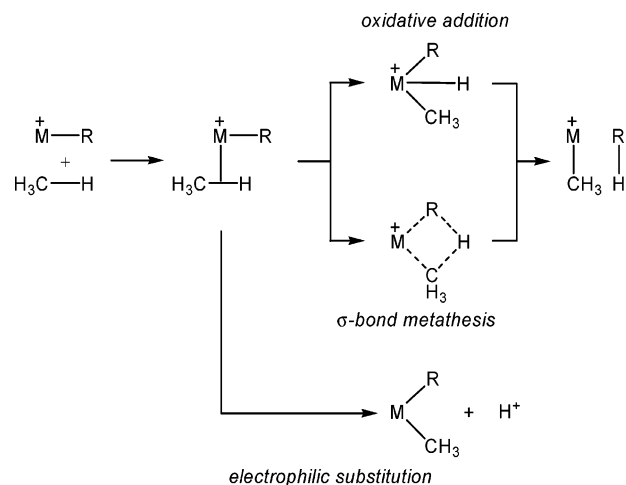
Today considerable insight has been accumulated concerning the mechanistic nature of metal-mediated C–H activations in general. Some essential and fairly general mechanistic features that will serve as a useful backdrop for the discussion of C–H activation at Pt will be reviewed in this section.

2.1. Classification of C–H Activation Reactions

Periana recently² defined C–H activation as “a facile CH cleavage reaction with an ‘MX’ species that proceeds by coordination of an alkane to the inner-sphere of ‘M’... leading to an M–C intermediate”. The C–H activation reactions have been subdivided according to reaction stoichiometries or possible reaction mechanisms in various ways, sometimes with rather unclear distinctions. We adhere to the subdivision into five different classes proposed by Stahl et al. according to reaction stoichiometries: oxidative addition, σ -bond metathesis, electrophilic substitution, 1,2-addition, and metalloradical activation.²¹ These classes, for which the notations do not necessarily bear mechanistic implications, are depicted in Scheme 5 for the particular case of methane activation.

2.2. C–H Bond Cleavage Event: Oxidative Addition vs σ -Bond Metathesis and Electrophilic Activation

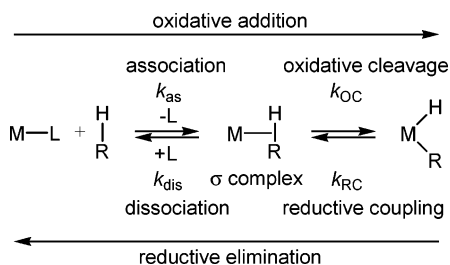
The terms “oxidative addition”, “ σ -bond metathesis”, and “electrophilic substitution” have strong

Scheme 6

mechanistic connotations in addition to the stoichiometrically based distinctions that were given in Scheme 5. The three mechanisms are depicted in Scheme 6 for a generic reaction in which a hydrogen atom is transferred from methane to a coordinated alkyl group or external base.

The oxidative addition mechanism usually operates for reactions at electron-rich, low-oxidation-state complexes, including those based on the Cp*Ir(I), Cp*Rh(I), and TpRh(I) moieties that have been thoroughly studied by the groups of Bergman^{17,36} and Jones.^{22,37} The σ -bond metathesis involves transfer of a hydrogen atom from one ligand to another in a concerted fashion through a four-center, four-electron transition state that avoids the formal two-electron oxidation of the metal. This mechanism offers an alternative for reactions at electron-deficient metal centers, in particular at d⁰ complexes which cannot undergo a formal oxidation of the metal. This applies especially to “early” transition metals in high oxidation states as well as lanthanide and actinide complexes.^{38–41} Interestingly, calculations⁴² have recently suggested that hydrogen transfer occurs by a σ -bond metathesis pathway from boron to carbon in the photochemically activated C–H borylation systems described by Hartwig.^{43,44} Although the behavior was attributed to the electropositive nature of B, these findings at relatively low-oxidation-state W and Fe complexes should serve as a reminder that σ -bond metathesis warrants consideration also at lower oxidation state and “late” transition metals. C–H activation by an electrophilic substitution pathway is closely related to the σ -bond metathesis pathway. Here, coordination of the alkane C–H bond at an electrophilic metal center leads to a C–H bond weakening that facilitates the following loss of a proton and generates the M–CH₃ species. The proton acceptor can be an external base or solvent or a sufficiently basic group in the coordination sphere of the metal. It is anticipated that soft electrophiles with low-lying, polarizable LUMOs should be most effective for this mode of C–H activation.² The alkane σ -complexes that will be discussed shortly bear strong similarities with the ubiquitous η^2 -H₂ complexes.^{45–50} It is well known that η^2 -H₂ complexes of metals that bear electron-withdrawing ligands and/or have a

Scheme 7



positive charge are quite acidic, and the coordinated H_2 molecule is strongly activated toward heterolytic cleavage. Analogous hydrocarbon C–H acidity enhancements are likely consequences of σ -alkane complex formation at electron-deficient metal centers and facilitate the electrophilic pathway for C–H activation (Scheme 6).

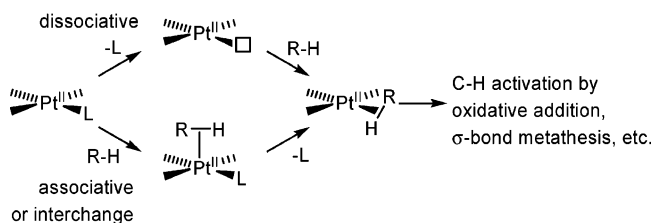
Bergman and co-workers have shown^{17,51–54} that cationic Ir(III) species $\text{Cp}^*\text{Ir}(\text{PMe}_3)(\text{CH}_3)(\text{ClCH}_2\text{Cl})^+$ and $\text{Cp}^*\text{Ir}(\text{PMe}_3)(\text{CH}_3)^+\text{BAR}_F^-$ activate alkane, arene, and other C–H bonds under very mild conditions. Ambiguities arose as to whether oxidative addition would still be favored relative to a σ -bond metathesis mechanism. The oxidative addition will involve cationic Ir(V) intermediates, somewhat unusual but not unprecedented in organometallic chemistry, whereas the σ -bond metathesis would avoid the Ir(V) oxidation state. Ab initio calculations by Su and Chu suggested⁵⁵ that the reactions at $\text{Cp}^*\text{Ir}(\text{III})$ likely proceed via oxidative addition, whereas σ -bond metathesis is competitive with oxidative addition when Ir is replaced with Rh, for which the +5 oxidation state is less prevalent.

2.3. Hydrocarbon Coordination

It is now well established that oxidative addition of C–H bonds to an unsaturated metal species M is a two-step reaction, depicted as a reversible process in Scheme 7. The first step is the association of the hydrocarbon at the metal. This requires a coordination site; the departing ligand L may be displaced in an associative or a dissociative fashion (Scheme 8). The association generates a hydrocarbon–metal complex intermediate. The second step is the oxidative cleavage of the C–H bond of the coordinated hydrocarbon. For the reverse process the reductive elimination comprises the two steps reductive coupling, generating the σ complex, followed by hydrocarbon dissociation. This terminology has been proposed recently by Jones⁵⁶ and Parkin⁵⁷ and helps distinguish the individual steps from the overall mechanistic connotations.

The hydrocarbon association leads to a crucial intermediate that appears to be involved in most, if not all, C–H activation reactions regardless of reaction mechanism, the so-called σ complexes (see section 2.4). Under thermal conditions this means that R–H must replace the two-electron-donor ligand L that is already bonded at the metal. The σ complexes are weakly bonded, and because most other ligands have significantly stronger bonds to the metal, hydrocarbon coordination will be thermodynamically unfavorable. The coordination of the hydrocarbon

Scheme 8



therefore will constitute a significant part of the activation barrier for a thermally driven C–H activation process. This will apply regardless of whether hydrocarbon coordination or oxidative cleavage is the rate-limiting step or whether hydrocarbon coordination occurs associatively or dissociatively.

To achieve high reactivity it is necessary to design systems in which all other ligands present in the medium are relatively weakly bonded. This has encouraged the search for poorly coordinating counteranions when cationic complexes are involved and the use of poorly coordinating solvents.

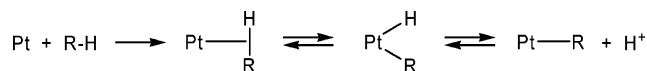
C–H activation at Pt has been mostly studied at Pt(II) precursors. Square-planar Pt(II) complexes constitute some of the most thoroughly studied systems for ligand substitution reactions. Substitutions may occur associatively, dissociatively, or by a concerted (interchange) mechanism.^{58,59} These possibilities are depicted in Scheme 8. The dissociative process proceeds via a three-coordinate, 14-electron intermediate, the associative process via a five-coordinate, 18-electron intermediate, and the interchange process via a five-coordinate transition state. It has been established that the majority of substitution reactions at Pt(II) occur associatively.^{60–62} Exceptions are known and tend to involve relatively electron-rich, often neutral, complexes with a strong σ donor (typically, an aryl group) trans to the leaving group.^{62,63} Reactions at more electron-deficient (cationic) complexes tend to occur associatively. Importantly, the well-studied substitution reactions at Pt(II) involve ligands that are far more nucleophilic than the hydrocarbon C–H bonds are expected to be. Thus, given the poor nucleophilicity of R–H in Scheme 8, one might suspect that dissociative reactions could be more prevalent in C–H activation chemistry than in the more traditionally studied systems.

The mode of alkane coordination has been addressed in the “pincer” complex (PCP)Ir-catalyzed dehydrogenation reactions (PCP = κ^3 -2,6-(R_2PCH_2)₂- C_6H_3). Recent calculations^{64,65} suggest that alkane coordination and H_2 displacement at neutral Ir(III) complexes (PCP)IrH₂ with bulky phosphine R groups proceed in a dissociative fashion, i.e., initial loss of H_2 followed by addition of R–H, under experimental conditions of high temperatures and low H_2 pressure.

2.4. σ Complexes of Alkanes and Arenes

The involvement of discrete metal–alkane σ complexes was mentioned in section 2.3. The first evidence that such species might be involved in C–H activation dates back to the 1960s. It was a remark-

Scheme 9



Scheme 10



able feature of the early Pt(II)-catalyzed H/D exchange reactions in acidic deuterated media that *multiple* H/D exchange into arene or alkane substrates was observed, even at early stages of the reaction.^{66,67} The observed isotopomer distributions required that multiple C–H bond-cleavage and bond-forming reactions occurred once a hydrocarbon molecule had entered the coordination sphere of Pt.

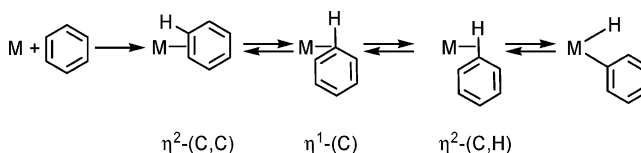
Mechanistically, this necessitated an intermediate metal–hydrocarbon complex *prior to a reversible* C–H bond cleavage/formation. For Shilov-type systems, multiple H/D exchange should result (Scheme 9) if (a) the oxidative addition product Pt(H)(R) undergoes reversible deprotonation at a greater rate than hydrocarbon dissociation in the deuterated acidic medium and (b) the Pt(R–H) intermediate is dynamic in nature such that the coordinated hydrocarbon “rotates” at Pt such as to expose its different C–H bonds toward the metal.

Garnett and Hodges in 1971 described this mechanistically required intermediate as “...a complex involving delocalized molecular orbitals of the alkane”.⁶⁸ This description is remarkably close to what is today described as σ -alkane complexes, quite astonishing considering the level of advancement of the science at that time. The σ complexes are commonly depicted with a hydrocarbon C–H bond acting as a two-electron donor toward an empty acceptor orbital at the metal, although different coordination modes have been envisioned.^{56,69}

The hydrocarbon σ complexes are now believed to be intermediates in most, if not all, metal-mediated C–H activation reactions. The experimental evidence that supports their existence includes transient spectroscopic observations, kinetic data, and isotopic labeling experiments.^{56,69–72} The incorporation of D label from deuterated protic media into coordinated hydrocarbyl groups, via the mechanism depicted above, is an obvious indicator. In other and numerous cases isotopic exchange between labeled and unlabeled hydride and methyl sites (Scheme 10) in a complex provides another line of evidence.^{73–85} There is a report that this exchange can be rapid even at low temperatures. In Cp*Os(dmpe)(H)(CH₃)⁺ the exchange of the hydride and methyl protons has been probed by spin-saturation transfer and line-shape analysis at temperatures below –100 °C; the exchange rate constant at this temperature was as high as 160 s^{–1}.⁷⁵ Similarly, spin-saturation transfer established rapid exchange between hydride and *phenyl* sites in Tp’Pt complexes; these will be discussed in section 7.2.^{86,87}

H/D label exchange according to Scheme 9 or 10 provides evidence for the existence of C–H(D)-bonded species even if these cannot be directly observed. However, stable, spectroscopically identifiable σ com-

Scheme 11



plexes remain rather elusive. There is only one report of a complex sufficiently stable to be observed by NMR spectroscopy, CpRe(CO)₂(cyclopentane).⁸⁸ An Fe(porphyrin) heptane complex⁸⁹ and a few U(III) alkane complexes,⁹⁰ all of which may gain additional stabilization by noncovalent interactions, have been crystallographically characterized. Neither of these relatively stable systems have been reported to exhibit C–H activation reactivity.

In terms of bonding there is a strong analogy^{46,48,71,72,91} between the situation in these σ -alkane complexes and the ubiquitous $\eta^2\text{-H}_2$ dihydrogen complexes,^{45,47–50} $\eta^2\text{-(Si,H)}$ silane,⁹² and metal alkyl complexes that exhibit agostic C–H interactions.⁹³

Analogous isotope exchange reactions occur in systems that involve arene C–H activation or complexes that contain phenyl ligands. Aromatic hydrocarbons are better ligands than alkanes by virtue of their electron-rich π -electron cloud, and $\eta^2\text{-(C,C)}$ -bonded arenes are commonly considered as intermediates in C–H activation reactions,^{21,37,57,94–99} although this is not always the case.^{100,101} A Pt benzene complex with a $\eta^2\text{-(C,C)}$ coordination mode has recently been characterized by X-ray crystallography.⁸⁷ In the cases where they are intermediates it is not obvious how C–H activation can occur directly from the $\eta^2\text{-(C,C)}$ coordination mode, and therefore, a “slip” of the arene to a less stable and therefore unobserved $\eta^2\text{-(C,H)}$ coordination mode¹⁰⁰ or even an $\eta^1\text{-mode}$ ¹⁰² might well precede the C–H activation (Scheme 11).¹⁰³ The involvement of an $\eta^2\text{-(C,H)}$ mode has been recently supported by DFT calculations for a tungstenocene-based C–H activating system.⁵⁷

2.5. Principle of Microscopic Reversibility

Obviously the direct observation of thermal oxidative addition of the C–H bonds of a hydrocarbon R–H at isolable metal complexes is desirable for mechanistic purposes, but normally this is not possible because the oxidative addition products M(R)(H) are thermodynamically unstable with respect to the reactants. Hydridoaryl and hydridoalkyl species have therefore been generated by other means, most commonly by protonation of stable metal alkyl or aryl precursors. The mechanism of the thermodynamically favorable reductive elimination, which is the microscopic reverse of the C–H activation reaction, can then be scrutinized. The principle of microscopic reversibility then suggests that the insight gained adds to the knowledge of the C–H activation process itself. It is important to note that the reaction conditions (solvent, temperature, etc.) that are applied in studying the reductive elimination reactions can be dramatically different from what is required to run the reaction in the opposite direction and that extrapolations of findings should be done with care.

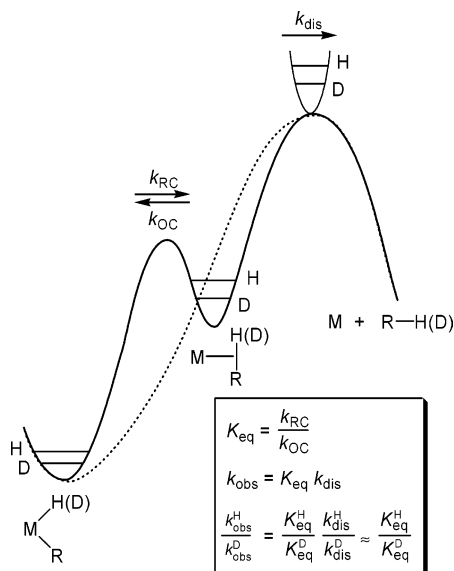


Figure 1. Reaction coordinate for two-step (—) and one-step (···) mechanisms for reductive elimination from a hydridoalkyl complex (RC = reductive coupling; OC = oxidative cleavage; dis = dissociation).

This principle has been successfully applied in order to understand reductive elimination/oxidative addition reactions and protonation/deprotonation reactions that are of significance in C–H activation chemistry.

2.6. Kinetic Isotope Effects

C–H activation chemistry involves the cleavage of C–H bonds, and it is not surprising that measurements of H/D kinetic isotope effects (KIEs) and interpretations of their physical meaning have been crucial to the mechanistic advancement of this chemistry.^{56,104,105}

The α -C H/D exchange of alkyl hydride complexes was noted early⁸⁰ and helped establish the intermediacy of σ complexes. The kinetics of reductive eliminations from alkyl hydride and alkyl deuteride complexes^{80,81} revealed observed H/D KIEs that were in many cases *inverse*, i.e., < 1 (ref 56 surveys a great number of cases of H/D exchange and inverse isotope effects). It became common to associate inverse KIEs with the intermediacy of σ -alkane complexes in the reductive elimination process. These isotope effects were considered to arise from the C–H(D) bond formation, i.e., the reductive coupling in Scheme 7, rather than the hydrocarbon dissociation, and were interpreted in terms of an *inverse equilibrium isotope effect* $K_{\text{eq}}^{\text{H}}/K_{\text{eq}}^{\text{D}} < 1$ for the formation of the σ complex from the alkyl hydride. The physical explanation for this is that the σ -alkane complex has formed an essentially complete C–H(D) bond, whereas the alkyl hydride has a weaker M–H(D) bond. Consideration of the zero-point energy differences for the vibrations of these bonds leads to an expected inverse equilibrium isotope effect for the reductive coupling step.¹⁰⁶ If there is only an insignificant isotope effect on the hydrocarbon dissociation step, the result will be an observed inverse kinetic isotope effect for the overall reductive elimination. This scenario is depicted with the solid line in Figure 1. The interpretation of

these KIEs has evoked considerable discussion.

One interesting issue has been whether the observed inverse isotope effects can be caused by a one-step reaction or whether a two-step mechanism is required.⁸⁴ A single-step mechanism may produce an inverse isotope effect,^{107,108} normally for a highly endothermic reaction in which the transition state is very “product-like”, i.e., a considerable amount of C–H bond formation has taken place. The dotted line in Figure 1 shows a trajectory for a hypothetical one-step reaction that passes through an *identical transition state for the rate-limiting step* as does the two-step reaction. The KIE should be dictated by the energy differences between the ground state and the rate-limiting transition state and hence would appear to be the same, regardless of the involvement of the preequilibrium. In this case strong support to the preequilibrium scenario is provided by the observed α -C H/D exchange phenomena.

A second issue has been how to interpret the inverse isotope effects given that a two-step mechanism is actually operative. It is important to note in Figure 1 that three different H/D rate constants, and therefore three different H/D isotope effects for elementary reactions, will contribute to the observed H/D isotope effect because $k_{\text{obs}} = k_{\text{RC}}k_{\text{dis}}/k_{\text{OC}} = K_{\text{eq}}k_{\text{dis}}$. The composite rate constant k_{obs} is usually established by normal kinetic measurements. Moreover, accepting that there is no significant isotope effect on the dissociation step, $(k^{\text{H}}/k^{\text{D}})_{\text{obs}} = K_{\text{eq}}^{\text{H}}/K_{\text{eq}}^{\text{D}} = (k_{\text{RC}}^{\text{H}}/k_{\text{RC}}^{\text{D}})/(k_{\text{OC}}^{\text{H}}/k_{\text{OC}}^{\text{D}})$. In a recent and insightful review⁵⁶ Jones points out that two different scenarios can lead to the observed inverse equilibrium isotope effects (Figure 2) and that detailed experimentation is needed before the contributions from each elementary step can be disentangled. The first scenario (left) is that the zero-point energy difference for the reductive coupling transition state (reflected in k_{RC}) is intermediate between those of the hydridoalkyl and σ -alkane complexes. In this case one would anticipate an inverse isotope effect for a *one-step* (see previous paragraph) reductive coupling and a normal isotope effect for the reverse oxidative cleavage. The second scenario (right) is that the zero-point energy difference for the C–H(D) stretch vanishes as the vibration becomes the reaction coordinate to break the bond. In this case a normal isotope effect is expected in both directions but with a greater magnitude for the oxidative cleavage than for the reductive coupling. In a series of elegant labeling experiments, the details of which will not be discussed here, Jones established that the reductive coupling from $\text{Tp}^*\text{Rh}(\text{CNR})(\text{CHMe}_2)\text{H}$ vs $\text{Tp}^*\text{Rh}(\text{CNR})(\text{CHMe}_2)\text{D}$ ($\text{R} = \text{CH}_2$ - $t\text{Bu}$) exhibits a *normal* KIE $k_{\text{RC}}^{\text{H}}/k_{\text{RC}}^{\text{D}} = 2.1$. In a related system, $\text{Tp}^*\text{Rh}(\text{CNR})(\text{CH}_2\text{D}_2)$ (generated by photolysis of $\text{Tp}^*\text{Rh}(\text{CNR})(\text{RN}=\text{C}=\text{NPh})$ in the presence of CH_2D_2) generated an initial 4.3:1 ratio of $\text{Tp}^*\text{Rh}(\text{CNR})(\text{CD}_2\text{H})(\text{H})$ and $\text{Tp}^*\text{Rh}(\text{CNR})(\text{CDH}_2)(\text{D})$, leading to the conclusion that the oxidative cleavage from the σ -methane complex also exhibited a *normal* KIE $k_{\text{OC}}^{\text{H}}/k_{\text{OC}}^{\text{D}} = 4.3$. It was concluded that observed inverse equilibrium isotope effects for C–H reductive coupling in these systems arise from *normal* isotope effects on each of the two opposing reactions with a

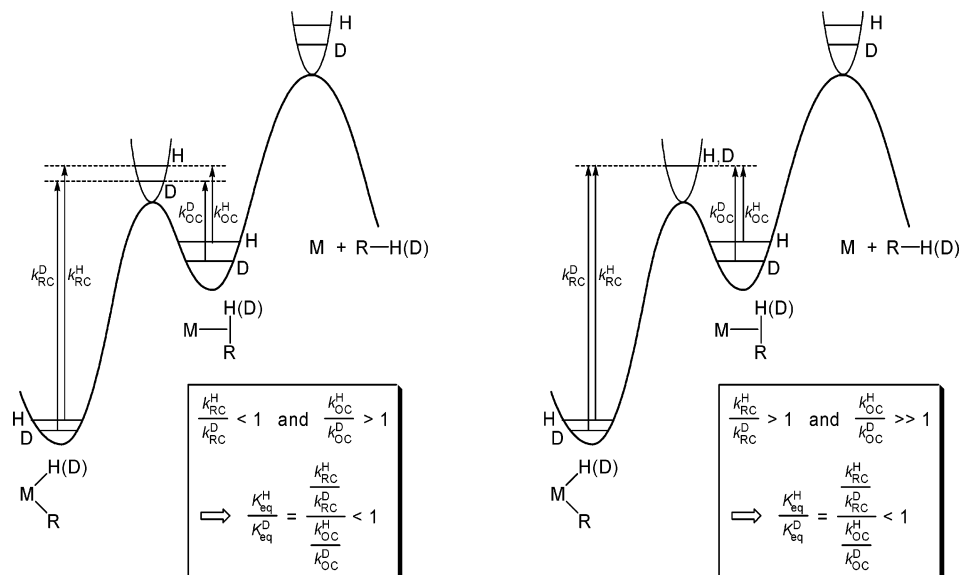


Figure 2. Two scenarios (see text) that can lead to inverse equilibrium isotope effects. (Adapted from ref 56.)

greater effect on the oxidative cleavage than on the reductive coupling. This corresponds to the second scenario, Figure 2 (right). A similar situation has been unraveled experimentally for methane elimination from a tungstenocene methyl hydride,⁵⁷ and the experimental findings have been further found to agree well with results from DFT calculations.¹⁰⁹ The complexity of the issue was underscored when Jones established that the inverse H/D KIE for reductive elimination of benzene from Cp*Rh(PMe₃)(Ph)(H/D) also originates in an inverse equilibrium isotope effect for η^2 -benzene formation (the additional involvement of σ -(C,H)-benzene intermediates suggested for other systems^{57,103} apparently cannot be ruled out). However, this time the inverse equilibrium isotope effect arises from an *inverse* isotope effect for the one-step reductive coupling and a normal effect on the oxidative cleavage, Figure 2 (left). Possible consequences of isotope effects on the “slip-page” from σ -(C,H) to η^2 -(C,C), perhaps via η^1 -(C)¹⁰² benzene complexes, have not been taken into account in the analysis.

A third issue arises from the fact that KIEs are commonly discussed in terms of the zero-point energies of the bonds being formed/broken and their relatively simple temperature dependency predicted by the van't Hoff relationship. Most reported KIEs arise from single-temperature measurements. Parkin and co-workers^{57,109,110} recently investigated isotope effects on C–H association, oxidative cleavage, and reductive coupling at molybdenocene and tungstenocene derivatives in detail. Equilibrium isotope effects (EIEs) are calculated by DFT¹¹⁰ from the expression $EIE = K^H/K^D = SYM \cdot MMI \cdot EXC \cdot ZPE$, where SYM is the symmetry factor, MMI is the mass-moment of inertia term, EXC is the excitation term, and ZPE is the zero-point energy term.¹⁰⁶ The calculations revealed that vibrations other than that involving the bond being broken/formed can make significant contributions to the ZPE part. Moreover, surprising temperature dependencies of the EIEs are implicated by the strikingly different response to the temperature of the ZPE and the SYM·MMI·EXC

terms. For example, coordination of CH₄ vs CD₄ at [H₂Si(C₅H₄)₂]W is predicted to exhibit an inverse EIE at temperatures below –204 °C and a normal EIE above –204 °C, whereas the EIE for oxidative cleavage starting from the corresponding methane complexes would be normal at all temperatures and increase with decreasing temperatures.¹¹⁰

With the above discussion in mind it is obvious that the interpretation of kinetic isotope data pertaining to C–H activation chemistry is far from trivial, even when simple molecules such as methane are concerned. In general, it is desirable to have KIE data for a wide range of temperatures. Even then, the fact that the measured rate constants are in reality composite rate constants makes interpretation of the physical meaning of the KIEs difficult as far as assigning the effects to elementary steps in the reaction sequence. The accumulated evidence today probably allows a generalization to be made: observed inverse KIEs for C–H reductive eliminations arise from inverse equilibrium effects for the reductive coupling step followed by a rate-limiting, isotope-insensitive dissociation of the hydrocarbon. Cases in which the reductive elimination KIEs are normal may be interpreted in terms of a change in the rate-limiting step, i.e., the hydrocarbon dissociation is rapid compared to the reductive coupling. This corresponds to the energy of the first transition state being above that of the second, representing a non-preequilibrium situation (Figure 3).⁵⁷

3. Shilov-type Chemistry

Shilov and co-workers have deservedly been widely credited for the discovery that Pt salts are capable of activating and functionalizing saturated hydrocarbons in acidic aqueous media, as previously expressed in excellent reviews.^{18,20,71,111} We find it pertinent to include details of this chemistry also in this review because interesting similarities in mechanistic thinking and analysis are revealed when these systems are compared with today's model systems and the widely acclaimed Catalytica system.

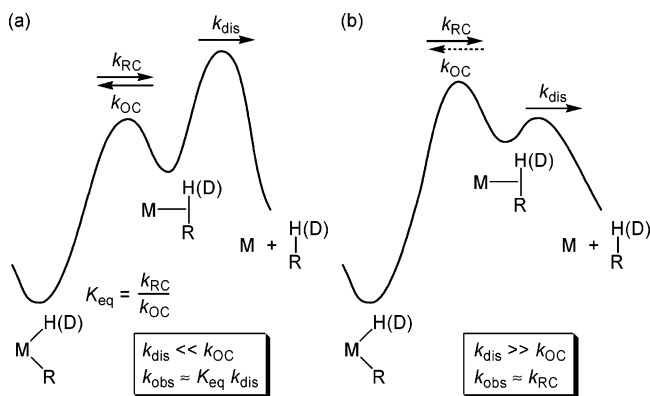


Figure 3. Reaction coordinate diagrams for R–H reductive elimination. (a) Rate-limiting hydrocarbon dissociation gives an inverse observed H/D isotope effect. (b) Rate-limiting reductive coupling gives a normal observed isotope effect.

3.1. C–H Activation by Pt(II)

Garnett and Hodges reported the first accounts of Pt-mediated aromatic C–H activation in 1967.²⁷ Dissolving K_2PtCl_4 in a D_2O/CD_3CO_2D mixture gave deuterium incorporation in benzene and benzene derivatives. Reactions with cyclohexane were reported to be slow, but no further details were given. Mechanistic details of the aromatic C–H activation were later reported in a series of remarkable papers.^{66,112–116} Despite early attempts by Garnett and Hodges to induce aliphatic C–H activation,²⁷ it was Shilov and co-workers who in 1969 were the first to successfully achieve H/D exchange into methane and ethane.²⁹ Influenced by the success of Garnett and Hodges (see section 1) with K_2PtCl_4 , Shilov chose the same system for reactions with methane and ethane. A deuterium incorporation of 2.5% was achieved for methane by heating with a solution of 30% CH_3CO_2D in D_2O acidified with 30% HCl at 100 °C for 6 h. More than 26% D incorporation into ethane was achieved after 9 h at 150 °C. This was the first homogeneous system ever to activate simple alkane C–H bonds. The results were later verified by Hodges, who also added linear and branched alkanes up to C6 to the list of reacting hydrocarbons.⁶⁸

Catalyst stability and Pt black formation, possibly by Pt(II) disproportionation, were early issues with the aqueous Pt(II) systems.¹¹⁷ Acidic conditions inhibited disproportionation, although too acidic conditions also inhibited the homogeneous metal-catalyzed H/D exchange and promoted acid-catalyzed exchange.^{27,66,114} The possible participation of heterogeneous species was also addressed.^{27,112} The acetic acid also served an important role by solubilizing benzene, precluding a two-phase system. Shteinman et al. speculated that a weak chelate complex, possibly $Cl_2Pt(\eta^2-HOOCCH_3)$, was the origin of acetic acid stabilization.⁶⁷ A 1H and ^{195}Pt NMR study of Pt(II) dicarboxylates shows multiple modes of complexation.¹¹⁸ Interestingly, a very recent study by Gerdes and Chen elaborates the role of interconverting η^1 and η^2 acetate ligands in Pt diimine complexes (see section 6.5).¹¹⁹ It was shown earlier that benzene and other aromatic hydrocarbons improved the stability of the catalytic system with respect to Pt

deposition.¹¹⁴ The inertness toward molecular oxygen is a desirable feature of the aqueous K_2PtCl_4 system;¹²⁰ the presence of air has even been suggested to inhibit disproportionation.¹¹⁴

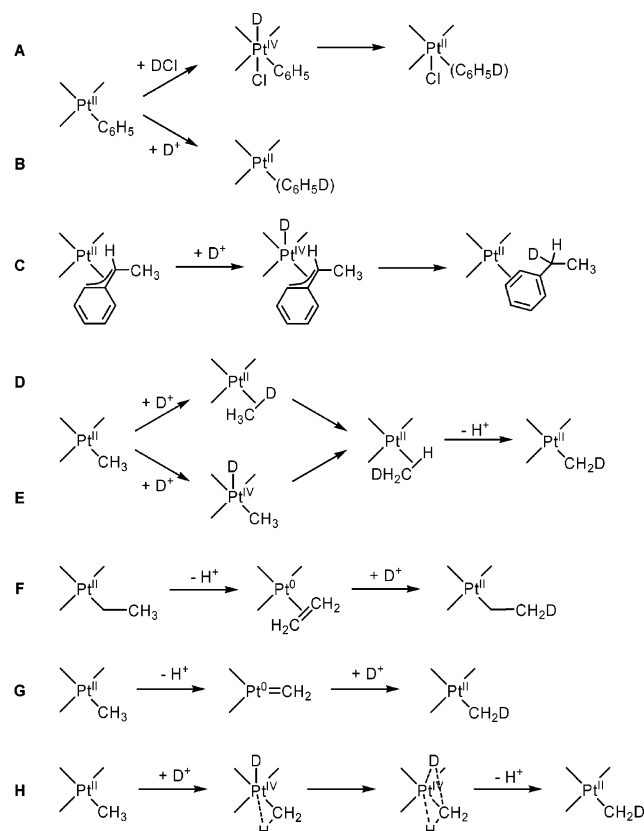
Reaction rates were shown to be first order in $[PtCl_4^{2-}]$ and [hydrocarbon] and inversely proportional to $[Cl^-]$,^{66,67} and perchloric acid was used to increase the acidity without accompanying inhibition by chloride. No simple correlation was found between the acidity and the reaction rates. A nonlinear dependence of the rate on added $PtCl_4^{2-}$ and Cl^- suggested initial displacement of chloride by one or two solvent molecules (D_2O , CH_3COOD) to yield $Pt(Solv)Cl_3^-$ or $Pt(Solv)_2Cl_2$.¹¹⁴ In fact, $PtCl_2(OAc)_2^{2-}$ as a catalyst led to increased H/D exchange rates in pyrene.¹¹⁵ The idea that an active Pt(II) complex with a coordination vacancy is formed by Cl^- dissociation was also suggested by Rudakov.¹²¹ ^{195}Pt NMR signals corresponding to $PtCl_4^{2-}$ as well as $PtCl_3(H_2O)^-$ were later observed by Bercaw and co-workers at an early stage in oxidation reactions where $PtCl_6^{2-}$ was used as the oxidant.¹²² Consumption of the oxidant gradually released Cl^- that during several hours inhibited the C–H activation reaction, and eventually the ^{195}Pt NMR signal of $PtCl_4^{2-}$ was the only one present. Again, it appears that at least one Cl^- must be displaced for C–H bond activation to proceed.

Ligand effects in $PtCl_2L_2$ and $PtCl_3L^-$ were studied, and it was shown that the rate of D incorporation into cyclohexane varied over 3 orders of magnitude in an order opposite of that expected from ligand trans effects,¹²³ suggesting that the rates of alkane C–H activation do not merely reflect the ease of ligand substitution. Rapid H/D exchange in alkanes and arenes is only observed when the ligands bonded to Pt are of low trans effect.¹¹⁵

The rate of deuterium incorporation into substituted benzenes (C_6H_5X , $X = F, Cl, Br, Me, CF_3, tBu, NO_2$) was relatively independent of X in reactions with aqueous Pt(II) in CH_3COOD/DCl .^{66,112} If one assumes that the electrophilic attack at the C–H bond is not rate determining, the invariance of rate exchange observed for the substituted benzenes is explained. For alkanes initial experiments showed H/D exchange rates that decreased in the order $C_2H_6 > CH_4 > CH_3COOH$.⁶⁷ Additional experiments showed that the rate of exchange decreased with the introduction of electronegative substituents ($CH_3F, CH_2F_2, CHCl_3, CH_3CHF_2$, etc.).^{116,124}

The reactivity order in alkane H/D exchange is cycloalkanes > primary C–H > secondary C–H > tertiary C–H, and steric factors appear to exert a major influence.^{68,114,125} Thus, in straight-chain and branched alkanes the methyl groups are more reactive. This observed reactivity is the opposite of what is normally found for electrophilic and radical oxidation reactions where reactivity largely depends on bond strength. Arenes are generally more reactive than alkanes, but reactivities nearly overlap, benzene reacting only twice as fast as cyclohexane.¹¹¹ In alkylbenzenes the aromatic C–H bonds are most reactive. In the side chain the α and ω positions are more reactive than the other methylene units,¹²⁶ and the extent of deuterium incorporation decreases with

Scheme 12



All steps are reversible as necessitated by the observed multiple H/D exchange, but have been drawn only in one direction and for the 1st H/D exchange for simplicity.

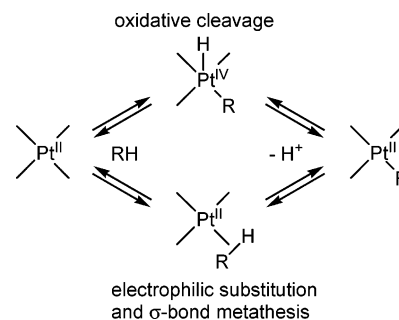
increasing chain length. For naphthalene H/D exchange is observed only in the β position,¹²⁷ and very little deuteration occurs in the aromatic positions of *p*-xylene compared to the methyl groups (2% vs 20%).^{113,128} Similar trends are observed for polycyclic aromatic hydrocarbons.¹²⁹

3.2. Mechanism of Multiple H/D Exchange

The fact that multiply deuterated species were formed even early in the reaction was a remarkable feature of the Pt(II)-catalyzed H/D exchange.^{66,67} Whether this occurred by a single multiexchange event or by consecutive single-exchange events was analyzed in detail by Garnett and Hodges, who estimated the so-called “*M* values” for the H/D exchange.⁶⁶ Originally introduced for heterogeneous exchange,¹³⁰ the *M* value gives an estimate of the number of D atoms that enter a substrate molecule that is bonded at a catalytic site before the molecule again dissociates. *M* values in the range 2.69–3.76 were found for benzene H/D exchange, depending on the CH₃COOD concentration. For H/D exchange into alkanes, *M* values were in the range 1.42–1.82.^{114,131}

Two mechanistic possibilities were originally favored. Repeated, reversible oxidative cleavage/reductive coupling of DCl/HCl (Scheme 12, **A**)⁶⁶ includes a Pt(IV) aryl hydride intermediate—a type of species which at that time had not yet been observed. The other possibility was repeated interconversions between σ -bonded and π -coordinated benzene combined with deprotonation/deuteration, not necessitating the Pt(IV) intermediate (**B**). The two options essentially

Scheme 13



amount to protonation at Pt vs at the C(aryl) atom or Pt–C(aryl) bond. In alkylbenzenes H/D exchange was observed in aromatic and aliphatic positions, aromatic C–H bonds generally being more reactive than aliphatic ones. The mechanism proposed to include this scrambling included a η^3 -benzyl species which interconverts with the π -benzene (**C**).¹²⁶ For alkanes, Garnett and Hodges proposed mechanism **D** including a complex described as involving “delocalized molecular orbitals of the alkane”.⁶⁸ This description is remarkably close to today’s description of Pt σ -alkane complexes. Bearing in mind that this was published as early as in 1971, it might indeed be the first mention of such intermediates in Pt-mediated C–H activation chemistry.

Rudakov and Shteinman suggested repeated interconversions between σ -bonded ethyl and π -coordinated ethene once ethane has reacted with the platinum center (**F**).¹³¹ For methane the postulated intermediate following the same pattern would necessitate a carbene species Pt=CH₂ (**G**). The carbene mechanism has not received much support in Pt-mediated C–H activation chemistry, although Pt hydrido(alkyl)carbene complexes have been suggested as intermediates in reactions of platinumacycloalkanes.¹³² Shestakov suggested a mechanism for H/D exchange avoiding both carbene species and alkane complexes (**H**).¹³³ Following addition of D⁺ at Pt, an agostic bond to the alkyl group is formed and the D on Pt is transferred to the alkyl group while the agostic H is transferred to Pt in a concerted fashion. Interestingly, a similar transition state involving D and SiMe₃, rather H and D, was recently proposed to be involved in the migration of Me₃Si from C to Pt in the protonolysis of a Pt–CH₂SiMe₃ complex.¹³⁴

Shilov and others proposed that H/D exchange proceeds by protonation at the Pt–CH₃ group followed by rotation of the coordinated methane and deprotonation, thereby avoiding a Pt(IV) methyl hydride that was believed to be thermodynamically unfavorable (**D**).^{121,135} Zamashchikov, however, proposed that H/D exchange could be accounted for by interconversions between a Pt(IV) alkyl hydride and the corresponding σ complex (**E**).^{136,137} Again, the two options amount to protonation at Pt vs at the C(alkyl) atom or Pt–C(alkyl) bond, and this addresses a key question, namely, whether C–H activation and the reverse reactions involve oxidative cleavage and Pt(IV) hydrido alkyl intermediates or electrophilic substitution and σ -bond metathesis processes (Scheme 13).

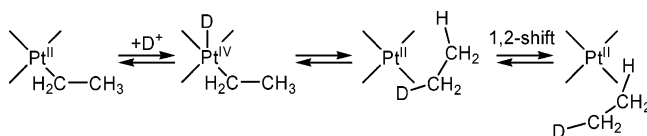
The idea that Pt(IV) alkyl, aryl, and hydride complexes were involved in C–H activation evolved during the 1960s,^{66,138} but it was not until the 1970s that experimental evidence for the existence of Pt(IV) alkyls and aryls was found,¹³⁹ and attempts were made to synthesize Pt(IV) alkyl complexes from RHgBr .¹⁴⁰ In 1982 Zamashchikov et al. recorded the ^1H NMR spectrum of a species believed to be $\text{PtCl}_4\text{Me}(\text{H}_2\text{O})^-$, where a signal corresponding to Pt–CH₃ was observed at δ 3.38 relative to $\text{Me}_3\text{Si-OSiMe}_3$ with characteristic ^{195}Pt satellites ($^2J_{\text{H-Pt}} = 77$ Hz).¹⁴¹ In the following years more Pt(IV) alkyl species were observed^{135,142} and eventually isolated.^{31,143–147} The Pt(II) methyl complex MePtCl_3^{2-} , believed to be the first intermediate after C–H bond breaking and deprotonation, proved more elusive. It was eventually obtained, admixed with $\text{Me}_2\text{PtCl}_2^{2-}$, from the reduction of MePtCl_5^{2-} with Cp_2Co by the Bercaw group.¹⁴⁸ Detailed studies showed that MePtCl_3^{2-} is much more water sensitive than $\text{Me}_2\text{PtCl}_2^{2-}$ and is readily protonolyzed in water, even at neutral pH. In the presence of PtCl_6^{2-} , however, oxidation of MePtCl_3^{2-} was shown to be competitive with protonolysis. At the temperature of alkane functionalization (120 °C), oxidation should completely dominate over the reversion of MePtCl_3^{2-} to methane by protonolysis.

Zamashchikov et al. suggested that deprotonation occurred from Pt(IV) alkyl hydrides after a complete oxidative cleavage.^{136,137} The conclusion was based on the assumption that the formation of an alkane complex would have no H/D isotope effect. Considering the current state of knowledge about isotope effects in C–H activation chemistry (see section 2.6) and agostic systems, this conclusion remains open.³¹ In a discussion of Shilov's mechanistic proposal, Bercaw et al. pointed out that oxidation of Pt(II) to Pt(IV) does not appear to be very attractive.^{31,149} By analogy with the known acidity of dihydrogen complexes¹⁵⁰ and the acidity of an agostic model complex,¹⁵¹ the authors argued that deprotonation from a methane σ complex would appear to be more favorable.

3.3. H/D Exchange—1,2 Shift in Ethane

The distribution of deuterioethanes arising from exchange in the presence of acetic acid shows a monotonically descending trend from d_1 to d_6 . When the reaction is performed in D_2O without acetic acid, a predominance of d_1 – d_3 over d_4 – d_6 is still seen but with an ascending trend within each group. This stepwise distribution suggests that exchange first takes place in one methyl group of ethane, and in a somewhat slower process the ethane molecule “turns around” and exchange occurs at the second methyl group.^{152,153} The formation of asymmetric d_2 and d_4 deuterioethanes is fully consistent with a mechanism involving σ -complex intermediates. The isotope distribution pattern implies that a 1,2-shift (shift of σ attachment of Pt from a C1–H to a C2–H) is slower than a 1,1-shift (shift of attachment from one C1–H to another; Scheme 14) or dissociation of ethane from Pt and that the presence of acetic acid somehow facilitates the 1,2-shift. Flood⁷⁶ and Jones⁷⁹ recently

Scheme 14



demonstrated that $(\text{Me}_3\text{tacn})\text{Rh}$ and $\text{Tp}'\text{Rh}$ fragments are capable of migrating along an alkane chain and that a Rh–D label can migrate intramolecularly to the α and ω termini of such chains.

3.4. Computational Studies of the Shilov System

A thorough review of quantum mechanical calculations on Pt and Pd molecular chemistry covering the literature from 1990 to 1999 has appeared.¹⁵⁴ An important DFT study by Siegbahn and Crabtree on *trans*- $\text{PtCl}_2(\text{H}_2\text{O})_2$ has addressed the importance of water in the second coordination sphere¹⁵⁵ and emphasizes the need to reliably include solvent and medium effects in calculations. Calculations were therefore done on reactions between methane and $\text{PtCl}_2(\text{H}_2\text{O})_2$ as well as an outer-sphere adduct containing an additional water molecule. The authors concluded that a σ -bond metathesis pathway was preferred. The rate-limiting step for the process is transfer of a hydrogen atom from the methane σ complex to a neighboring (cis) chloride ligand with an energy barrier 69 kJ/mol above the methane σ complex. In this process the H atom is not very protonic, as indicated by the fact that the transition state was not significantly stabilized by additional water molecules in the bond-breaking region. However, an oxidative addition pathway was still competitive for reactions at Pt and could not be discounted. A more clear-cut preference for σ -bond metathesis was found for reactions at Pd. The role of the second solvent coordination sphere at Pt was manifest in two ways: by acting as the terminal proton acceptor from the heterolytic cleavage of the C–H bond of methane and by improving the energetics of the methane binding at Pt. Attempts were also made to address the remarkable selectivity for terminal C–H bonds vs internal C–H bonds using propane as a model.¹⁵⁵ The origin of this effect was attributed to the greater polarity of the primary vs secondary M–C bonds¹⁵⁶ that are formed in the σ -bond metathesis. An increasing number of methyl substituents on a carbon decreases the negative charge on carbon, resulting in a weaker metal–carbon bond. This is an interesting observation, especially since the selectivities have been largely attributed to steric effects (see section 3.1).

In a study of methane C–H activation at *cis*- and *trans*- $\text{PtCl}_2(\text{NH}_3)_2$ in aqueous media Hush and co-workers calculated that ammonia is bound more tightly than water as a ligand by ca. 80 kJ/mol.¹⁵⁷ Consequently, and in contrast to the findings in the above paragraph, displacement of ammonia by methane in $\text{PtCl}_2(\text{NH}_3)_2$ is rate limiting in the overall activation of methane with energy barriers that are comparable to those of the C–H bond cleavage. The *trans* complex exhibited a clear preference for oxidative addition over σ -bond metathesis, whereas the

two were competitive for reactions at the cis complex. Further details about the ammine complexes are discussed in relation to the Catalytica system (section 4).

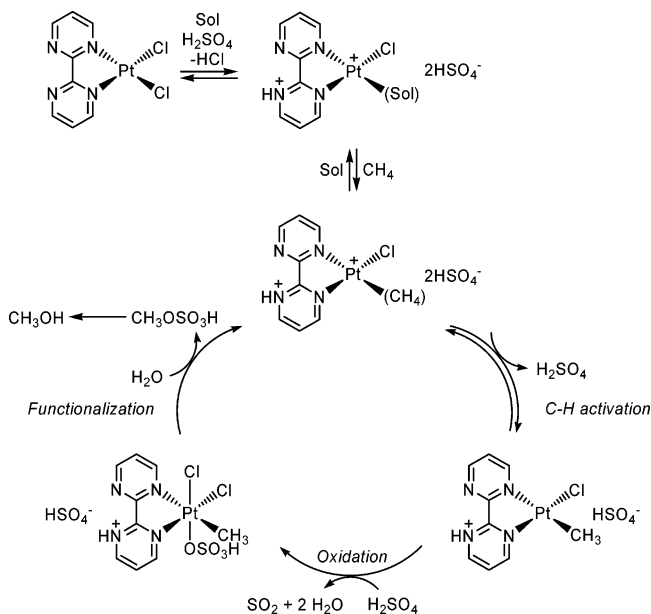
3.5. C–H Activation by Pt(IV)

Pt(II) systems have been most frequently studied for C–H activation, yet it has been shown that Pt(IV) species are also capable of activating aromatic C–H bonds, affording Pt(IV) aryl complexes (aryl)-PtCl₅²⁻ or (aryl)PtCl₄(H₂O)⁻.^{158–161} Refluxing benzene with H₂PtCl₆ in CF₃COOH/H₂O for 10 min followed by workup on silica gel containing ammonia yielded PtCl₄(C₆H₅)(NH₃)⁻NH₄⁺. With monosubstituted benzenes only meta and para isomers are observed with a kinetic preference for para. With increasing reaction time a near statistical meta and para distribution is obtained. No σ -aryl products were isolated from *p*-xylene and mesitylene. The reactions were first order with respect to PtCl₆²⁻ and arene, and LiCl inhibited the reaction. Electronic effects were probed in competition experiments between C₆H₆ and various C₆H₅X species and demonstrated that initial rates decreased by 3 orders of magnitude going from X = OH to NO₂. Kinetic isotope effects in benzene-*d*₆ and toluene-*d*₈ were 3 and 2.3, respectively. The mechanism that was proposed involves Cl⁻ dissociation followed by coordination of the arene to give a Pt(IV) π -arene complex which transforms into a Wheland-type complex. Deprotonation leads to the σ -aryl complex. The observed meta/para isomerization may proceed via a Wheland-type intermediate or via the π complex. The relatively small kinetic isotope effects led to the suggestion that the rate-limiting step is the formation of the Wheland complex rather than the subsequent deprotonation. The reaction of PtCl₆²⁻ with arenes also proceeds at room temperature under photochemical or γ -irradiation (⁶⁰Co source).¹⁶¹ Contrasting the thermal reaction, only the para Pt–aryl isomer is obtained from monosubstituted benzenes, and no meta/para isomerization was observed. Subjecting hexane to H₂PtCl₆ in CH₃COOH/H₂O under photochemical¹⁶² or γ -irradiation¹⁶³ yields a π -alkene product which can be trapped by workup on silica with pyridine.

4. “Catalytica” System for Catalytic Methane Functionalization

Apart from the use of expensive Pt(IV) as an oxidant, the aqueous K₂PtCl₄ system suffered one major drawback, namely, short catalyst life due to reduction of platinum and deposition of insoluble (PtCl₂)_n.¹⁶⁴ As discussed already, this could be prevented to some extent by the addition of aromatic compounds including benzene, toluene, and pyrene. Addition of chloride inhibited catalyst reduction but unfortunately also attenuated the rate of the C–H activation reaction. These issues were addressed by Catalytica Advanced Technology Inc., where Periana et al. described a (bpym)PtCl₂/H₂SO₄ system which converts methane to methyl bisulfate, a potential precursor for methanol (Scheme 15). The process is *catalytic in Pt* and utilizes SO₃ in fuming H₂SO₄ as

Scheme 15



oxidant.¹⁶⁴ The catalyst is severely inhibited by water or methanol, so that unattractive rates are observed below 90% H₂SO₄.² This system is frequently referred to as the “Catalytica system”. Regarding yields, selectivity, and catalyst turnover numbers, the Catalytica system is a true landmark for catalytic low-temperature methane functionalization. It accomplishes C–H activation, oxidation, and functionalization in the best way so far achieved for a homogeneous system without significant overoxidation to CO₂ or formation of chloromethane.¹⁶⁵ Although the process at present is not economically competitive compared to existing heterogeneous industrial processes, it serves as an important lead for future developments.

The Catalytica system is stable and active for the conversion of methane to methyl bisulfate with yields greater than 70% based on methane, selectivities greater than 90%, and catalyst turnover numbers greater than 300.² The ester can be hydrolyzed to methanol, and the SO₂ formed can, in principle, be reoxidized to SO₃, leading to O₂ as the terminal and very attractive oxidant. A remarkable feature of the system is the “self-assembling” and “self-cleaning” feature of the catalyst: treatment of (PtCl₂)_n with one equivalent of the bpym ligand in concentrated H₂SO₄ at 150 °C leads to complete dissolution of (PtCl₂)_n and catalyst formation. Even Pt metal is dissolved by bpym in hot, 96% H₂SO₄ to produce homogeneous (bpym)Pt(HSO₄)₂. It has been recently reported that the precatalyst (bpym)PtCl₂ dissolves in superacidic HF/SbF₅ with formation of the dinuclear cation [(H₂bpym)Pt(μ-Cl)]₂⁶⁺, which has been crystallographically characterized with SbF₆⁻ and Sb₂F₁₁²⁻ counterions.¹⁶⁶ It was reported that at temperatures up to about 80 °C this complex shows no reaction with methane (higher temperatures are difficult to handle due to the vapor pressure of HF). Nevertheless, both uncomplexed N atoms of the bpym ligand are protonated under these conditions and presumably could be under true catalytic conditions in concentrated sulfuric acid, resulting in a highly electrophilic Pt center.

Multiple H/D exchange is observed into gas-phase methane over a catalyst prepared in D_2SO_4 , suggesting again the involvement of σ -methane intermediates. No H/D exchange is observed into the methyl group when CH_3OSO_3H is added to the catalyst in D_2SO_4 . The ability of the catalyst to discriminate between C–H bonds in CH_4 and CH_3OSO_3H is of crucial importance for the desired selectivity and is thought to be due to the electron-withdrawing bisulfate group which inhibits electrophilic reactions between the metal complex and CH_3OSO_3H .

The original Catalytica paper¹⁶⁴ discusses whether C–H activation occurs by oxidative cleavage, with deprotonation from a Pt(IV) methyl hydride, or by electrophilic substitution, with proton loss from a Pt(II) σ -methane complex. Experimental data do not allow a distinction to be made between these two mechanisms. A great number of computational studies has followed concerning the mechanism of the C–H activation in the Catalytica system and in the simpler $(NH_3)_2PtCl_2$ system, which experimentally was shown to have a higher catalytic activity but was more prone to dissociation of the ammine ligand under acidic conditions.¹⁶⁴ The calculations are particularly challenging because reliable modeling of the highly polar and acidic medium is expected to be of great importance.

DFT calculations on $(NH_3)_2PtCl_2$ using a dielectric continuum to model solvation were used by Hush and co-workers to study oxidative addition vs electrophilic substitution.¹⁵⁷ The replacement of ammonia by methane and formation of a σ -methane complex was effectively rate limiting for this system. The two alternative pathways from the σ -methane complex through either a five-coordinate Pt(IV) methyl hydride or deprotonation of the σ -methane ligand were investigated. The activation barriers for σ -bond metathesis and oxidative addition were found to be comparable for *cis*- $(NH_3)_2PtCl_2$, whereas oxidative addition was strongly favored for *trans*- $(NH_3)_2PtCl_2$. It was concluded that the results support the thermodynamic feasibility of oxidative addition of methane to $(NH_3)_2Pt(OSO_3H)_2$ or $(NH_3)_2Pt(OSO_3H)(H_2SO_4)^+$. In a later DFT study on the same system using the Poisson–Boltzmann continuum to model solvation, Goddard and co-workers investigated the possibility of methane displacing chloride instead of ammine. A comparison of oxidative addition and electrophilic substitution pathways suggested that for *cis*- $(NH_3)_2PtCl_2$ the oxidative addition pathway is favored by 42 kJ/mol.¹⁶⁷

DFT calculations on the Catalytica system using the conductor-like screening model for solvation corrections were used by Ziegler and co-workers.¹⁶⁸ Calculations were performed on cations $(bpym)PtCl^+$ and $(bpym)Pt(OSO_3H)^+$ and interestingly led to different conclusions with regard to the mechanism. Oxidative addition was favored for $(bpym)PtCl^+$, whereas a σ -bond metathesis in which deprotonation occurs by proton transfer to the coordinated HSO_4^- ligand was preferred for $(bpym)Pt(OSO_3H)^+$. However, the authors pointed out that the solvation model used was not accurate enough to model the equilibrium between $(bpym)Pt(OSO_3H)^+$ and $(bpym)PtCl^+$.

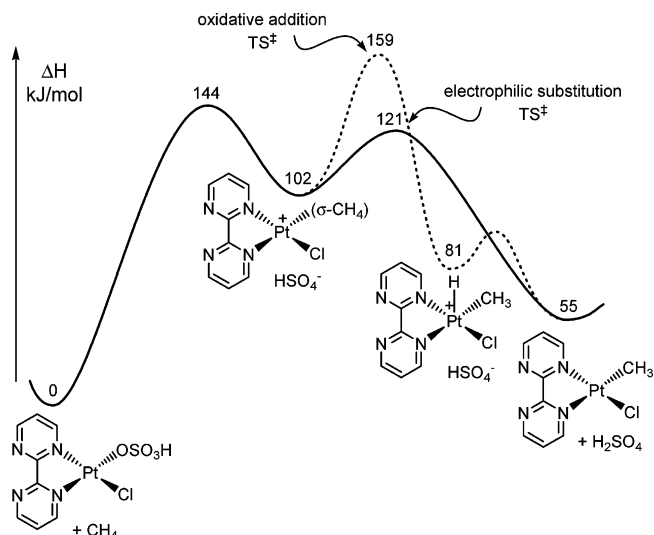


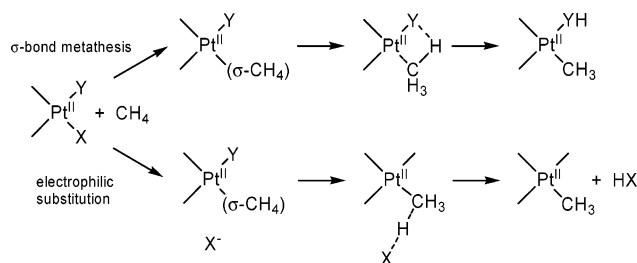
Figure 4. DFT-calculated energy diagram for C–H activation at the Catalytica system. (Adapted from ref 167.)

Protonation of the noncoordinated N atoms of the bpym ligand increased the tendency toward a σ -bond metathesis pathway. However, it was found that both ligand protonation steps were endothermic and that the noncoordinated N atoms of bpym are not protonated in the Catalytica system or that if they are protonated the counterions probably coordinate to Pt as well.

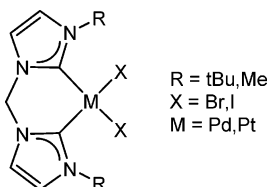
The study by Goddard that was mentioned above also includes calculations on the $(bpym)PtCl_2$ system.¹⁶⁷ Extensive computations were done to map the energies and relationships of the many species that might be involved in the concentrated H_2SO_4 medium. Contrary to Ziegler's findings it was observed that Cl^- remains closely associated to form a tight ion pair $(bpym)PtCl(CH_4)^+Cl^-$; T-shaped three-coordinate Pt cation $(bpym)PtCl^+$ and N-protonated analogues were not favored as discrete intermediates. Contrasting the behavior of the ammine system *cis*- $(NH_3)_2PtCl_2$, an electrophilic substitution was now favored over oxidative addition and Cl^- was shown to assist the deprotonation of the σ -bound methane. The calculations indicated that the bpym ligand was likely to be protonated at one nonligated N under actual catalytic conditions,¹⁶⁹ which causes a greater preference for electrophilic substitution. Periana argues that a reason for the apparent changeover in mechanism from the oxidative addition observed in the Shilov system to electrophilic substitution in the Catalytica system is the increased electrophilicity of the metal due to protonation of the bpym ligand.² Figure 4 depicts a reaction coordinate diagram for C–H activation at the unprotonated bpym catalyst system. The relative energies of the electrophilic substitution TS^\ddagger and the methane association TS^\ddagger are consistent with multiple H/D exchange in deuterated media.

At this point it is appropriate to address the use of the terms “electrophilic substitution” and “ σ -bond metathesis” (Scheme 16). The major differences between Goddard's electrophilic substitution and Ziegler's σ -bond metathesis appear to be whether the base X^- (Cl^- and HSO_4^-) is attached to Pt or not

Scheme 16



Scheme 17



when the deprotonation occurs: X^- is detached in the case of electrophilic substitution but attached in the case of a σ -bond metathesis. The two studies do however agree that deprotonation occurs from the σ -methane complex. In other words, no oxidative addition occurs, so no Pt–H bond is formed. Hush indicates the similarities between the two pathways in a DFT study on $(NH_3)_2PtCl_2$ but uses the term σ -bond metathesis similarly for a mechanism where Cl^- remains bonded to Pt during the deprotonation of the weakly coordinated methane.¹⁵⁷

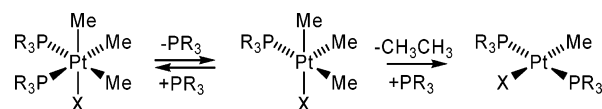
There have been recent reports that Pd and Pt complexes bearing chelating *N,N*-heterocyclic carbene complexes show interesting activities in Shilov-type chemistry.^{170,171} For example, the Pd bis-(carbene) complex with $R = Me$ and $X = Br$ in Scheme 17 catalyzes the conversion of CH_4 (20–30 atm) to CH_3OCOCF_3 in CF_3COOH at 80–100 °C using $K_2S_2O_8$ as the oxidant with at least 30 turnovers. The Pd complexes are stable in this reaction medium, but analogous Pt complexes decompose to Pt black. The *N,N*-heterocyclic carbene ligands have had a major impact on organometallic chemistry and catalysis during the past decade.^{172,173} Insofar as they have hardly been used in Pt-mediated C–H activation chemistry, there appears to be a significant potential for new discoveries with these novel ligand systems.

5. Reactions at Pt Complexes with Phosphine Ligands

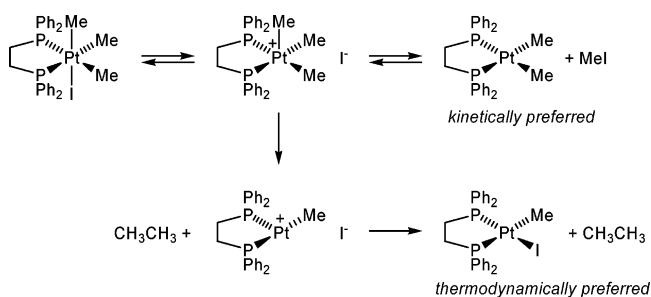
5.1. C–C and C–X Reductive Elimination from Octahedral Pt(IV) Complexes

A considerable part of the current understanding of C–H activation processes stems from investigation of C–H reductive elimination processes. Hydride and alkyl ligands are both σ -donors toward the metal, and therefore, insight gained from studies of C–C and C–heteroatom eliminations is useful.²⁰ The reactivity of octahedral Pt(IV) complexes will be particularly important for us. C–C reductive eliminations from *fac*-(PR_3)₂PtMe₃X complexes have been extensively studied. Inhibition by added phosphine was seen in

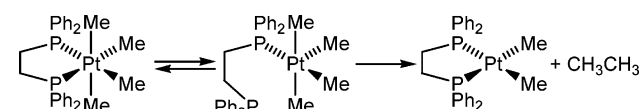
Scheme 18



Scheme 19



Scheme 20



early work, and this is considered to imply a dissociative mechanism in which phosphine dissociation generates a five-coordinate species that is responsible for the reductive elimination (Scheme 18).¹⁷⁴

In accord, chelating diphosphines, which are less prone to dissociation, should lead to reduced reactivity. However, eliminations from *fac*-(diphosphine)-PtMe₃X systems also undergo eliminations by dissociative pathways. In these cases it is the X^- group that dissociates. For example, (dppe)PtMe₃I undergoes dissociative eliminations—elimination of MeI is kinetically preferred but reversible whereas ethane elimination is thermodynamically favored. Both reactions proceed via the same five-coordinate intermediate (Scheme 19).^{13,175} Competing C–O and C–C reductive eliminations from (dppe)PtMe₃OAc, (dppe)-PtMe₃(*O-p*-C₆H₄OMe), and related systems proceed according to similar mechanisms.^{176,177}

C–C elimination also occurs from (diphosphine)-PtMe₄ compounds. In these cases no readily dissociable ligand is present. Nevertheless, it has been concluded that C–C elimination occurs by dissociation of one arm of the diphosphine to generate the five-coordinate species that undergoes elimination (Scheme 20).^{178,179} It appears that no definitive examples of a direct C–C coupling from octahedral Pt(IV) alkyl complexes have been reported to date.

With the above experimental findings in mind and considering the many similarities between alkyl and hydride ligands—both being σ donors with strong trans influence properties—one might anticipate dissociative C–H elimination reactions to be prevalent for Pt(IV) alkyl hydrides. However, C–H eliminations are generally more facile than C–C eliminations, and therefore, there is a definite possibility that a direct elimination pathway may be available, in particular for systems that have no easily dissociated ligand.¹⁸⁰

5.2. C–H Reductive Elimination from Pt(II)

There are relatively few reported stable Pt(II) hydridoalkyl complexes, and consequently, alkane

elimination from Pt(II) has not been extensively studied. The first demonstration of an intramolecular alkane elimination from a *cis*-hydridoalkyl complex was reported by Halpern and co-workers.¹⁸⁰ The formation of methane from *cis*-(PPh₃)₂Pt(H)(CH₃) at –25 °C was shown to be intramolecular by a crossover experiment. The rate of methane loss ($4.5 \pm 0.5 \times 10^{-4} \text{ s}^{-1}$) was unaffected by addition of PPh₃, which however trapped the Pt fragment to cleanly yield Pt(PPh₃)₃. A normal k^H/k^D isotope effect of 3.3 ± 0.3 was determined for the reaction of (PPh₃)₂Pt(H)(CH₃) vs (PPh₃)₂Pt(D)(CD₃). These results were interpreted in terms of rate-limiting reductive elimination. Electronic effects on the methane elimination were investigated with a series of *cis*-(PAr₃)₂Pt(H)(CH₃) complexes (Ar = *p*-XC₆H₄; X = Cl, H, Me, MeO). The observed rate decreased by a factor of almost 20 through the series, which correlates with the relative abilities to stabilize the low Pt(0) oxidation state. For *cis*-(PPh₃)₂Pt(H)(R') compounds the elimination rate decreased in the series R' = Ph, Et, Me, vinyl. Normal KIEs for reductive elimination from Pt(II) alkyl hydride phosphine complexes have also been reported for the more stable *cis*-(PPh₃)₂Pt(H)(CH₂CF₃)¹⁸¹ ($k^H/k^D = 2.2$) and (dcpe)Pt(H)(CH₂CMe₃)¹⁸² ($k^H/k^D = 1.5$). The normal isotope effects imply a rate-limiting reductive cleavage rather than alkane elimination when considered with the background on kinetic isotope effects that was given in section 2.6.^{83,109} Small values of ΔS^\ddagger for elimination from *cis*-(PPh₃)₂Pt(H)(CH₂CF₃) ($21 \pm 8 \text{ J K}^{-1} \text{ mol}^{-1}$) and from (dcpe)Pt(H)(CH₂CMe₃) ($21 \pm 4 \text{ J K}^{-1} \text{ mol}^{-1}$) are clearly in accord with nondissociative processes.

The nondissociative nature of these elimination reactions has been confirmed by recent DFT-B3LYP computational studies on *cis*-(PH₃)₂Pt(H)(CH₃)¹⁸³ and *cis*-(PMe₃)₂Pt(H)(CH₃)¹⁸⁴ model systems. The three-coordinate species (PR₃)Pt(H)(CH₃) have a considerably lower barrier toward methane elimination (producing an η^2 -(H,H) σ -methane complex) than (PR₃)₂Pt(H)(CH₃) (which yields a weakly bonded CH₄ adduct with $d(\text{Pt}\cdots\text{HCH}_3)$ of 3.31 Å). However, the high energy cost of PR₃ predissociation rendered the dissociative pathway considerably less favorable by 32 and 40 kJ/mol for the two ligand systems (Figure 5). The experimentally determined activation energy $\Delta G^\ddagger_{248\text{K}} = 78 \text{ kJ/mol}$ for *cis*-(PR₃)₂Pt(H)(CH₃)¹⁸⁰ (calculated from the rate constant given) agrees well with DFT-computed values for *cis*-L₂Pt(H)(CH₃), $\Delta G^\ddagger_{248\text{K}} = 69$ and 82 kJ/mol for L = PH₃ and PMe₃, respectively.

5.3. C–H Activation at Pt(0) Complexes

The transient (PR₃)₂Pt⁰ fragments that result from the alkane eliminations discussed above are capable of oxidatively adding hydrocarbon C–H bonds. In particular, (dcpe)Pt⁰ has been generated in situ by the above-mentioned reductive elimination of neopentane from (dcpe)Pt(CH₂CMe₃)(H) and has been particularly well studied.¹⁸² The (dcpe)Pt⁰ fragment is not stable but can be trapped with diphenylacetylene or added dcpe. In the presence of benzene, (dcpe)Pt(C₆H₅)(H) is quantitatively formed. Reductive elimination of neopentane was inferred to be the rate-

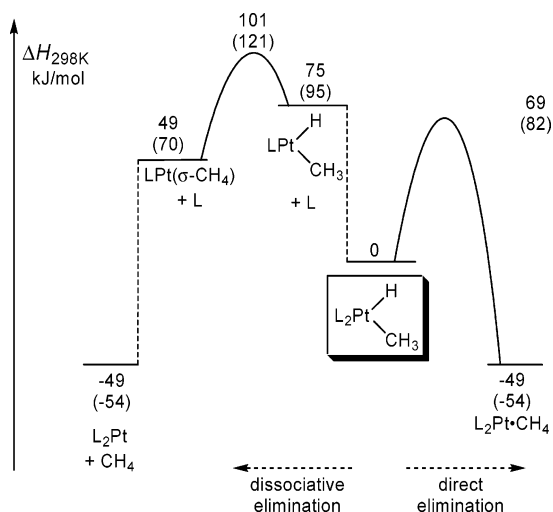
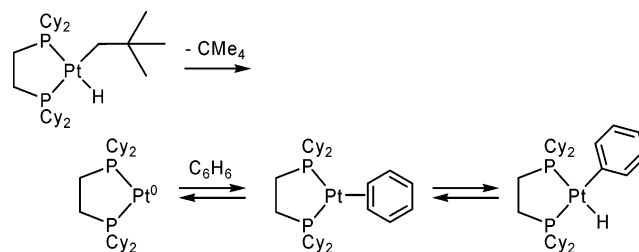


Figure 5. Energy diagram for dissociative and direct methane elimination from *cis*-L₂Pt(H)(CH₃) with L = PH₃ and PMe₃ (in parentheses).

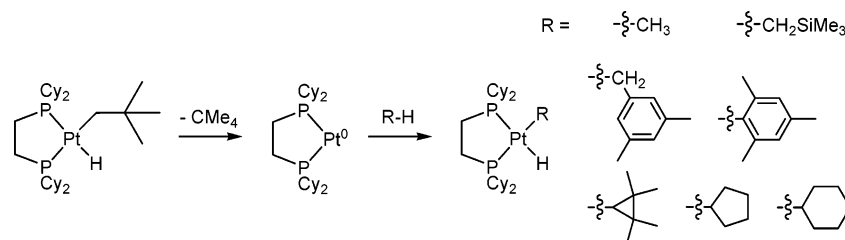
Scheme 21



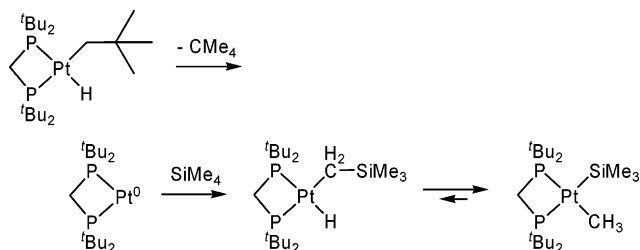
limiting step for the overall reaction on the basis of observed first-order kinetics, indistinguishable rates for C₆H₆ and C₆D₆ activation, and a kinetic isotope effect ($k^H/k^D = 1.5$) for reductive elimination of (dcpe)Pt(CH₂CMe₃)(D). No H/D exchange involving the methylene or methyl groups of the neopentyl ligand was seen during thermolysis of (dcpe)Pt(CH₂CMe₃)(D), mitigating against metalation of the neopentyl ligand to access Pt(IV) intermediates. No D from C₆D₆ was incorporated into the neopentane. D scrambling into the hydride site was observed by ²H NMR during thermolysis of (dcpe)Pt(C₆D₅)(H) in C₆H₆, suggesting that η^2 -benzene intermediates are involved. Exchange with the solvent C₆H₆ was also seen. It is likely that η^2 -benzene complex formation precedes benzene activation, although this was not rigorously proven. Scheme 21 summarizes the mechanism of these reactions.

A range of other hydrocarbons with alkyl, aryl, benzyl, or trimethylsilyl C–H bonds add to in-situ-generated (dcpe)Pt⁰ (Scheme 22) with highly variable yields.¹⁸⁵ Reaction with alkynes and alkenes mainly produces coordination complexes. When (dcpe)Pt(CH₂CMe₃)(H) was thermolyzed in the presence of mesitylene, products of aromatic and benzylic activation were formed with an 85:15 kinetic preference for aromatic C–H activation. Upon prolonged heating in mesitylene at 69 °C, the two products isomerized to give a 46:54 mixture of aromatic and benzylic products, which translates to a 0.4 kJ/mol thermodynamic preference for the sterically less hindered benzylic product. Independently synthesized samples of the two also equilibrated in mesitylene but not in

Scheme 22



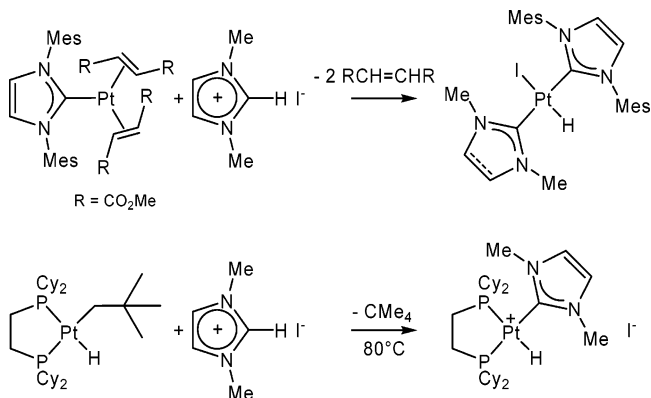
Scheme 23



benzene-(dcpe)Pt(C₆H₅)(H) formed instead. These findings suggest that the mechanism of isomerization between the aromatic and benzylic activation products does not involve a cyclometalated Pt(IV) intermediate but rather proceeds by reductive elimination of mesitylene followed by re-addition of mesitylene by aryl or benzylic C–H bond activation. Addition of benzene solvent then competes favorably with the re-addition of mesitylene. The driving force for an aromatic preference, in the absence of overriding steric effects, is normally a stronger Pt–C(aryl) than Pt–C(benzylic) bond. A kinetic preference for aromatic activation but thermodynamic preference for benzylic activation was recently reported in a cationic (diimine)Pt system (section 6.6); in this case the benzylic preference was attributed to η^3 coordination of the benzylic moiety.¹⁸⁶

MO calculations¹⁸⁷ suggest that a smaller P–Pt–P bite angle leads to increased reactivity of the P₂Pt⁰ moiety toward C–H and C–X bonds. Thus, a highly strained system (dtbpm)Pt(CH₂CMe₃)(H) with a P–Pt–P angle of 74.7° was prepared.¹⁸⁸ The reactive intermediate (dtbpm)Pt⁰ was trapped as stable alkyne or olefin adducts after room-temperature elimination of neopentane. Surprisingly, heating (dtbpm)Pt(CH₂CMe₃)(H) in benzene did not lead to C–H activation but instead produced a dimer of the alkyl hydride. Independently prepared (dtbpm)Pt(C₆H₅)(H) was stable under the reaction conditions. Heating (dtbpm)Pt(CH₂CMe₃)(H) in neat SiMe₄ produced (dtbpm)Pt–(SiMe₃)(Me) by selective cleavage of a Si–C bond (Scheme 23). The Si–C bond cleavage is believed to occur by prior C–H activation to yield an intermediate (dtbpm)Pt(CH₂SiMe₃)(H) which was not observed during the reaction. However, independently prepared (dtbpm)Pt(CH₂SiMe₃)(H) underwent smooth isomerization to the thermodynamically more stable (dtbpm)Pt(SiMe₃)(Me). Labeling studies demonstrated that the isomerization occurred intramolecularly and without elimination of Me₄Si. Isomerization of (dtbpm)Pt(CH₂SiMe₃)(D) selectively produced (dtbpm)Pt(SiMe₃)(CH₂D) with no evidence for D incorporation into the Si–Me groups. Remarkably, this C–H/Si–C activation occurs even in the presence of

Scheme 24



benzene. This unprecedented reactivity toward the Me₄Si sp³ C–H bonds in a system that does not activate benzene C–H bonds is quite surprising. The mechanism of this isomerization is not known, but the reaction does show a close resemblance with recent Me₄Si C–H activating cationic Pt(II) diimine systems^{134,189} (see section 6.7).

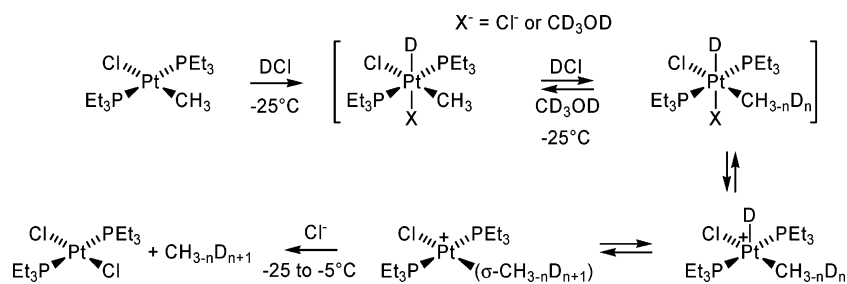
A comparison of the reactivity of bent (dcpe)Pt⁰ with that of linear bis(phosphine) Pt(0) complexes led to the suggestion that these complexes may serve as models for *edge* and *terrace* atoms in heterogeneous catalysts, respectively.^{182,185} The latter were thought to be completely unreactive with respect to hydrocarbon addition,^{190,191} but opposite claims¹⁹² have since been made for Pt systems.

An *N*-heterocyclic carbene Pt(0) alkene complex has recently been shown to activate C–H bonds of imidazolium salts to yield isolable Pt(II) bis(carbene) compounds.¹⁹³ The reaction is complete within 1 h in refluxing THF or acetone. Comparing the reactivity of the Pt(0) carbene with (dcpe)Pt⁰ toward imidazolium salts, it was shown that the former is more efficient in the C–H bond activation (Scheme 24). The mechanism of these reactions has not been investigated in detail, but the established C–H acidity of imidazolium salts^{194–196} suggests that initial proton transfer toward a neutral and presumably quite basic Pt center may be operative.

5.4. Protonation of Pt(II) and Reductive Elimination from Pt(IV) Complexes with Labile Anionic Donors

As discussed above, methane elimination from neutral Pt(II) hydridoalkyl complexes (PR₃)₂Pt(H)–(CH₃) proceeds without prior phosphine dissociation. The situation is quite different for octahedral Pt(IV) complexes (PR₃)₂Pt(H)(CH₃)(X)(Y) with a strong predominance for dissociative processes, although a

Scheme 25

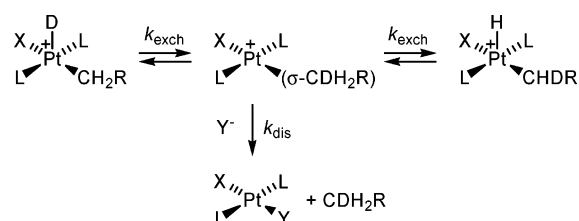


limited number of apparently nondissociative processes have been documented.

Several studies have served to provide a detailed understanding of the mechanism of protonation of (PEt₃)₂Pt(Me)Cl and closely related systems. Protonations have been proposed to occur directly at the metal, by electrophilic attack at the Pt–C bond, or by a concerted (σ -bond metathesis) pathway,^{138,197–201} interestingly, the current view (Scheme 25) is in essence a slightly modified form of the initial mechanism proposed by Belluco et al.¹⁹⁸ The Pt(IV) phosphine complex (PEt₃)₂PtCl₂(Me)(H) was obtained from (PEt₃)₂Pt(Me)Cl and HCl at –78 °C and eliminated methane at –45 °C in CD₂Cl₂.⁸⁴ Addition of DOTf to (PEt₃)₂Pt(Me)Cl in CD₃OD produced no observable hydride, but slow generation of (PEt₃)₂PtCl₂ was accompanied by production of all methane isotopomers in solution; multiple D incorporation into unreacted Pt–methyl was also seen. In the absence of added chloride, full D incorporation took place prior to methane loss (Scheme 25). Addition of chloride caused methane elimination to compete with D incorporation. The rate of H/D exchange was first-order-dependent on [Cl⁻] but with a nonzero positive intercept of k_{obs} vs [Cl⁻] ($\Delta H^\ddagger = 61 \pm 6 \text{ kJ mol}^{-1}$, $\Delta S^\ddagger = -62 \pm 19 \text{ J K}^{-1} \text{ mol}^{-1}$, $k^{\text{H}}/k^{\text{D}} = 0.80 \pm 0.05$ at –27 °C). The rate of protonolysis (methane elimination) was first-order-dependent on [Cl⁻] with a zero intercept of k_{obs} vs [Cl⁻] ($\Delta H^\ddagger = 70 \pm 3 \text{ kJ mol}^{-1}$, $\Delta S^\ddagger = -52 \pm 11 \text{ J K}^{-1} \text{ mol}^{-1}$, $k^{\text{H}}/k^{\text{D}} = 0.11 \pm 0.02$ at –12 °C). The mechanism in Scheme 25 appears to accommodate the findings.⁸⁴ An initial solvent- or chloride-assisted protonation generates the six-coordinate Pt(IV) hydride. Dissociation of the solvent or chloride provides the five-coordinate species that after reductive coupling gives the σ -methane species that is responsible for the H/D exchange. This exchange is reversible in the absence of chloride; excess chloride facilitates the rate-limiting methane elimination. This suggests that methane elimination from the cationic σ -methane intermediate is an associative process with chloride acting as the nucleophile. A corollary, given by the principle of microscopic reversibility, is that if C–H activation were to occur in this system, methane would enter the coordination sphere of Pt in an associative fashion, despite the fact that methane is an exceptionally poor nucleophile!

Complexes *trans*-(PEt₃)₂Pt(CH₂R)Cl (CH₂R = Et, CH₂Ph) also undergo H/D exchange into the alkyl α position (not into the β position for CH₂R = Et) in CD₃OD/D⁺ without observable Pt(IV) hydride intermediates.²⁰² The rates of H/D exchange decreased in the order Et > Me > CH₂Ph, which is the same order

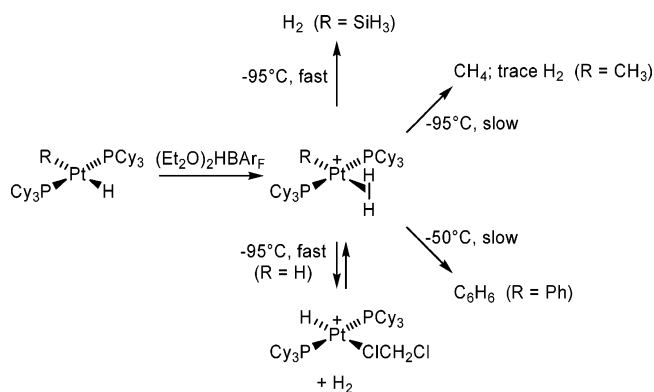
Scheme 26



as that for alkane elimination.¹⁹⁷ The neopentyl complex (CH₂R = CH₂tBu) did *not* incorporate D into the CH₂ group but did release neopentane-*d*₁ at –23 °C. The extent of α -D incorporation will depend on the relative rates of the exchange process (hence on the energy of the alkane σ complex) and the loss of alkane (k_{exch} and k_{dis} in Scheme 26; simplified by showing only first H/D exchange and disregarding isotope effects). The properties of the nonobservable alkane complexes are not straightforwardly assessed. However, the similarities in trends of rate of D incorporation and alkane loss suggest that for the Pt–Et/Me/CH₂Ph series the relative rates of the two key processes are affected in the same direction when R is altered. For Pt–CH₂tBu, the alkane dissociation must be fast relative to the H/D exchange via the σ complex. The trans influence of the X group (Scheme 26) should considerably affect the rate of alkane loss (a strong trans influence might also increase the rate of reductive coupling, and hence H/D exchange rate, through a Pt–CH₂R bond weakening effect). In accord, *cis* bis(phosphine) complexes (depe)PtMe₂ and *cis*-(P(OMe)₃)₂Pt(Cl)Me as well as *trans*-(PEt₃)₂Pt(I)Me give only CH₃D upon deuteriolysis whereas *trans*-(PEt₃)₂Pt(Cl)Me, *trans*-(PEt₃)₂Pt(Br)Me, and (tmeda)PtMe₂ give multiple exchange, all in accord with the standard trans influence series PR₃ > I⁻ > Br⁻ > Cl⁻ > amine.

Whereas protonolysis of *trans*-(PEt₃)₂Pt(Me)X (X = Cl, Br) led to multiple D incorporation in CD₃OD/DOTf and proceeded at greater rates in CD₃OD than in CD₂Cl₂, the initially surprising finding was that H/D exchange did not occur and protonolysis reactions were slower in methanol for X = OTf, F, NO₃. The key to understanding this is that the latter more weakly bonded ligands completely dissociate in methanol to give the cationic solvento complex *trans*-(PEt₃)₂Pt(Me)(MeOH)⁺. By virtue of its positive charge, this species is more difficult to protonate than the neutral species, and the hydridoalkyl complex that must be accessed in order to achieve H/D exchange as well as methane elimination is more slowly formed. In other words, the rate-limiting step is the protonation rather than the methane elimination as it is for X =

Scheme 27



Cl (Scheme 25) and Br. On the other hand, the triflate complex is protonated in CD_2Cl_2 to reversibly give *trans,cis*-(PEt_3) $_3\text{Pt}(\text{CH}_3)(\text{H})(\text{OTf})_2$, which eliminated methane at room temperature; DOTf in this case provided a mixture of isotopomers. The triflate ligand, as expected, exerts a weak σ -methane labilizing effect.²⁰²

Studies of the protonation of a variety of *trans*-(PCy_3) $_2\text{Pt}(\text{H})(\text{X})$ complexes revealed that there are three thermodynamic sites of proton attack: hydride, platinum, or the *trans* ligand X, depending on the nature of X and the resulting basicity of the *trans* hydride.²⁰³ Relative stabilities of observable $\eta^2\text{-H}_2$ complexes *trans*-(PCy_3) $_2\text{Pt}(\text{X})(\text{H}_2)^+$, which have large $^1J_{\text{H-D}}$ values for the HD isotopomers (indicative of a rather unactivated H–H bond), lend further support to the suggested labilization of the σ complex by the *trans* ligand. Protonation of *trans*-(PCy_3) $_2\text{Pt}(\text{SiH}_3)(\text{H})$ with $\text{H}(\text{Et}_2\text{O})_2\text{BAR}_F$ at -95°C in CD_2Cl_2 immediately liberated H_2 . Under the same conditions *trans*-(PCy_3) $_2\text{Pt}(\text{H})(\text{CH}_3)$ is reversibly protonated to give *trans*-(PCy_3) $_2\text{Pt}(\eta^2\text{-H}_2)(\text{CH}_3)^+$, which gradually eliminated CH_4 and small quantities of H_2 . The reaction of *trans*-(PCy_3) $_2\text{Pt}(\text{D})(\text{CH}_3)$ with a large excess of $\text{HBAR}_F/\text{DBAR}_F$ in CH_2Cl_2 at -60°C furnished CH_3D and CH_4 and no evidence for multiple H/D exchange; the methane isotopomer ratios led to an estimated $k^{\text{H}}/k^{\text{D}} = 2.5 \pm 0.4$ for protonolysis of the Pt– CH_3 bond. The phenyl analogue *trans*-(PCy_3) $_2\text{Pt}(\text{H})(\text{Ph})$ gave a dihydrogen complex *trans*-(PCy_3) $_2\text{Pt}(\eta^2\text{-H}_2)(\text{Ph})^+$ from $\text{H}(\text{Et}_2\text{O})_2\text{BAR}_F$; benzene was liberated at -50°C with no indication of H_2 . On the other hand, when *trans*-(PCy_3) $_2\text{Pt}(\text{H})(\text{Ph})$ was treated with HCl at -80°C , H_2 was rapidly produced along with *trans*-(PCy_3) $_2\text{Pt}(\text{H})(\text{Cl})$; the H_2 ligand in *trans*-(PCy_3) $_2\text{Pt}(\eta^2\text{-H}_2)(\text{Ph})^+$ was immediately replaced with chloride at -80°C .²⁰³ Protonation of *trans*-(PCy_3) $_2\text{PtH}_2$ with $\text{H}(\text{Et}_2\text{O})_2\text{BAR}_F$ yielded *trans*-(PCy_3) $_2\text{Pt}(\eta^2\text{-H}_2)(\text{H})^+$, which was in equilibrium with H_2 and the dichloromethane solvate; when generated from HOTf, *trans*-(PCy_3) $_2\text{Pt}(\eta^2\text{-H}_2)(\text{H})^+$ irreversibly lost H_2 at -95°C . HCl provided *trans*-(PCy_3) $_2\text{Pt}(\text{Cl})(\text{H})$ and H_2 with no observable dihydrogen precursor at -95°C . In summary (Scheme 27), the rate of H_2 loss from these complexes correlates with the *trans* influence of X ($\text{SiH}_3 > \text{H} \approx \text{CH}_3 > \text{Ph}$). Furthermore, the combined data suggest that displacement of H_2 by chloride from *trans*-(PCy_3) $_2\text{Pt}(\eta^2\text{-H}_2)(\text{X})^+$ (X = H, Me, Ph) proceeds associatively. (An alternative explanation, preequilibrium dissociation of H_2 followed by rate-limiting

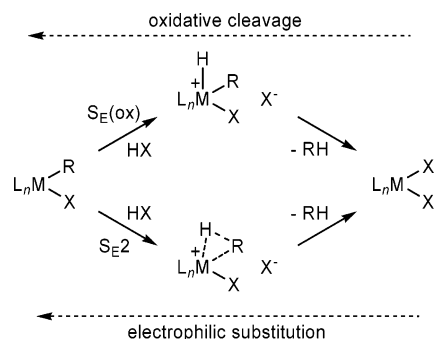
trapping by chloride, cannot be ruled out).²⁰³ The mechanism of proton transfer from H_2 to R ligand in forming the CH_4 and C_6H_6 products is not established. Of potential relevance, these and other known Pt(II) dihydrogen complexes have not shown signs of being in equilibrium with the Pt(IV) dihydride tautomers.^{204–206} For example, a 75 kJ mol^{-1} energy difference has been calculated between $(\text{PH}_3)_2\text{Pt}(\text{H}_2)\text{-H}^+$ (most stable) and $(\text{PH}_3)_2\text{PtH}_3^+$; in $(^t\text{Bu}_3\text{P})_2\text{Pt}(\text{H})(\text{H}_2)^+$ there is no sign of intramolecular H/ H_2 scrambling by NMR even at room temperature. The large $^1J_{\text{H-D}}$ value of 34.7 Hz suggests an H–H bond with little back-bonding and therefore negligible H–H bond weakening.²⁰⁵

When *trans*-(PCy_3) $_2\text{Pt}(\text{H})(\text{Ph})$ is treated with MeOTf in CD_2Cl_2 , methane is liberated at -45°C .²⁰³ There was no mention of the identity of the Pt-containing product or any observable intermediates. The apparently selective formation of methane rather than benzene contrasts with the mixture (ca. 80:20) that results from protonation of (diimine)Pt(Me)(Ph) complexes^{103,207} (section 6.5).

More electrophilic Pt centers are available using the *dfep*, $(\text{C}_2\text{F}_5)_2\text{PCH}_2\text{CH}_2\text{P}(\text{C}_2\text{F}_5)_2$, ligand. Whereas donor phosphine complexes $(\text{PR}_3)_2\text{PtMe}_2$ react with HOTf to give $(\text{PR}_3)_2\text{Pt}(\text{OTf})_2$,^{202,208} (*dfep*)PtMe $_2$ undergoes protolytic cleavage of only one Pt–Me bond to give (*dfep*)Pt(Me)(OTf) at ambient temperature²⁰⁹ and without detectable (*dfep*)Pt(Me)(H)(OTf) $_2$ intermediates. Heating at 100°C for 15 min in neat HOTf (!) is required to form (*dfep*)Pt(OTf) $_2$ from the methyl triflate precursor.²¹⁰ The (*dfep*)Pt moiety of the bis(triflate) is remarkably robust even in superacid media, reminiscent of the Catalytica catalyst (see section 4),¹⁶⁴ and provides a source of “(*dfep*)Pt $^{2+}$ ” in SbF_5 and $\text{SbF}_5/\text{HSO}_3\text{F}$.²¹⁰ Only monodeuterated methane was detected when DOTf was reacted with (*dfep*)Pt(Me)(OTf). Protonolysis of (*dfep*)Pt(Me)(OCOCF $_3$) with CF_3COOD led to some D incorporation into Pt–methyl and produced some CH_2D_2 and CHD_3 in addition to CH_3D . It was concluded that this exchange was *not* a consequence of the normal scrambling via reversible protonation and σ -methane complex formation but rather was catalyzed by heterogeneous Pt decomposition products *prior* to protonolysis. Some caution is therefore warranted when similar H/D scrambling effects are investigated and mechanistically interpreted.²¹⁰

Ambiguities existed regarding whether the protonolysis of (*dfep*)Pt(Me)(OTf) and (*dfep*)Pt(Me)(OCOCF $_3$) occurred at Pt (oxidative addition, or $\text{S}_{\text{E}}(\text{ox})$ mechanism) or at the Pt–C bond (concerted $\text{S}_{\text{E}}2$ mechanism, corresponding to reverse of C–H activation by electrophilic substitution), Scheme 28. In the presence of excess HOTf, NMR data for (*dfep*)Pt(Me)(OTf) suggested hydrogen bonding between Pt–OTf and HOTf, but no other intermediates were seen. Puddephatt and co-workers²⁰¹ noted a contrasting selectivity of mixed $\text{Au}^{\text{III}}(\text{alkyl})(\text{aryl})$ and $\text{Pt}^{\text{II}}(\text{alkyl})(\text{aryl})$ complexes toward protonolysis: $k_{\text{Au-R}}/k_{\text{Au-Ar}} \ll 1$ and $k_{\text{Pt-R}}/k_{\text{Pt-Ar}} \gg 1$. It was proposed that relative $k_{\text{M-Me}}$ and $k_{\text{M-Ph}}$ rates might be used to distinguish between the protonation pathways: $\text{S}_{\text{E}}(\text{ox})$ if $k_{\text{M-Me}}/k_{\text{M-Ph}} \gg 1$ and $\text{S}_{\text{E}}2$ if $k_{\text{M-Me}}/k_{\text{M-Ph}} \ll 1$. The rationale for this would be (a) $\text{S}_{\text{E}}(\text{ox})$ should be generally

Scheme 28

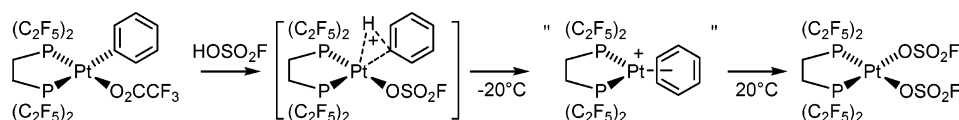


preferred for M–Me vs M–Ph with other factors being equal and (b) S_E2 is promoted via a charge-delocalized Wheland-type intermediate. For Au(III) the $S_E(\text{ox})$ mechanism is unlikely because of the unavailable +5 oxidation state, and an S_E2 mechanism is consistent with the observations. The reverse applies to Pt(II), where Pt(IV) is usually accessible. The analysis is rather simplistic today considering current knowledge of possible differences in rate-limiting steps even for a “straightforward” metal protonation—proton transfer, reductive coupling, associative or dissociative alkane dissociation—but nevertheless offers an interesting diagnostic tool.

The kinetics of the protonation of (dfep)Pt(R)(OCOCF₃) was investigated for R = Me, Ph, CH₂-Ph.²¹¹ Protonolysis in neat TFE proceeded to give (dfep)Pt(OCOCF₃)₂ in all cases. However, the phenyl complex underwent complete reaction within hours at 20 °C, whereas the methyl and benzyl species required hours at 150 °C, and it was concluded that the (dfep)Pt(R)(X) compounds most likely undergo protonolysis by the S_E2 mechanism. Protonolysis of (dfep)Pt(Ph)(OCOCF₃) or addition of benzene to a solution of (dfep)Pt(OCOCF₃)₂ or the analogous bis(triflate) species in FSO₃H at –70 °C led to detection of a species formulated as (dfep)Pt(η^6 -C₆H₆)²⁺ (Scheme 29). The spectroscopic data do not appear to distinguish between the proposed η^6 -C₆H₆ bonding mode, a fluxional η^4 -C₆H₆ mode (which would give a more conventional square-planar Pt(II) species), and a fluxional (dfep)Pt(η^2 -C₆H₆)(OSO₂F)⁺ species. An analogous species is *not* seen when (dfep)Pt(Me)(OSO₂F) is treated with benzene in FSO₃H.

The properties of Pt complexes of dfep have been recently compared with fluorinated monophosphine complexes.²¹² Whereas (dfep)PtMe₂ resists H₂ up to 150 °C, *cis*-(PMe(C₂F₅)₂)₂PtMe₂ slowly reacts with H₂ to form methane and Pt(PMe(C₂F₅)₂)₄ at ambient temperature, presumably via phosphine dissociation and H₂ addition. The monomethyl complexes *trans*-(PMe(C₂F₅)₂)₂Pt(Me)(X) readily form upon dissolution in neat HX (X = OTf, OCOCF₃, OSO₂F), and prolonged heating furnishes *cis*-(PMe(C₂F₅)₂)₂PtX₂. A kinetic isotope effect for the protonation of the methyl triflate species was measured in HOTf vs DOTf with

Scheme 29

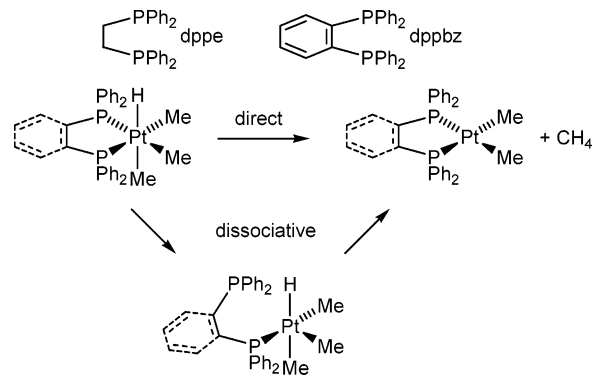


$k^H/k^D = 2.7$, identical to the value for (dfep)Pt(Me)(OTf). Interestingly, deuteriolysis of *trans*-(PMe(C₂F₅)₂)₂Pt(Me)(OCOCF₃) with CF₃COOD led to complete deuterium incorporation into remaining Pt–methyl within 15 min at 150 °C and generation of CH₃D and CH₂D₂ (CHD₃ was not mentioned).²¹² Deuteration of the methyl ligand in the triflate analogue occurred under milder conditions. Reversible protonation and methane σ -complex formation appears to be accessible for this system, in contrast to the dfep system. This difference is readily understood since the σ -CH₄ ligand in the dfep complex will be labilized as it must be *trans* to a strong *trans* influence phosphine group, whereas in the bis-(monophosphine) system the σ -CH₄ ligand is less labile as it will be *trans* to the much weaker *trans* influence triflate or trifluoroacetate groups.

5.5. C–H Reductive Elimination from Pt(IV) Complexes without Labile Anionic Ligands

The only thoroughly studied alkyl–H reductive eliminations from neutral Pt(IV) complexes without dissociable “X” ligands appear to be those of *fac*-(dppe)PtMe₃H and *fac*-(dppbz)PtMe₃H.¹⁷⁹ Methane elimination occurs from both complexes at ambient temperature (Scheme 30). The kinetic parameters

Scheme 30



were essentially identical for both: k_{obs} (50 °C) = $(1.3 \pm 0.1) \times 10^{-4} \text{ s}^{-1}$, $\Delta H^\ddagger = 108 \pm 4 \text{ kJ mol}^{-1}$, $\Delta S^\ddagger = 13 \pm 13 \text{ J K}^{-1} \text{ mol}^{-1}$, $k^H/k^D = 2.2$ for *fac*-(dppe)PtMe₃H(D) and k_{obs} (50 °C) = $(1.2 \pm 0.1) \times 10^{-4} \text{ s}^{-1}$, $\Delta H^\ddagger = 111 \pm 2 \text{ kJ mol}^{-1}$, $\Delta S^\ddagger = 25 \pm 8 \text{ J K}^{-1} \text{ mol}^{-1}$, $k^H/k^D = 2.5$ for *fac*-(dppbz)PtMe₃H(D). Thermolysis of the monodeuterides in C₆D₆ yielded CH₃D as the only methane isotopomer. C–C reductive elimination proceeded dramatically faster from (dppe)PtMe₄ than from (dppbz)PtMe₄, which led to the conclusion that C–C elimination was a dissociative process despite the presence of chelating phosphine ligands. The similarities of the kinetic parameters for elimination from the two hydridoalkyl complexes, with very different chelate rigidity, strongly suggest that a chelate opening cannot be operative here and that a

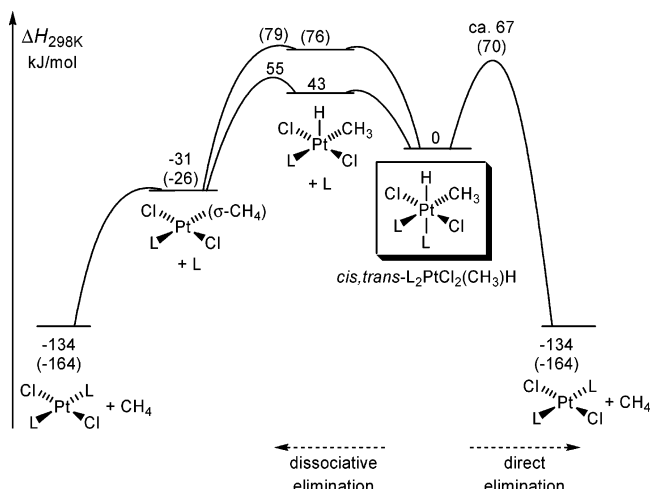


Figure 6. Energy diagram for dissociative and direct methane elimination from *cis,trans*- $L_2PtCl_2(H)(CH_3)$ with $L = PH_3$ and PMe_3 (in parentheses).

direct elimination occurs. The ΔS^\ddagger values were near zero for C–H elimination, whereas a value of $63 \pm 17 \text{ J K}^{-1} \text{ mol}^{-1}$ was found for C–C elimination (dppe only); this difference is also in accord with the proposed mechanistic change. The isotope effects cannot be used to distinguish the mechanisms but do suggest that C–H reductive coupling, rather than alkane dissociation, is rate limiting. These are the only well-documented cases of a direct C–H reductive elimination from octahedral Pt(IV) complexes, irrespective of charge or supporting ligand types. By the principle of microscopic reversibility, a direct C–H oxidative addition at square-planar Pt(II) should therefore be possible, as suggested by calculations.²¹³

The dissociative vs nondissociative nature of these elimination reactions has, in part, been confirmed by recent DFT-B3LYP computational studies on different stereoisomers of *cis*-(PH_3)₂PtCl₂(H)(CH₃)¹⁸³ and *cis*-(PMe_3)₂PtCl₂(H)(CH₃)¹⁸⁴ model systems. Some essential features for the *cis,trans* isomers are reproduced in Figure 6. A transition state for direct methane elimination was not located for $L = PH_3$ because PH_3 trans to hydride dissociated concomitantly with methane elimination. (Ligand dissociation occurred in concert with C–H coupling for the two other *cis*-phosphine isomers as well). The barrier for a *hypothetical* transition state was estimated at 67 kJ/mol with artificial geometrical constraints. This pathway was disfavored relative to the true dissociative pathway by ca. 13 kJ/mol. The activation energy for elimination starting from the five-coordinate species was only 13 kJ/mol, but the cost of PH_3 dissociation provides an additional enthalpic cost of 43 kJ/mol.¹⁸³ For the more realistic system with $L = PMe_3$, the phosphine is more strongly bonded and transition states for the direct reaction were located. In enthalpy terms, the direct elimination is now slightly favored by 8 kJ/mol relative to the dissociative pathway. It is likely that when entropy contributions are accounted for, dissociative behavior may be expected for bis(monodentate phosphines) and direct elimination may be countered for chelating bis(phosphines).¹⁸⁴ The major contributor for the reversal in preferred elimination pathway between (PH_3)₂-

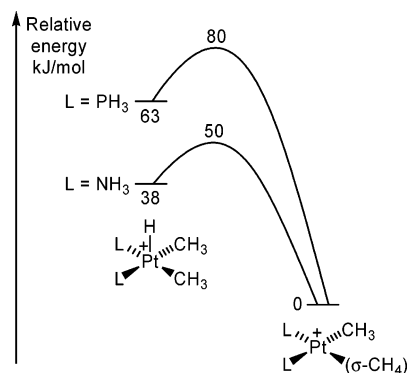


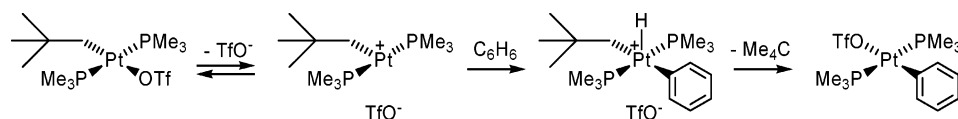
Figure 7. Energy diagram for reductive coupling from *cis*- $L_2PtMe_2H^+$ ($L = PH_3, NH_3$).

Pt(H)(CH₃) and (PH_3)₂PtCl₂(H)(CH₃) is the stronger binding enthalpy of the dissociating PH_3 ligand at Pt(II) than at Pt(IV); the two Cl ligands at Pt(IV) lower the enthalpic cost of phosphine dissociation by 33 kJ/mol.¹⁸³ For PMe_3 the corresponding binding enthalpies at Pt(II) and Pt(IV) differ by only 19 kJ/mol, possibly because of the steric repulsions with the Cl ligands that are *cis* disposed relative to PMe_3 .¹⁸⁴

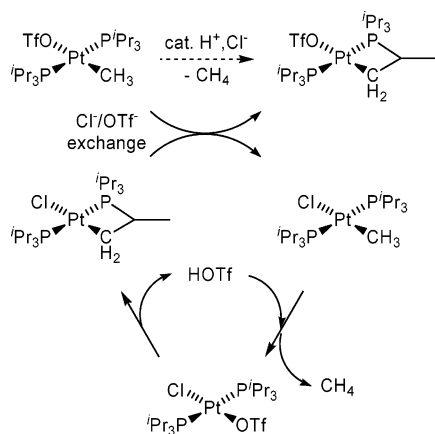
Calculations on elimination from five-coordinate *cis*-(PH_3)₂Pt(Cl)(H)(CH₃)⁺, derived from (PH_3)₂PtCl₂(H)(CH₃) by dissociation of Cl[−] rather than PH_3 (see above), were also reported. The square-pyramidal structure with H apical was enthalpically preferred over that with CH₃ apical by 5 kJ/mol. An almost barrier-free reductive coupling was predicted from the H-apical isomer to give *cis*-(PH_3)₂Pt(Cl)(σ -CH₄)⁺ with methane bonded in an η^2 -(H,H) fashion.¹⁸³ The calculated methane binding enthalpy in *cis*-(PH_3)₂Pt(Cl)(σ -CH₄)⁺ was 40 kJ/mol, significantly stronger than 15 kJ mol^{−1} in (PH_3)₂PtCl₂(σ -CH₄), presumably reflecting the effect of the positive charge in the former.

The reductive elimination of methane and ethane from five-coordinate model complexes $L_2PtMe_2H^+$ and $L_2PtMe_3^+$ ($L = NH_3, PH_3$) and the microscopic reverse oxidative additions have been investigated by DFT calculations.²¹⁴ The five-coordinate Pt(IV) species were found to prefer a square-pyramidal geometry with the L ligands *cis* disposed and a “pinched” trigonal-bipyramidal structure with the two L ligands *trans*. The four-coordinate alkane complexes preferred the *trans* arrangement of the two L groups. C–H reductive eliminations were predicted to be easier than C–C reactions for $L = NH_3$ and PH_3 , and differences in activation barriers for C–H vs C–C reactions were relatively insensitive to the identity of L. However, barriers for both types of oxidative additions were considerably lower for $L = NH_3$ than PH_3 , consistent with the general view that N-based ligands are able to stabilize the Pt(IV) oxidation state better than P-based ligands (Figure 7).^{215,216} C–H reductive eliminations resulted in Pt(II) σ -methane complexes that preferred to have the weakly bonded alkane *trans* disposed with respect to the high *trans* influence H or CH₃ ligands. The σ -alkane species were invariably more stable than the Pt(IV) precursors, the exothermicity of the C–H coupling being greatest for $L = NH_3$. The implied instability of

Scheme 31



Scheme 32



pentacoordinate Pt(IV) is a manifestation of the experimental fact that stable Pt(IV) hydrides are almost invariably stabilized by a sixth ligand.²¹⁷

5.6. C–H Activations at Cationic Pt(II) Phosphine Complexes

When *trans*-(Me₃P)₂Pt(CH₂CMe₃)(OTf)—assumed to have a covalently bonded triflate ligand—is heated in C₆D₆ at 133 °C, loss of neopentane-*d*₁ with concomitant C–D activation of C₆D₆ yielding *trans*-(Me₃P)₂Pt(C₆D₅)(OTf) is the dominant reaction.²¹⁸ An observed inhibition of the reaction rate by addition of Bu₄N⁺OTf[−] suggests that triflate dissociates prior to the rate-limiting step. Addition of Bu₄N⁺BF₄[−] on the other hand increases the rate, presumably due to enhanced triflate dissociation caused by the increased ionic strength. A large normal kinetic isotope effect was observed ($k^H/k^D = 20 \pm 6$; the authors were not confident about the magnitude as many uncertain assumptions were made). Substituting toluene for benzene yielded *trans*-(Me₃P)₂Pt(*m*-tolyl)(OTf) and *trans*-(Me₃P)₂Pt(*p*-tolyl)(OTf) in a 65:35, near statistical, ratio. No *o*-tolyl or benzyl products were observed. This lack of selectivity along with indistinguishable rates for benzene and toluene activation suggest that there is insignificant positive charge localization on the aromatic ring. These findings suggest that after the triflate dissociation a Wheland-type intermediate of an electrophilic substitution pathway cannot be involved in the product-determining or rate-limiting step. The authors concluded that an oxidative addition pathway is more likely (Scheme 31).

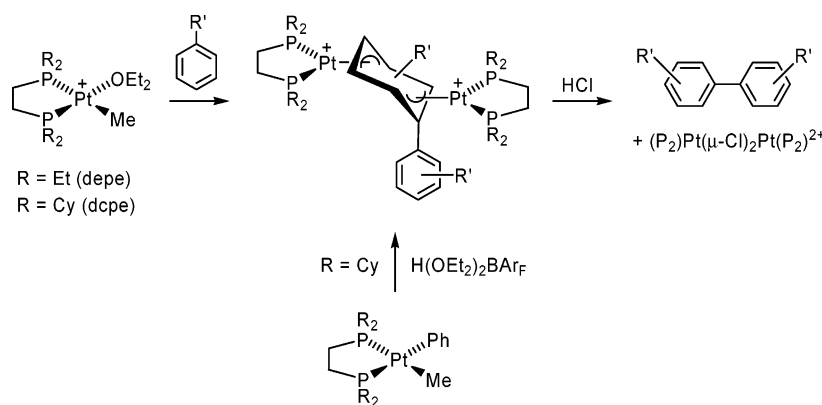
Thorn reported that *trans*-(P^{*i*}Pr₃)₂Pt(Me)(OTf) is robust for days in CD₂Cl₂ at ambient temperature.²¹⁹ Addition of catalytic amounts of HCl causes an efficient catalytic cyclometalation of a phosphine ligand with concomitant expulsion of methane (Scheme 32, top). This reaction does not occur in the presence of chloride alone or triflic acid alone. The catalytic cycle in Scheme 32 was proposed to account for all observations. When the reactant (P^{*i*}Pr₃)₂Pt(Me)(OTf) is not

efficiently protonated by HOTf, this may be attributed to the weak trans influence of the triflate ligand. The Cl[−]/OTf[−] ligand exchange produces (P^{*i*}Pr₃)₂Pt(Me)(Cl), which is more susceptible to protonation followed by methane loss to give (P^{*i*}Pr₃)₂Pt(Cl)(OTf). The chloride might enhance this step by facilitating the protonation event as well as labilizing the trans-located methane in an intermediate σ -methane complex; chloride might even associatively assist the methane displacement (cf. the discussion of *trans*-(PEt₃)₂Pt(Me)(Cl) in section 5.4). Cyclometalation occurs from (P^{*i*}Pr₃)₂Pt(Cl)(OTf), possibly by prior triflate dissociation, and results in the cyclometalated Pt–Cl complex, which initiates another catalytic cycle. The authors favored an electrophilic mechanism for the C–H activating cyclometalation step, although the data appear to be entirely compatible with an oxidative addition mechanism.

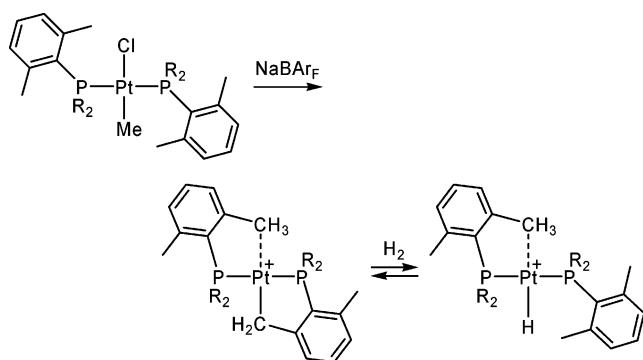
In an attempt to activate aromatic C–H bonds with (PPh₃)₂Pt(Me)(OEt₂)⁺BAR_F[−], Kubas and co-workers instead observed an unusual B–C bond cleavage of the BAR_F[−] anion at Pt yielding (PPh₃)₂Pt-[3,5-(CF₃)₂C₆H₂]₂.²²⁰ The closely related Pt(II) chelating diphosphine complexes (P–P)Pt(Me)(OEt₂)⁺BAR_F[−] (P–P = depe or dcpe) behaved differently. The cations, available by protonolysis of Pt dimethyl precursors with H(OEt₂)₂BAR_F, reacted with benzene and toluene in the neat hydrocarbons with concomitant extrusion of methane during 4 h at ambient temperature or immediately at 80 °C.²²¹ The unusual Pt₂(μ - η^3 : η^3 -biaryl) products were formed as a result of C–H activation and C–C coupling reactions (Scheme 33). Free biaryls were liberated upon treatment with HCl or I₂. The bitolyl product gave a statistical mixture of *m,m'*, *m,p'*, and *p,p'* isomers. The distribution suggests that an electrophilic aromatic substitution mechanism (which should provide more *p* isomers) is not responsible for the C–H cleavage. Biphenyl formation is believed to occur from dimerizing (P–P)Pt(Ph)(Solv)⁺ species; accordingly, protonolysis of (dcpe)Pt(Ph)(Me) with H(OEt₂)₂BAR_F furnished the same Pt₂ biphenyl product. C–H activation of furan furnished a dimeric Pt–furyl species that did not undergo furyl–furyl coupling. Intractable products (except methane) arose from attempted reactions with cyclohexane or fluorobenzene, presumably due to intramolecular reactions involving the diphosphine ligands.

The sterically encumbered *trans*-(PR₂Ar)₂Pt(Cl)(Me) (R = Ph, Cy; Ar = 2,6-Me₂C₆H₃) undergoes chloride abstraction with NaBAR_F with subsequent C–H bond cleavage of an *o*-methyl group and methane extrusion to give a formally 14-electron complex that is stabilized by agostic interactions to an aryl methyl group (Scheme 34), as demonstrated by an X-ray crystallographic analysis for R = Cy.²²² The agostic complexes reversibly react with H₂ giving cationic hydrides which are stabilized by time-aver-

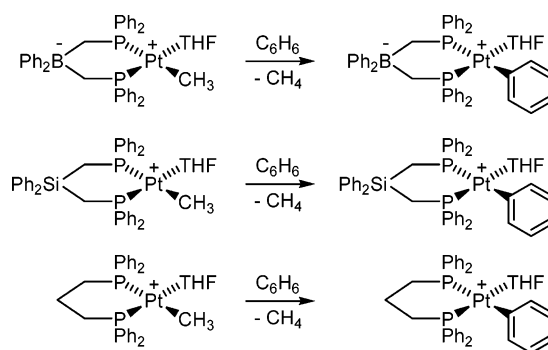
Scheme 33



Scheme 34



Scheme 35



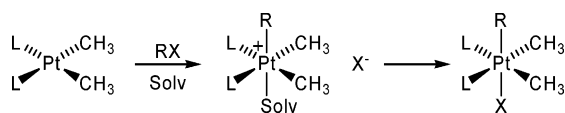
aged agostic interactions of the four *o*-methyl groups. The exact mechanisms for these C–H bond-forming and cleavage reactions are not known. The dynamic agostic complexes may be considered models for the still elusive σ -alkane Pt(II) complexes. A somewhat weaker agostic interaction has also been observed recently for $(P^iPr_3)_2Pt(Me)^+$ by X-ray crystallographic analysis.²²³

5.7. C–H Activation at Zwitterionic Pt(II) Complexes

In many cases discussed above it has been evident that the nature of the counteranion X^- that is displaced from $L_2Pt(R)(X)$ compounds has a strong influence on the reaction mechanisms. In an interesting attempt to eliminate or attenuate possible counteranion effects and avoid the use of polar media that are required to dissolve salts, Thomas and Peters prepared the zwitterionic Pt(II) complex $[Ph_2B(CH_2PPh_2)_2]Pt(Me)(THF)$ (Scheme 35).²²⁴ The THF ligand is weakly bound and easily substituted by other neutral donors. Heating of this compound in benzene at 50 °C for 4 h affords $[Ph_2B(CH_2PPh_2)_2]Pt(Ph)(THF)$ (80%) and methane. Added THF, as might be anticipated, inhibits the reaction but results in greater yields. An analogous reaction with toluene results in exclusive aromatic C–H activation (tentatively assigned *o:m:p* ratio of 1:1:3) with no evidence of benzylic activation. Attempts to activate methane or cyclohexane have not been successful, possibly due to the limited solubility of $[Ph_2B(CH_2PPh_2)_2]Pt(Me)(THF)$ in nonaromatic hydrocarbons; the unavoidable use of THF as a solvent would appreciably inhibit the desired reaction.

The electron-donating capability of the ligand in the zwitterionic methyl complex in Scheme 35 has been compared to that of the diphosphines in the related cationic compounds $Ph_2Si(CH_2PPh_2)_2Pt(Me)(THF)^+B(C_6F_5)_4^-$ and $(dppp)Pt(Me)(THF)^+B(C_6F_5)_4^-$ on the basis of IR ν_{CO} data for Pt and Mo carbonyl complexes.²²⁵ The electron density at Pt in the zwitterion is appreciably higher than that in the two cationic species. It was suggested that some of the anionic character of the borane is distributed to the ligand phenyl groups in the zwitterion, making these phenyl groups better electron-pair donors than the respective phenyl groups in the cationic species. This effect would explain several unusual observations. For example, the rate of THF self-exchange is THF independent for $[Ph_2B(CH_2PPh_2)_2]Pt(Me)(THF)^+$, presumably anchimerically assisted by a P–Ph group, whereas it is a THF dependent, associative process for $Ph_2Si(CH_2PPh_2)_2Pt(Me)(THF)^+$. All three complexes activate benzene (Scheme 35), but the Pt–phenyl products were unstable. The two cationic complexes underwent phenyl coupling reactions analogous to those observed in the (depe)Pt and (dcpe)Pt complexes in Scheme 33. The zwitterionic system also gave some phenyl coupling, although the major product $[Ph_2B(CH_2PPh_2)_2]PtPh_2^-[Ph_2B(CH_2PPh_2)_2]Pt(THF)_2^+$ arose from disproportionation. As a consequence of the electronic differences of the ligand systems, metalation of the more electron-rich phenyl group in the ligand is competitive with benzene C–H activation for $[Ph_2B(CH_2PPh_2)_2]Pt(Me)(THF)$ but not for $Ph_2Si(CH_2PPh_2)_2Pt(Me)(THF)^+$. This explains significant D incorporation into the ligand during C_6D_6 activation with $[Ph_2B(CH_2PPh_2)_2]Pt(Me)(THF)$. Kinetic measurements demonstrated that the benzene

Scheme 36



activation proceeds about twice as fast with the zwitterion as with the two cationic systems at 55 °C and that the kinetic isotope effect was much lower, 1.3 in the zwitterionic vs 6–6.5 in the cationic systems. Thermolysis of the three Pt–methyl complexes in C_6D_6 produced CH_4 and CH_3D but no higher-D-containing methane isotopomers. CH_4 dominated for the zwitterionic complex but not for the cationic ones. This is in accord with NMR evidence that established reversible insertion of Pt into C–H bonds of B-bonded as well as P-bonded phenyl groups of the $Ph_2B(CH_2PPh_2)_2^-$ ligand. Mechanistically, the cationic complexes were suggested to activate benzene by associative, reversible displacement of THF by benzene followed by a rate-limiting C–H oxidative addition that resulted in large kinetic isotope effects. In the zwitterionic system, however, the predominant pathway was proposed to be THF displacement by a P-bonded phenyl and intramolecular C–H activation of the phenyl group before benzene coordination and C–H activation. The resulting multistep mechanism readily accommodates the observed small kinetic isotope effect and other observations. The zwitterionic system importantly has established that increasingly electrophilic Pt centers are not a prerequisite in the search for systems that activate C–H bonds more rapidly.

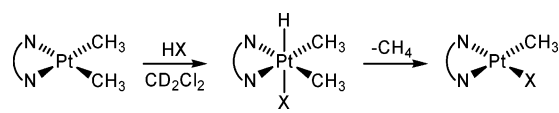
6. Reactions at Pt Complexes with Neutral Nitrogen Donor Ligands

The chemistry of Pt complexes bearing neutral N_2 - and N_3 -donor ligands that is of relevance to C–H activation is extensive. This section will include Pt complexes with bpy, phen, diimine, tmeda, and related ligands. Recent relevant reviews by Puddephatt cover oxidative addition reactions at Pt(II) complexes²¹⁵ and the chemistry of stable Pt(IV) hydrides.²¹⁷ Importantly, it has been pointed out that the nitrogen-based ligands stabilize higher oxidation state complexes to a greater extent than do phosphine ligands.^{215,216} Consequently, this section will largely deal with Pt(II)/Pt(IV) chemistry.

6.1. Protonation of Pt(II) Alkyl Complexes and Reductive Elimination from Pt(IV) Hydridoalkyl Complexes with Neutral N_2 Ligands

Crespo and Puddephatt²²⁶ reported in 1987 that oxidative addition of alkyl halides at L_2PtMe_2 complexes ($L_2 =$ bpy and $2PMe_2Ph$) occur by a two-step mechanism (Scheme 36) in which the first step was an S_N2 -type attack by the metal at RX (see section 5.1 for the microscopic reverse). Solvent capture, suggested to occur in concert with the S_N2 attack, provided observable cationic solvento complexes that underwent substitution of solvent by X^- . The better solvent ligand (MeCN) provided more stable solvent complexes than poorer ones (MeOH, acetone). The

Scheme 37



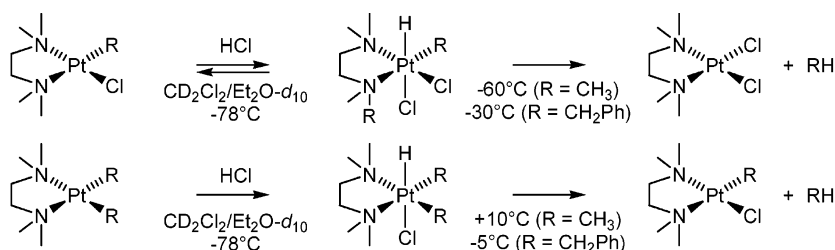
initial oxidative addition product was trans; by use of CD_3I it was established that CH_3/CD_3 positional scrambling occurred later. As we shall see, numerous reactions at (N–N)Pt(II) complexes, including important protonation reactions, occur by the same general mechanism.

Treatment of (N–N)PtMe₂ (N–N = ^tBu₂bpy, bpy, phen) with a range of acids HX leads to an oxidative addition/reductive elimination reaction to give (N–N)Pt(Me)(X) and methane (Scheme 37).²²⁷ Intermediate Pt(IV) hydridoalkyl complexes (N–N)PtMe₂(H)(X) formed by trans addition of HX could be detected for the more soluble ^tBu₂bpy complexes by ¹H NMR at –78 °C. The qualitative order of stability of the Pt(IV) hydrides was X = Cl > Br > I > CF₃COO, CF₃SO₃ (the last two could not be detected even at –90 °C). The trend reflects the need to dissociate the X[–] ligand, accessing the reactive five-coordinate species, prior to reductive elimination of methane.²²⁷ (N–N)Pt(IV) hydridomethyl complexes were also seen in reactions where HCl or HBr was generated in situ from Me₃SiX and residual water in the NMR solvents.²²⁸

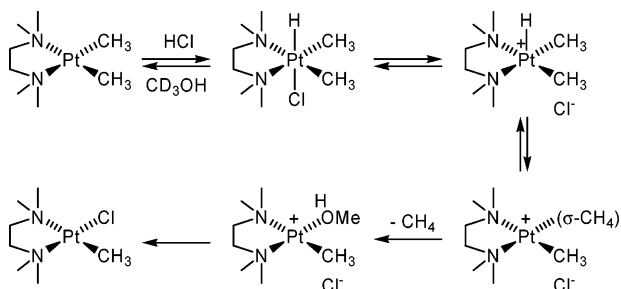
A dinuclear, stable Pt(IV) hydridomethyl complex [(^tBu₂bpy)PtMe₃]₂(μ-H)⁺OTf[–] that was crystallographically characterized resulted from reduction of *fac*-(^tBu₂bpy)PtMe₃(OTf) with NaBH₄.^{229,230} The hydridic character of the Pt–H bond in the incipient product *fac*-(^tBu₂bpy)PtMe₃H presumably renders it a superb ligand by displacement of triflate from *fac*-(^tBu₂bpy)PtMe₃(OTf). Excess NaBH₄ established an equilibrium between the dinuclear hydride and *fac*-(^tBu₂bpy)PtMe₃H, but the latter could not be isolated. Both hydrido species, unable to access five-coordination by easy ligand dissociation, were robust with respect to methane elimination (no (^tBu₂bpy)PtMe₂ was formed) and isotopic exchange between Pt–D and Pt–CH₃ groups in *fac*-(^tBu₂bpy)PtMe₃D at ambient temperature.

The Bercaw group explored reactions of Pt alkyl complexes bearing the tmeda supporting ligand.^{84,231} Protonation of (tmeda)Pt(R)(Cl) (R = Me, CH₂Ph) with HCl in CD₂Cl₂ at –78 °C led to reversible formation of observable Pt(IV) hydrides which eliminated methane or toluene upon warming (Scheme 38). The more stable benzyl system was employed for mechanistic evaluation. HCl addition was reversible, $K_{eq}^H/K_{eq}^D = 0.51 \pm 0.05$ at –28 °C. The reductive elimination obeyed kinetics that exhibited first-order behavior with respect to Pt and HOTf, a negative ΔS^\ddagger of -77 ± 29 J K^{–1} mol^{–1}, inhibition by added Brønsted or Lewis acids (HCl, HOTf, SnCl₄), and $k_{obs}^H/k_{obs}^D = 1.55 \pm 0.10$ for Pt–H vs Pt–D (i.e., $k^H/k^D = 3.1 \pm 0.6$ for the elimination step). The data are in accord with acid-assisted dissociation of Cl[–] to give the pentacoordinate (tmeda)Pt(H)(CH₂Ph)(Cl)⁺ that is responsible for the reductive elimination. Within the context of the isotope effect discussion in

Scheme 38



Scheme 39

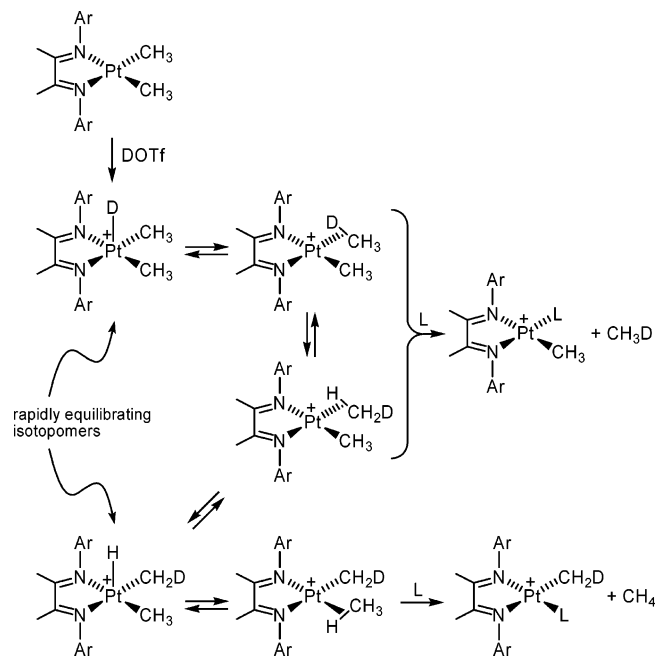


section 2.6, the kinetic isotope effect implies that C–H reductive coupling, rather than toluene elimination, is the rate-limiting step. The dialkyl complexes (tmeda)PtR₂ (R = Me, CH₂Ph) produced Pt(IV) hydrides that were thermally more stable (Scheme 38).

Addition of HCl to (tmeda)Pt(CH₃)₂ in CD₃OD/CD₂-Cl₂ generated the Pt(IV) hydride, which at –40 °C revealed gradual D incorporation from the solvent into the Pt–methyl groups; methane loss at ambient temperature gave all methane H/D isotopomers. The H/D exchange kinetics gave $\Delta H^\ddagger = 66 \pm 8 \text{ kJ mol}^{-1}$, $\Delta S^\ddagger = -20 \pm 31 \text{ J K}^{-1} \text{ mol}^{-1}$, $k^H/k^D = 1.9 \pm 0.2$ (–47 °C), and a rate inversely dependent on [Cl[–]]. Similarly, the overall reductive elimination gave $\Delta H^\ddagger = 80 \pm 3 \text{ kJ mol}^{-1}$, $\Delta S^\ddagger = 17 \pm 9 \text{ J K}^{-1} \text{ mol}^{-1}$, $k^H/k^D = 0.29 \pm 0.05$ (–27 °C), and inverse dependence of the rate on [Cl[–]]. The observations are readily accommodated by Scheme 39, which involves (1) reversible protonation to give the observed Pt(IV) hydridoalkyl which facilitates H/D exchange with the medium, (2) reversible Cl[–] dissociation which gives rise to inhibition by Cl[–] for exchange and elimination via the common five-coordinate species that (3) reversibly undergoes reductive coupling to give the σ -methane intermediate, crucial to H/D exchange and the inverse isotope effect, and (4) irreversible elimination of methane. This represents the first report of alkyl–hydride reductive coupling at Pt to give a σ -alkane intermediate that is reasonably robust with respect to alkane elimination under conditions where H/D exchange occurs. The loss of methane was considered to be dissociative because of the inverse dependence of the rate on [Cl[–]] (the inverse dependence would be canceled if methane dissociation were associative).⁸⁴ It appears that an associative displacement cannot be ruled out because the methanol solvent may well function as the incoming nucleophile for methane displacement.

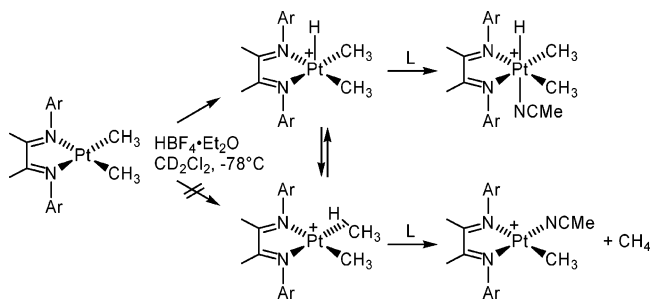
We recently addressed the point of whether the methane loss was associative or dissociative.²³² The

Scheme 40



strategy that was employed, based on competitive trapping of interconverting intermediates,²³³ is outlined in Scheme 40. Treatment of (diimine)Pt(CH₃)₂ (diimine = Ar–N=CMe–CMe=N–Ar with Ar = 3,5-(CF₃)₂C₆H₃ (N^f–N^f) or 2,6-Me₂C₆H₃ (N^r–N^r)) with DOTf provides the deuteride (diimine)Pt(CH₃)₂D⁺ (if protonation occurs at Pt) or (diimine)Pt(CH₃)(σ -DCH₃)⁺ (protonation at methyl). The site of protonation is irrelevant because the Pt–D complex reductively couples to give the σ -DCH₃ complex. σ -DCH₃ rotation at Pt then provides (diimine)Pt(CH₃)(σ -HCH₂D)⁺, which oxidatively inserts into the H–C bond to give (diimine)Pt(H)(CH₃)(CH₂D)⁺, which again can reductively couple to provide (diimine)Pt(CH₂D)(σ -HCH₃)⁺. Release of methane from (diimine)Pt(CH₃)(σ -DCH₃)⁺ and (diimine)Pt(CH₃)(σ -HCH₂D)⁺ yields CH₃D and (diimine)Pt(CH₃)(L)⁺, whereas (diimine)Pt(CH₂D)(σ -HCH₃)⁺ produces CH₄ and (diimine)Pt(CH₂D)(L)⁺. The CH₃D:CH₄ ratio (and Pt–CH₃:Pt–CH₂D) will depend on the relative rates of methane release and H/D scrambling. Dissociative methane release will give a product ratio that is independent of the concentrations of any externally added nucleophile L (competitive trapping of a putative three-coordinate species by L and methane can be ruled out because methane loss is irreversible under the experimental conditions²³²). If methane is released associatively, the product ratio will depend on [L] in the event that equilibration and intermo-

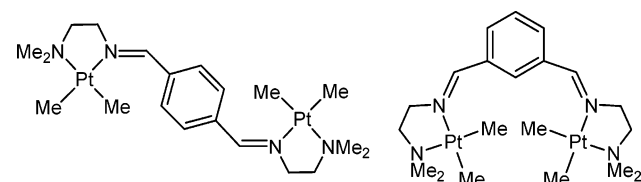
Scheme 41



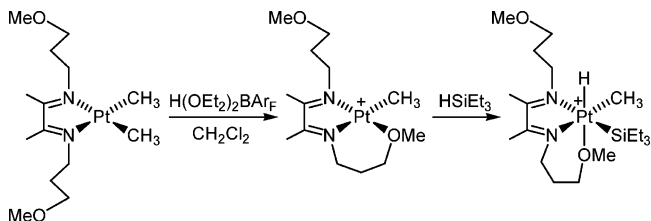
lecular displacement of methane by L occur at comparable rates. (If trapping by L is extremely fast, only CH_3D will form; if trapping by L is very slow, a constant ratio mixture will result since Curtin–Hammett conditions apply^{101,234}). Consistent results were obtained when L was acetonitrile at variable concentrations. For diimine = $\text{N}^f\text{--N}^f$, a 59:41 ratio of CH_3D and CH_4 (essentially statistical, 57:43) was produced in the non-nucleophilic solvent trifluoroethanol (TFE). Addition of increasing amounts of MeCN inhibited the scrambling (72:28 ratio at 6.0 M MeCN). Added water at 0.5 M had no trapping effect, but at 6.0 M, all methane isotopomers $\text{CH}_m\text{D}_{4-m}$ were seen, presumably because the initial protonation event becomes reversible. For diimine = $\text{N}^r\text{--N}^r$, where the Pt is considerably more sterically shielded, a not quite statistical distribution was seen in TFE (63:37) and more efficient trapping ensued with MeCN (85:15 at 6.0 M). In a more recent contribution complete scrambling was seen in neat TFE for Ar = 3,5- $\text{tBu}_2\text{C}_6\text{H}_3$, with 2.5 M MeCN inhibiting the scrambling (67:33).²³⁵ The experiments establish that methane is released associatively, and the principle of microscopic reversibility then implies that methane coordination will be an associative process for a C–H activation reaction. (Extensions to reactions at other complexes, in particular uncharged ones, and under different reaction conditions should of course be done with extreme care.)

Another important question pertaining to these protonation reactions is: does the protonation occur at Pt or at the methyl group? Various mechanisms have been proposed, and the process is probably dependent on the nature of the substrate, acid, solvent, and other parameters.^{84,138,155,197,199,201} The question bears direct relevance on the Shilov chemistry since by the principle of microscopic reversibility these two situations correspond to deprotonation from a Pt(IV) hydride (i.e., an oxidative addition mechanism) or from an activated, acidic σ -alkane ligand (i.e., an electrophilic substitution mechanism). The mere observation of Pt(IV) hydrides at low temperatures does not provide conclusive evidence that metal protonation occurs since the barrier for converting an incipient σ -methane complex to an observable, thermodynamically favored six-coordinate Pt(IV) hydridoalkyl species is expected to be rather low. Again, we addressed the question²³⁶ with competitive trapping of interconverting intermediates²³³ as outlined in Scheme 41. In this case advantage is taken of the fact that trapping of the five-coordinate (diimine)Pt(CH_3) $_2\text{H}^+$ by L must be associative and that methane displacement from

Scheme 42



Scheme 43

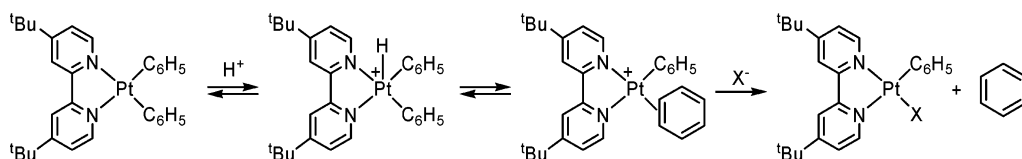


(diimine)Pt(CH_3)($\sigma\text{-CH}_4$)⁺ is also associative for L = MeCN (see above), i.e., both are bimolecular processes. Protonation of (diimine)PtMe₂ at temperatures low enough that the Pt(IV) hydridoalkyl complexes are stable on the experimental time scale should give product ratios that are [MeCN] dependent if the rate of trapping and reductive coupling/oxidative cleavage occur at comparable rates. The experiments consistently showed that the (diimine)-Pt(Me)(NCMe)⁺ to (diimine)PtMe₂(H)(NCMe)⁺ ratio decreased with increasing [MeCN] for Ar = *p*-MeC₆H₄, 2,6-Me₂C₆H₃, and 2,6-*i*Pr₂C₆H₃ and that the trapping was most efficient for the least hindered diimine. These results are only consistent with Pt being the kinetically preferred site of protonation. For a C–H activation reaction the principle of microscopic reversibility then implies that a deprotonation reaction analogous to that in the Shilov cycle occurs from a Pt(IV) hydride rather than from a σ -alkane complex. (Extensions to reactions at other complexes and under different reaction conditions should of course be done with great care.)

The Pt(II)/Pt(II) dinuclear complexes in Scheme 42 reacted with HCl to give Pt(II)/Pt(IV) and Pt(IV)/Pt(IV) hydridoalkyl products, observed by low-temperature NMR, by addition of one and two HCl per molecule.²³⁷ The following methane elimination proceeded faster from the Pt(IV)/Pt(IV) compound than from the Pt(II)/Pt(IV) compound. This indicates some intermetal communication, but the chemistry of these compounds is otherwise well understood in terms of the relatively independent behavior of two monometallic fragments. In CD₃OD/CD₃CN treatment with DOTf produced the full range of methane isotopomers $\text{CH}_n\text{D}_{4-n}$.

Pt(IV) intermediates can be intramolecularly trapped by a pendant ligand sidearm, as shown in Scheme 43.²³⁸ Protonolysis of the methoxyalkyl-substituted diimine Pd complex resulted in intramolecular C–H activation α to the methoxy group, but for Pt, no C–H activation was observed. The loss of methane was instead followed by coordination of the methoxy group to the vacant site to give a κ^3 -ligated Pt(II) intermediate. Further reaction with HSiEt₃ gave a chelation-stabilized Pt(IV) hydridoalkyl silyl complex.

Scheme 44



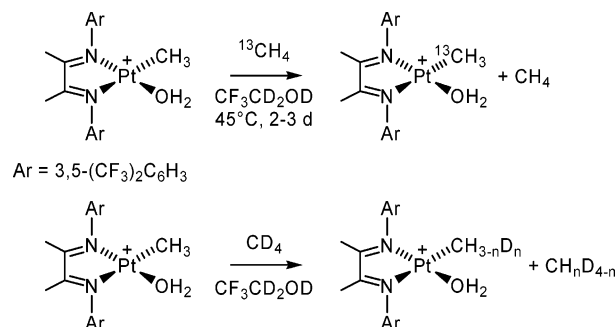
6.2. Protonation of Pt(II) Aryl Complexes and Reductive Elimination from Pt(IV) Hydridoaryl Complexes with Neutral N₂ Ligands

Protonolysis of the diphenyl Pt(II) complex (*t*Bu₂bpy)PtPh₂ with HX (X = Cl, BF₄, CF₃SO₃, CF₃CO₂) has been recently reported.²³⁹ The Pt(IV) phenyl hydride (*t*Bu₂bpy)PtPh₂(H)(Cl) was seen at low temperatures in CDCl₃; reductive elimination of benzene occurred at ca. -20 °C. The other acids gave no detectable hydrides, presumably due to the absence of sufficiently strongly coordinating anions. The acetonitrile adduct (*t*Bu₂bpy)PtPh₂(H)(NCCD₃)⁺ was obtained with HBF₄ or CF₃SO₃H in the presence of CD₃CN; this adduct also eliminated benzene at -20 °C. Treatment of (*t*Bu₂bpy)PtPh₂ with DBF₄ in CDCl₃/CD₃OD produced C₆H₆ (8%), C₆H₅D (77%), and C₆H₄D₂ (15%) along with ca. 10% D incorporation evenly distributed into the ortho, meta, and para positions of Pt-Ph in the (*t*Bu₂bpy)Pt(Ph)(Cl) product. These observations are consistent with a sequence of reversible protonation and reversible Ph-H reductive coupling/oxidative cleavage prior to elimination of benzene (Scheme 44); the rate of elimination must be competitive with the rate of oxidative cleavage. There was no mention of observable (*t*Bu₂bpy)Pt-(π -benzene) complexes. Protonation of the pincer system (NCN)PtPh (NCN = κ^3 -2,6-C₆H₃(CH₂NMe₂)₂) with HCl analogously led to (NCN)Pt(Ph)(H)(Cl), observed at -78 °C, and elimination of benzene upon warming. In this case only C₆H₅D was obtained in CDCl₃/CD₃OD. Presumably the π -benzene ligand is labilized by the strong trans influence of the pincer aryl group and is displaced before oxidative cleavage occurs. The involvement of the five-coordinate Pt(IV) and the Pt(II) π -benzene intermediates was modeled by DFT calculations of protonation at the simplified *cis*-(NH₃)₂Pt(CH₃)(C₆H₅) system.²³⁹

6.3. Stoichiometric Methane C-H Activation at Cationic Pt(II) Complexes with Neutral N₂ Ligands

The (tmeda)Pt complexes discussed in section 6.1 were capable of stoichiometric, intermolecular hydrocarbon C-H activation.^{240,241} Protonation of (tmeda)PtMe₂ with H(OEt₂)₂BAR_F in ether generated (tmeda)Pt(CH₃)(OEt₂)⁺. This complex decomposed at ambient temperature by activation of an α -C-H bond of coordinated ether to give a Fischer carbene complex. Intermolecular C-H activation was demonstrated when protonation was done in pentafluoropyridine C₅F₅N, a poorly coordinating solvent. The solvento cation (tmeda)Pt(CH₃)(NC₅F₅)⁺ reacted with benzene at 85 °C to give the phenyl complex (tmeda)Pt(C₆H₅)(NC₅F₅)⁺ and methane within 2-3 days. Under 30 atm of ¹³CH₄ at 85 °C (tmeda)Pt(¹³CH₃)(NC₅F₅)⁺ was formed during 1 week—definitive proof that methane C-H activation occurred. Heating of

Scheme 45



(tmeda)Pt(CH₃)(NC₅F₅)⁺ with cyclohexane-*d*₁₂, toluene-*d*₈, or benzene-*d*₆ produced CH₄, CH₃D, CH₂D₂, and CHD₃ during several days. The data imply that σ -alkane complexes (tmeda)Pt(σ -RD)(CH₃)⁺ and (tmeda)Pt(R)(σ -CDH₃)⁺ are involved in the H/D exchange processes.

We reported that treatment of the diimine complex (N^f-N^f)PtMe₂ with HBF₄·Et₂O in slightly moist CH₂Cl₂ led to the isolated aqua complex (N^f-N^f)Pt(CH₃)(H₂O)⁺BF₄⁻.^{242,243} (N^f-N^f = Ar-N=CMe-CMe=N-Ar with Ar = 3,5-(CF₃)₂C₆H₃). This and related diimine species are capable of activating a wide range of hydrocarbon C-H bonds. Particularly successful reactions proceeded in trifluoroethanol, TFE, a highly polar, ionizing, hydrogen-bonding, yet low-nucleophilicity solvent that has been widely used for mechanistic organic chemistry.⁵ TFE solutions of (N^f-N^f)Pt(CH₃)(H₂O)⁺BF₄⁻ reacted under 20-25 atm of ¹³CH₄ to give (N^f-N^f)Pt(¹³CH₃)(H₂O)⁺BF₄⁻ with a half-life of ca. 48 h at 45 °C. Analogously, reaction with CD₄ resulted in formation of all CH_nD_{4-n} isotopomers (Scheme 45), indicative of the intermediacy of σ -methane complexes. Addition of water inhibited the reaction, suggesting that a preequilibrium dissociation of water from the aqua complex must occur. This will be addressed in the context of the kinetics of benzene activation at (diimine)Pt complexes (see section 6.5). Protonation of (N^f-N^f)PtMe₂ in CD₂Cl₂ with HBF₄·Et₂O at -70 °C produced two (N^f-N^f)PtMe₂(H)(X) species (X remains unidentified) with H and X occupying the apical sites. Both hydrides decomposed by methane loss at ca. -40 °C, so oxidative addition to access the Pt(IV) state appears to be a viable pathway.

6.4. Computational Studies of Stoichiometric Methane C-H Activation at Cationic Pt(II) Complexes with Neutral N₂ Ligands

The reductive elimination of methane from five-coordinate model complexes L₂PtMe₂H⁺ (L = NH₃, PH₃) and the microscopic reverse were investigated by DFT calculations,²¹⁴ and the results reflect a greater stabilization of the Pt(IV) oxidation state as

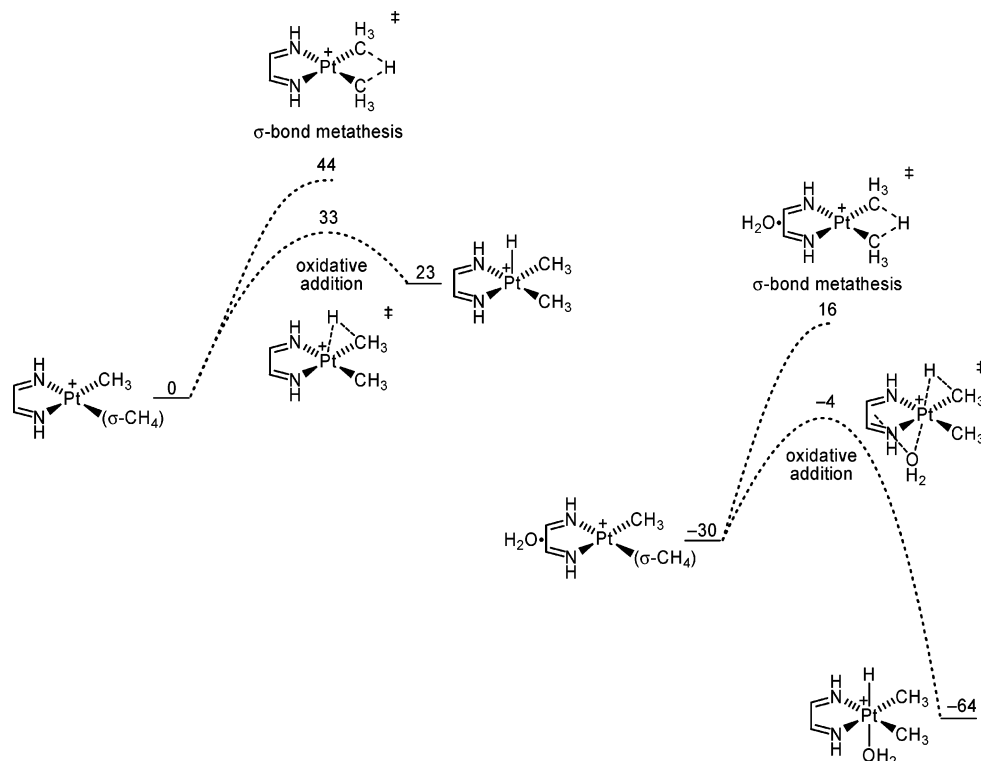


Figure 8. Energy diagram (kJ mol^{-1}) for oxidative addition and σ -bond metathesis pathways in the C–H activation at $(\text{N}^{\text{h}}-\text{N}^{\text{h}})\text{Pt}(\text{CH}_3)^+$ with (right) and without (left) H_2O . Energies are relative to that of $(\text{N}^{\text{h}}-\text{N}^{\text{h}})\text{Pt}(\text{CH}_3)(\sigma\text{-CH}_4)^+$ plus H_2O .

well as the transition state connecting Pt(II) and Pt(IV) by NH_3 than by PH_3 , as already discussed in section 5.5.

Bercaw's (tmeda)Pt system²⁴⁰ was modeled by the (eda)Pt fragment (eda = ethylenediamine) in a DFT study.²⁴⁴ The σ -methane complex $(\text{eda})\text{Pt}(\text{Me})(\sigma\text{-CH}_4)^+$ had a calculated Pt–methane bond strength of 92 kJ mol^{-1} , and oxidative cleavage with a barrier of 15 kJ mol^{-1} resulted in a square-pyramidal $(\text{eda})\text{PtMe}_2\text{H}^+$ product with H in the apical position, 7 kJ mol^{-1} above the σ complex. A σ -bond metathesis pathway for the degenerate CH_3/CH_4 H-atom exchange had a much greater barrier of 39 kJ mol^{-1} .

The energetics of the methane activation at (diimine)Pt complexes were investigated by DFT calculations with the simple imine $\text{HN}=\text{CH}-\text{CH}=\text{NH}$ ($\text{N}^{\text{h}}-\text{N}^{\text{h}}$) as the ligand.²⁴³ According to the calculations the bond energies between the three-coordinate $(\text{N}^{\text{h}}-\text{N}^{\text{h}})\text{Pt}(\text{CH}_3)^+$ and H_2O , TFE, and CH_4 are 158, 148, and 99 kJ mol^{-1} (zero-point energy corrections not included). Binding energies of H_2O and TFE at five-coordinate $(\text{N}^{\text{h}}-\text{N}^{\text{h}})\text{PtMe}_2\text{H}^+$ are 87 and 78 kJ mol^{-1} , so although the five-coordinate oxidative addition product $(\text{N}^{\text{h}}-\text{N}^{\text{h}})\text{PtMe}_2\text{H}^+$ with H apical is 20 kJ mol^{-1} uphill from $(\text{N}^{\text{h}}-\text{N}^{\text{h}})\text{Pt}(\text{Me})(\sigma\text{-CH}_4)^+$, the overall oxidative addition of methane at $(\text{N}^{\text{h}}-\text{N}^{\text{h}})\text{Pt}(\text{Me})(\text{Solv})^+$ is essentially thermoneutral (the unfavorable entropy change is not included) because of the binding of Solv (H_2O , TFE) at Pt(IV). The mechanism of the reaction was also probed by DFT, now with ZPE corrections included. The results are summarized in Figure 8. The oxidative cleavage from $(\text{N}^{\text{h}}-\text{N}^{\text{h}})\text{Pt}(\text{CH}_3)(\sigma\text{-CH}_4)^+$ (Figure 8, left) is unfavorable by 23 kJ mol^{-1} and has a barrier of 33 kJ mol^{-1} . The σ -bond metathesis pathway has a barrier of 44 kJ mol^{-1} , so the oxidative addition is preferred. If the

reductive coupling is initiated with the axial water ligand (right), the calculations suggested that dissociation of H_2O occurs in concert with C–H coupling and that H_2O remains primarily electrostatically attached at the diimine moiety of the Pt(II) σ -methane complex. H_2O is seen to stabilize all entities but to a different extent. The oxidative cleavage now is favorable by 34 kJ mol^{-1} and has a barrier of 26 kJ mol^{-1} , to be compared with 46 kJ mol^{-1} for the σ -bond metathesis. Oxidative addition is therefore preferred. The axial H_2O ligand lowers the barrier for oxidative cleavage and raises the barrier for reductive coupling because the formation/cleavage of the Pt– OH_2 bond is part of the process.²⁴³

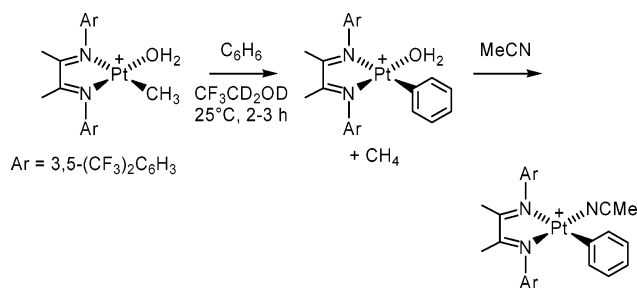
6.5. Stoichiometric Arene C–H Activation at Cationic Pt(II) N_2 Complexes

As already mentioned, $(\text{tmeda})\text{Pt}(\text{Me})(\text{NC}_5\text{F}_5)^+$ reacted with benzene at 85°C to give $(\text{tmeda})\text{Pt}(\text{C}_6\text{H}_5)(\text{NC}_5\text{F}_5)^+$ and methane within 2–3 days. Multiple H/D exchange from C_6D_6 into methane signaled the intermediacy of σ -methane and σ/π -benzene intermediates.^{240,241}

The aqua complex $(\text{N}^{\text{f}}-\text{N}^{\text{f}})\text{Pt}(\text{Me})(\text{H}_2\text{O})^+\text{BF}_4^-$ (Scheme 46) is capable of activating benzene under milder conditions in TFE. (Trapping of TFE/aqua complexes by MeCN addition after complete reaction was commonly done to obtain more stable products that were easier to characterize.) Again, C_6D_6 resulted in multiple H/D exchange into the methane and signaled σ -complex intermediates.²⁴²

The mechanism of benzene activation in TFE at (diimine)Pt(Me)(H_2O)⁺ complexes has been explored in detail, initially with $\text{Ar} = 2,6\text{-Me}_2\text{C}_6\text{H}_4$ (diimine = $\text{N}^{\text{r}}-\text{N}^{\text{r}}$)¹⁰³ and later systematically with a wide range

Scheme 46



of substituents at the diimine.²³⁵ The reaction between (N'-N')Pt(Me)(H₂O)⁺BF₄⁻ and benzene was first order with respect to benzene and Pt and inverse first order with respect to water. The H/D kinetic isotope effect for reaction with C₆H₆ vs C₆D₆ was 1.06 ± 0.05, and the activation parameters were $\Delta H^\ddagger = 80 \pm 1 \text{ kJ mol}^{-1}$ and $\Delta S^\ddagger = -67 \pm 4 \text{ J mol}^{-1} \text{ K}^{-1}$. Almost statistical H/D exchange occurred between CH₃ and C₆D₆ or 1,3,5-C₆H₃D₃, as inferred from analysis of the liberated methane, but there was no D incorporation from TFE-*d*₃. The kinetics require an *equilibrium dissociation* of water prior to the rate-limiting transition state. This can be achieved by either reversible dissociation of the aqua ligand, generating a transient three-coordinate species that is irreversibly reacting with benzene, or reversible, associative substitution of the aqua ligand by TFE accompanied by irreversible associative substitution of benzene for TFE.¹⁰³ The latter was favored, in part based on the observed negative ΔS^\ddagger . A solvent-assisted, associative mechanism for benzene coordination, a and b in Scheme 47, is therefore proposed; the direct associative route (c) is inconsistent with the kinetics. The near-unity kinetic isotope effect for the reaction is consistent with this mechanism as long as the rate-limiting step is benzene coordination rather than C-H bond cleavage (see discussion of Figure 10 later in this section).

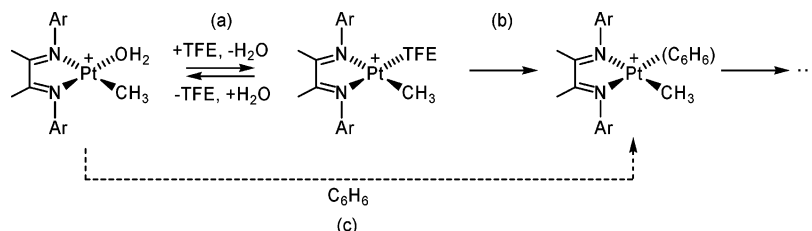
Consistent with this scheme, the aqua complexes (diimine)Pt(Me)(H₂O)⁺ are in equilibrium with the corresponding TFE-*d*₃ complexes in TFE-*d*₃, with H₂O binding being strongly favored.²³⁵ Equilibrium and rate measurements at high pressures^{245,246} have later supported the proposed associative mechanism.²⁴⁷ ΔH° , ΔS° , and ΔV° for reaction a were determined by variable-temperature and variable-pressure equilibrium measurements, and ΔH^\ddagger , ΔS^\ddagger , and ΔV^\ddagger for the overall reaction with benzene were determined from variable-temperature and variable-pressure kinetics. The parameters for the rate-limiting second step were obtained from the difference between the two, $\Delta H^\ddagger(\text{b}) = 66 \pm 2 \text{ kJ mol}^{-1}$, $\Delta S^\ddagger(\text{b}) = -57 \pm$

$5 \text{ J K}^{-1} \text{ mol}^{-1}$, and $\Delta V^\ddagger(\text{b}) = -9.5 \pm 1.3 \text{ cm}^3 \text{ mol}^{-1}$,²⁴⁷ which is quite typical for associative substitutions at square-planar Pt(II) complexes.^{246,248,249}

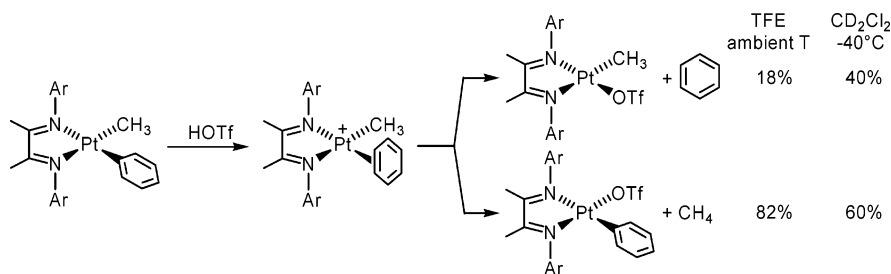
A series of protonation experiments shed light on what happens after benzene coordination at Pt.¹⁰³ First, protonation of (N'-N')Pt(Me)(Ph) in TFE at ambient temperature followed by MeCN quench after complete hydrocarbon elimination yielded benzene and (N'-N')Pt(Me)(NCMe)⁺ (18%) and methane and (N'-N')Pt(Ph)(NCMe)⁺ (82%). Low-temperature protonation of (N'-N')Pt(Me)(Ph) in CD₂Cl₂ generated the observable η^2 -benzene complex (N'-N')Pt(Me)-(η^2 -C₆H₆)⁺ (Scheme 48), which eliminated benzene and methane in a 40:60 ratio upon warming above -40 °C. Clearly, protonation accesses interconverting (N'-N')Pt(H)(Me)(Ph)⁺, (N'-N')Pt(Me)(η^2 -C₆H₆)⁺, and (N'-N')Pt(σ -CH₄)(Ph)⁺ species. The last two eliminate benzene and methane (presumably associatively) in a ratio that is somewhat dependent on the reaction conditions. Figure 9 summarizes the details in a qualitative energy diagram. The rate-limiting step is benzene coordination. Once benzene has entered the coordination sphere of Pt, Curtin-Hammett conditions prevail, intermediates C-G interconvert rapidly, and the preference for ultimate loss of methane (major) vs benzene (minor) is dictated by the difference in transition-state energies for C → B and G → H. In CD₂Cl₂ the η^2 -benzene complex is most stable in the C-G manifold;¹⁰³ in more coordinating solvents F is stabilized relative to C. In CD₂Cl₂ containing CD₃CN F is seen exclusively.²⁵⁰

Thus far we have established that repeated C-H oxidative cleavage and reductive coupling reactions occur fast, requiring no more than a few minutes at -78 °C for acquisition of low-temperature NMR spectra, but it still remains to be established exactly *how* rapid these processes are. We recently found by 2D EXSY ¹H NMR spectroscopy that exchange correlations can be seen between hydride, methyl, and phenyl signals even at -78 °C. Variable-temperature, quantitative EXSY measurements show that hydrogens of the phenyl and π -benzene ligands in a series of (diimine)Pt(C₆H₅)(η^2 -C₆H₆)⁺ complexes undergo exchange via symmetrical (diimine)PtPh₂H⁺ intermediates with $\Delta G^\ddagger = \text{ca. } 64 \text{ kJ mol}^{-1}$.²⁵¹ These values are somewhat greater than 54 kJ mol⁻¹ reported by Templeton and co-workers⁸⁶ for exchange in (κ^2 -HTp')Pt(C₆H₅)(η^2 -C₆H₆)⁺ at comparable temperatures. The difference may reflect the greater ease of formal oxidation from Pt(II) to Pt(IV) at the κ^2 -HTp' system, which is neutral at Pt, than at the cationic diimine complexes. Thermodynamic data for Pt(II) benzene hydride/Pt(IV) phenyl dihydride equilibria

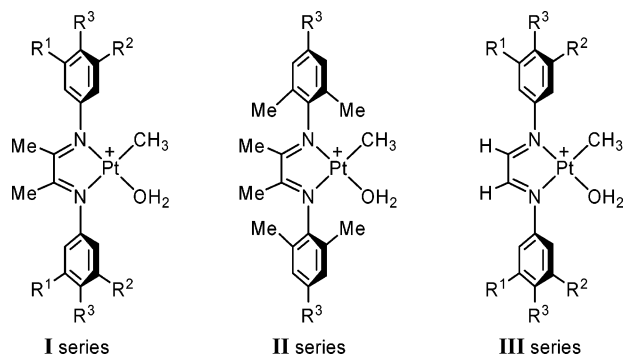
Scheme 47



Scheme 48



Scheme 49



have been recently reported for related systems,²⁵² as will be discussed in section 7.2.

Recently, Zhong et al. thoroughly investigated ligand electronic and steric effects on benzene C–H activation at a wide range of (diimine)Pt(Me)(H₂O)⁺ complexes in TFE.²³⁵ Three series of ligands were employed (Scheme 49). Series **I** complexes have N-aryl groups with substituents in the 3,4,5-positions that do not appreciably sterically shield the axial access to Pt. Series **II** members bear methyl groups in the 2,6-positions that will restrict access to Pt because the aryl groups are expected to be more or less perpendicularly oriented with respect to the Pt coordination plane. Series **III** complexes differ from series **I** in having H atoms instead of methyl groups

at the diimine backbone. Within each series it is assumed that the substituents alter the electronic environment without significantly affecting the sterics. The electronic effects were assessed from the infrared ν_{CO} frequencies of the (diimine)Pt(Me)(CO)⁺ complexes.

Some important findings may be summarized with Figure 9 as the starting point (not all reactions and kinetics were done with all members of a series). Within each series of complexes the most electron-rich members were more reactive, as inferred from correlations of $\log k_{\text{obs}}$ vs ν_{CO} of the CO adducts. The **II** series reacted more slowly than the **I** series, obviously for steric reasons. Within the **III** series reaction rates were considerably slower than for compounds within the **I** series with comparable electron density at Pt. Neither series incorporated D from the solvent when C₆H₆ was activated in TFE-*d*₃, implying that deprotonation from all intermediates **C–G** in Figure 9 must be considerably slower than the lifetime of these interconverting species. All three series followed the same rate law, first order with respect to (diimine)Pt(Me)(H₂O)⁺ and benzene and inverse first order with respect to water. Series **I** exhibited kinetic isotope effects (C₆H₆ vs C₆D₆) in the range 1.6–2.2, exhibited partial D scrambling between C₆D₆ and the reacting methyl group, and D is incorporated in up to 20% of unconsumed starting material during the reaction. Series **II** had isotope

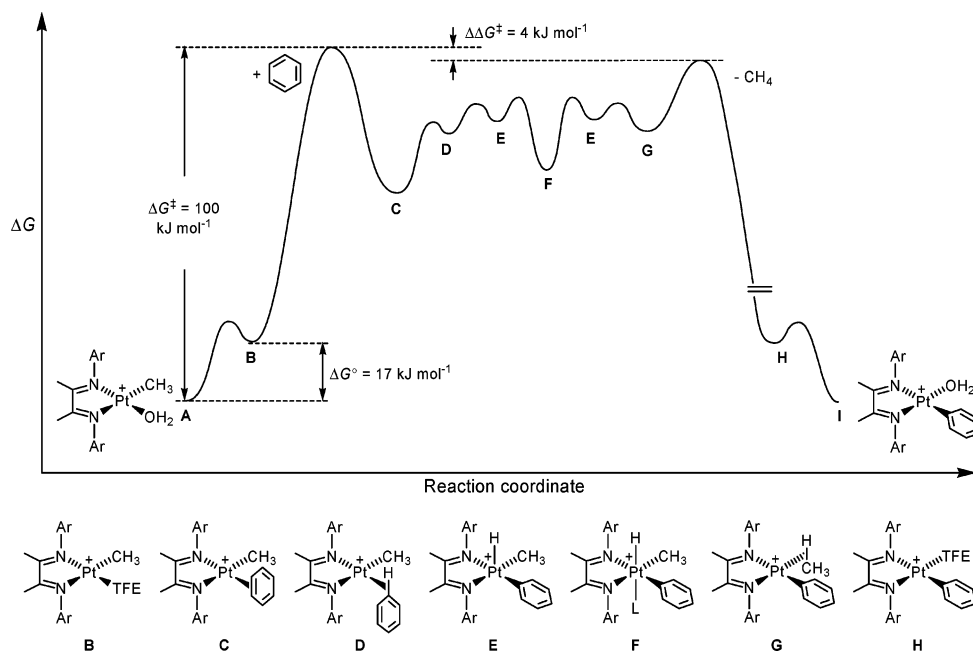


Figure 9. Qualitative reaction coordinate diagram for the C–H activation of benzene by (N'–N')Pt(CH₃)(H₂O)⁺ in TFE.

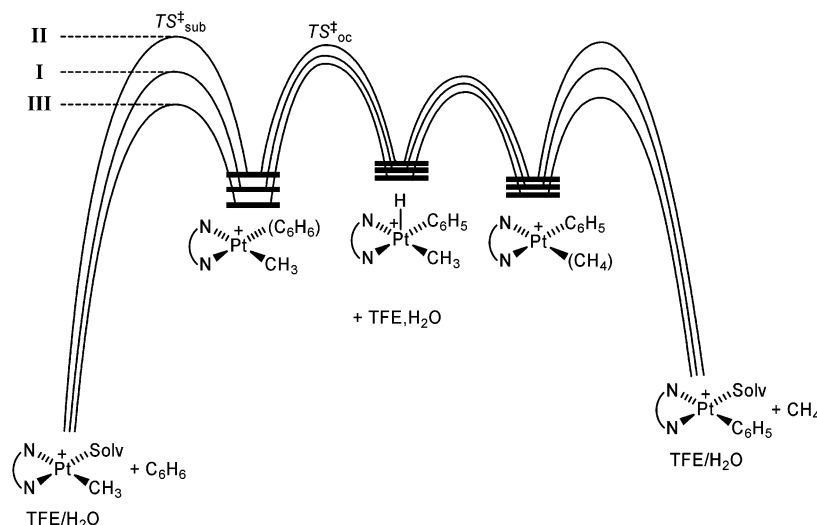


Figure 10. Qualitative reaction coordinate diagram for reactions between series **I**, **II**, and **III** diimine–Pt complexes and benzene.

effects of ca. 1.1, essentially complete statistical isotopic scrambling between Pt–CH₃ and C₆D₆ into the products, and some (not quantified) scrambling into unreacted starting material. Series **III** had isotope effects as great as 3.6–5.9 and had even less scrambling between C₆D₆ and reacting Pt–methyl than **I**, and up to 20% of unconsumed starting material became deuterated. These observations are largely understood with Figure 9 as a basis, but slight modifications (Figure 10) are called for to compare series **I**, **II**, and **III**.

One noteworthy detail in Figure 10 is that whereas the substitution of benzene for TFE is the rate-limiting step for series **II** complexes, it is the oxidative cleavage of a coordinated benzene C–H bond that is rate limiting for series **I** and **III**. This is reasonable because the approach of benzene is subject to severe steric hindrance in **II**. The rate law should be the same for both cases. The switch in rate-limiting step nicely explains that k^H/k^D is greater for **I** and **III** since the C–H bond is cleaved in TS_{oc}⁺ for **I** and **III** but has yet to be cleaved in TS_{sub}⁺ for **II**. The change in rate-limiting step also provides a rationale for the differences in extent of isotope label exchange between C₆D₆ and Pt–CH₃ in the products as well as in unreacted starting complexes. Complete activation parameters are available for Ar = 2,6-Me₂C₆H₃ (type **I**), with $\Delta S^\ddagger = -70 \text{ J K}^{-1} \text{ mol}^{-1}$, and Ar = 3,5-^tBu₂C₆H₃ (type **II**), with $\Delta S^\ddagger = -21 \text{ J K}^{-1} \text{ mol}^{-1}$ (the reported ΔS^\ddagger of +21 J K⁻¹ mol⁻¹ in ref 235 was miscalculated; see ref 16 in ref 253). This is also consistent with the diagram—the rate-limiting TS[‡] for type **I** has a solvent (TFE) molecule still attached, whereas this is not the case for **II**.

All three series **I**, **II**, and **III** exhibit increased reactivity with increasing electron density at Pt. A similar trend has been reported for related reactions at cationic Ir complexes.^{53,254} This immediately makes sense if the oxidative cleavage reaction is rate limiting (**I** and **III**) but is less intuitive for **II** where the opposite trend might be expected for a rate-limiting ligand substitution. This trend is rationalized as a *ground-state effect*: the energies of the reactants (i.e., bond strength to the aqua ligand) within each series

are more sensitive to changes in the diimine ligand than either of the two possible rate-limiting transition states TS_{sub}⁺ or TS_{oc}⁺. The model therefore explains most observations nicely, but there are still some unexplained effects of replacing the methyl group at the diimine backbone with a hydrogen (**I** vs **III**).²³⁵

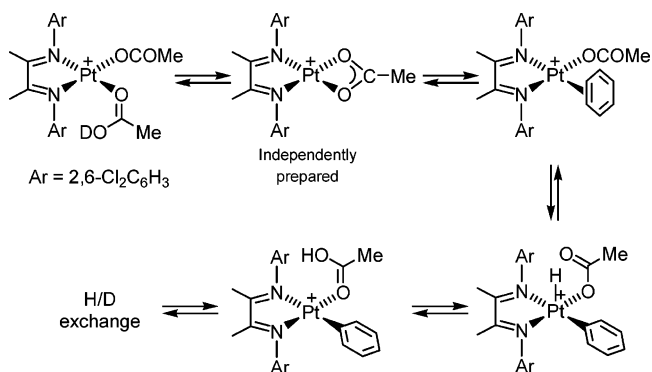
The Bercaw group recently reported that arene C–H activation can also be effected with cationic (diimine)Pd(Me)(H₂O)⁺ complexes with substitution patterns belonging to type **I** in Scheme 49.²⁵³ The reaction of benzene did not produce the corresponding phenyl complexes; however, they were invoked as intermediates that decomposed by disproportionation or ligand redistribution to give biphenyl. This is quite reminiscent of benzene activation at cationic Pt phosphine complexes, see section 5.6. The metal ended up as Pd(0) and unidentified materials under anaerobic conditions and as (diimine)Pd(H₂O)₂²⁺ and [(diimine)Pd(μ-OH)]₂²⁺ under aerobic conditions. Most important aspects of the kinetics and mechanistic details of the benzene activation at Pd are well described by Figure 10 with rate-limiting C–H activation. The observed rate was proportional to [C₆D₆]/[H₂O], $k^H/k^D = 4.1 \pm 0.5$, $\Delta H^\ddagger = 84 \pm 8 \text{ kJ mol}^{-1}$, and $\Delta S^\ddagger = -8 \pm 25 \text{ J K}^{-1} \text{ mol}^{-1}$, and there was no detection of deuteration levels beyond CH₃D in reactions with C₆D₆. The more electron-rich complex (R² = ^tBu, **I** in Scheme 49) reacts faster than the electron-poor complex (R² = CF₃), and Pd reacts faster than Pt with the same ligands. This is consistent with the ground-state stabilizing effect that was invoked for Pt.²³⁵ The nature of the rate-limiting step—C–H activation vs σ -bond metathesis—is not known; oxidative addition is less likely at Pd than at Pt because the Pd(IV) oxidation state is less accessible.

Gerdes and Chen recently compared the mechanisms of benzene activation at (diimine)Pt(CH₃)(L)⁺ complexes in solution and in the gas phase.²⁰⁷ Solution studies were reported for Ar = 2,6-Me₂C₆H₃ (N'–N') and 2,6-Cl₂C₆H₃ (N^{Cl}–N^{Cl}) and gas-phase studies for N^{Cl}–N^{Cl}. The consistency between data arising from the two approaches appeared to be remarkable. The reaction coordinate diagram in Figure 9 implies

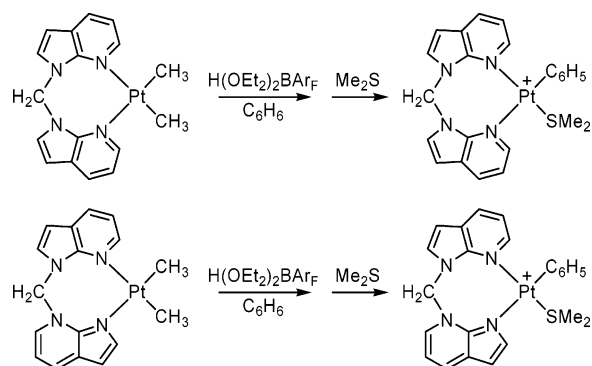
that TFE must be associated with Pt in the rate-limiting step for oxidative addition of benzene and, by the principle of microscopic reversibility, also for the elimination of benzene from any preformed species in the C–G manifold. Electrospray ionization tandem mass spectrometry studies of collision-induced elimination of methane and benzene from preselected $(N^{Cl}-N^{Cl})Pt(CH_3)(C_6H_6)^+$ or $(N^{Cl}-N^{Cl})Pt(CH_4)(C_6H_5)^+$ ions indicated that TFE caused no acceleration of the reaction compared to other, presumably inert, collision gases. No adducts or product ions containing TFE were detected, leading to the conclusion that TFE was *not* a component of the rate-limiting transition state. TFE solution kinetics for benzene activation at $(N'-N')Pt(CH_3)(H_2O)^+BF_4^-$ and $(N^{Cl}-N^{Cl})Pt(CH_3)(H_2O)^+BF_4^-$ indicated first-order behavior in [Pt] and $[C_6H_6]$ and inverse first order in $[H_2O]$, in agreement with earlier reports.^{103,235} Rates in TFE containing benzene and in neat (wet) benzene were virtually identical. Reaction-order data for the individual components in benzene were not reported, but it was nevertheless concluded that the apparent zero-order dependence on [TFE] rules out a TFE-assisted pathway even in solution. This view is contrary to the strong evidence provided by the earlier studies, including the high-pressure volume of activation data,²⁴⁷ that quite convincingly established this pathway. It was inferred that rate-limiting transition states different from those connecting B–C and G–H (Figure 9) and devoid of TFE must be involved.²⁰⁷ Proposed candidates, not supported by experiment, include η^2 -(H,H) σ -methane complexes or four-coordinate structures in which the fourth site is occupied by the ortho substituent of the diimine N-aryl group. It appears to us that the mechanistic discrepancies may just as well reflect significant differences between the gas-phase and solution-phase processes.²⁵⁵ There is no doubt that in solution the $(N-N)Pt(CH_3)(Solv)^+$ ($Solv = H_2O, TFE$) species are involved in the chemistry—both are in fact directly observed and in equilibrium with each other. The gas-phase collision-induced activation of $(N^{Cl}-N^{Cl})Pt(CH_3)(C_6H_6)^+/(N^{Cl}-N^{Cl})Pt(CH_4)(C_6H_5)^+$ with TFE leads to the products of methane and benzene elimination. Neither the reactants nor the products of these collision-induced reactions contain TFE. Hence, it may be safely argued that the gas-phase data pertain to a reaction manifold entirely different from that of the C–H activation observed in solution.

Gerdes and Chen recently¹¹⁹ utilized the phenyl complex $(N^{Cl}-N^{Cl})Pt(C_6H_5)(Solv)^+$, prepared by protonolysis of $(N^{Cl}-N^{Cl})Pt(CH_3)_2$ with $H(OEt_2)_2BAR_F$ in benzene, as a catalyst for H/D exchange into benzene in CD_3COOD solution. Turnover numbers in the thousands were seen, and kinetics established that the exchange process was first order in catalyst and benzene and inverse first order in acetic acid. The M value (number of H/D exchanges per pass through the catalytic cycle, see section 3.2) was 2.6 ± 0.3 . Electrospray MS analysis indicated that the catalyst resting state was the Pt(II) complex $(N^{Cl}-N^{Cl})Pt(OCOD_3)(DOCOD_3)^+$ and that the turnover-limiting step of the reaction was displacement of the acetic acid ligand by benzene to give a π -benzene complex.

Scheme 50



Scheme 51



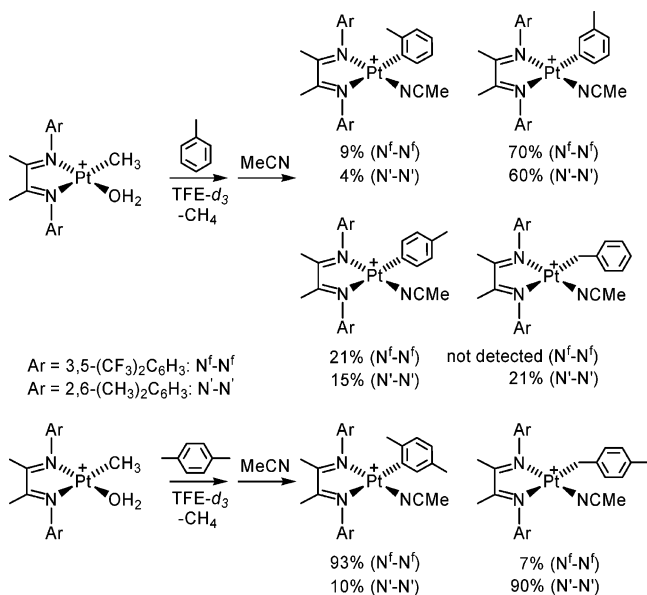
The benzene ligand undergoes relatively rapid (accounting for the M value) oxidative cleavage and H/D exchange via proton transfer from Pt–H to the Pt–OAc group; isotopic exchange then must occur either via H/D exchange with the medium or by substitution of CD_3COOD for CD_3COOH . Dissociative benzene coordination at the cationic Pt acetate was inferred on the basis of the rate law, although an anchimerically assisted, i.e., intramolecularly assisted associative mechanism, was favored. The latter is in accord with the general associative substitution behavior of cationic Pt(II) complexes (see section 5.1). The first half of the catalytic cycle is depicted in Scheme 50.

Wang and co-workers noted that the $(N-N)PtMe_2$ complexes of the two isomeric $(N-N)$ ligands bis(*N*-7-azaindoly)methane activate benzene after protonation with $H(OEt_2)_2BAR_F$ (Scheme 51).^{256,257} Interestingly, the reaction of the complex with the unsymmetrical ligand (bottom) exclusively furnished the product with the phenyl group trans to the pyrrole, rather than the pyridine, nitrogen. A related dinuclear tetramethyl complex^{257,258} yielded products of double benzene C–H activation in moderate yields; the mechanism of this transformation is only poorly understood.

6.6. Regioselectivities in Aromatic Activation

The establishment of rapidly interconverting Pt(II) and Pt(IV) species after hydrocarbon coordination is a fairly general feature of C–H activations at cationic Pt(diimine) complexes. This raises intriguing possibilities concerning regioselectivities of C–H activation of substituted aromatics. The reactions of toluene and *p*-xylene were investigated at $(N^f-N^f)Pt(Me)(H_2O)^+$ and $(N'-N')Pt(Me)(H_2O)^+$ in TFE

Scheme 52



(Scheme 52). MeCN trapping was done after completed reaction and did not affect the observed product distributions. The N^f-N^f system preferentially gave products of aromatic C-H activation, whereas benzylic activation was preferred at the N[']-N['] complex.²⁵⁹ For Ar = 3,5-*t*Bu₂C₆H₃, *p*-xylene gave almost exclusively aromatic activation whereas mesitylene gave 95:5 benzylic and aromatic activation at 25 °C.²³⁵ The differences are believed to result from the greater steric demands of the 2,6-disubstituted ligands (more crowded Pt favors benzylic activation) vs 3,5-disubstituted ligands (less crowded Pt favors aromatic activation). These findings are contrasted by H/D exchange in *p*-xylene in the Shilov system where a 91:9 selectivity for the benzylic positions over the aromatic positions was observed.^{113,128} This is surprising as PtCl₄²⁻ or PtCl₃(H₂O)⁻ are not

particularly crowded compared to the 2,6-disubstituted diimine ligand (N[']-N[']), and aromatic activation—giving stronger Pt-aryl bonds in crucial intermediates—would normally be anticipated. Simple steric considerations appear to be insufficient to explain the deviating selectivity patterns even in this simple system. A recent study on C-H activation of acetophenone and nitrobenzene by an iridium phosphine pincer complex showed a similar counterintuitive selectivity.²⁶⁰ In this case low-temperature NMR revealed a kinetic meta and para selectivity, whereas the thermodynamic product was the ortho isomer due to formation of a favorable chelate.

Protonation of the three isomeric ditolyl complexes (N^f-N^f)Pt(*o*-Tol)₂, (N^f-N^f)Pt(*m*-Tol)₂, and (N^f-N^f)Pt(*p*-Tol)₂ in TFE to which was added 0–1.7 M MeCN further illuminated how these regioselectivities might arise. In neat TFE all substrates gave exactly the same product distribution (no observed ortho or benzylic, 77% meta, 23% para) for the resulting (N^f-N^f)Pt(Tol)(NCMe)⁺ complexes after trapping with MeCN. Extensive positional isomerization had occurred. When MeCN was present during the protonolysis, the extent of positional isomerization was effectively inhibited. This is most readily accommodated by the already established associative displacement of hydrocarbons from the cationic complexes. MeCN is the better nucleophile, and hydrocarbon displacement competes with positional isomerization. TFE is a poor nucleophile, positional isomerization is very rapid compared to displacement of products (Curtin–Hammett conditions prevail), and the product distribution is independent of the identity of the substrate. The qualitative energy diagram in Figure 11 illustrates the situation.

Interestingly, the meta:para ratio for the toluene activation was unusual, as it was significantly *greater* than the statistical 2:1 for the N^f-N^f and N[']-N[']

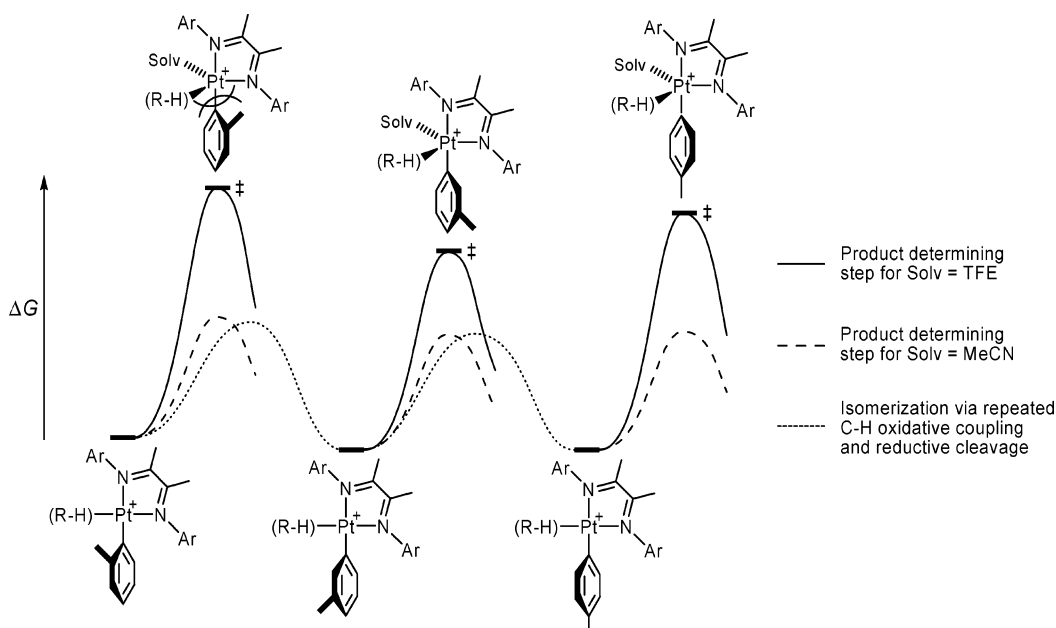
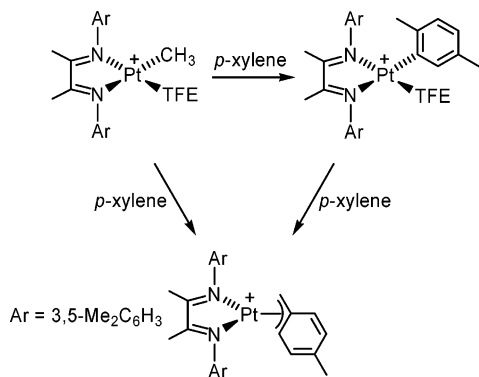


Figure 11. Qualitative energy diagram that illustrates the product-determining events during (a) toluene C-H activation, with (R-H) = σ -CH₄ and Solv = TFE, and (b) protonolysis of di(tolyl) complexes, where (R-H) = π -toluene and Solv = TFE/MeCN. Benzylic species have been omitted.

Scheme 53

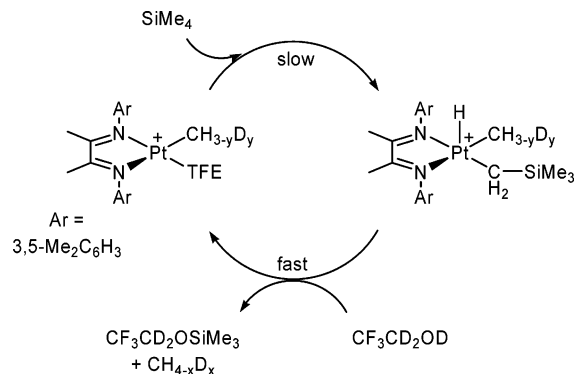


ligand systems. The same meta preference is seen in the protonation of the $(N^I-N^I)Pt(Tol)_2$ isomers in TFE. The surprising meta preference has been tentatively suggested to arise from a poorer delocalization of the positive charge by resonance in (diimine)- $Pt(R-H)(Tol)^+$ for $Tol = m-Tol$ than for $p-Tol$. This leads to a harder Pt center that is more susceptible to nucleophilic attack by TFE.²⁵⁹ The meta:para ratio, for kinetically as well as thermodynamically controlled reactions, is usually statistically 2:1 or less in other C–H activating systems that have been studied.^{160,161,185,218,261–263}

Protonation of $(N'-N')Pt(p-Tol)_2$ in TFE/0.05 M MeCN furnished $(N'-N')Pt(R)(NCMe)^+$ (8% $R = o-Tol$, 65% $m-Tol$, 15% $p-Tol$, 12% benzyl).²⁵⁹ A control experiment showed that the isomerization was not caused by a sequence of elimination and re-addition of toluene. The formation of the benzylic isomer is therefore significant because it demonstrates a rearrangement between “aromatic” and “benzylic” C–H coordination modes prior to hydrocarbon elimination. This contrasts a report by Legzdin and co-workers, who concluded that separate C–H activation pathways exist for benzylic vs aromatic toluene C–H activation at thermally generated $Cp^*W=CH^tBu$ and $Cp^*W=CHPh$ fragments.²⁶⁴

The Bercaw group recently reported surprising selectivity patterns in the reaction between the (diimine) $Pt(CH_3)(TFE)^+$ complex in Scheme 53 and substituted benzenes.^{186,265} This complex, generated as the $[CF_3CD_2OB(C_6F_5)_3]^-$ salt from the Pt dimethyl precursor and $B(C_6F_5)_3$ in TFE, is a water-free analogue of the (diimine) $Pt(CH_3)(H_2O)^+$ complexes described above and does exhibit an expected reactivity increase toward benzene compared to the aqua complex. C–H activation at mesitylene occurred exclusively at the benzylic position at a rate an order of magnitude more slowly than with benzene (rates are not statistically corrected for number of equivalent C–H bonds), with $k^H/k^D = 1.1 \pm 0.2$. With p -xylene aromatic activation was preferred ($k^H/k^D = 4.0 \pm 1.8$) over benzylic activation ($k^H/k^D = 0.8 \pm 0.3$) by a factor of 2, but only the product of benzylic activation was observed on a longer time scale and is thermodynamically preferred. The reason for this surprising preference appears to be a η^3 coordination mode of the benzylic moiety. Curiously, and in contrast with the findings for toluene activation at $N'-N'$ discussed above, a first-order dependence of the isomerization rate on the p -xylene concentration

Scheme 54



suggests that the isomerization from aromatic to benzylic product may occur intermolecularly. Toluene behaves qualitatively similar to p -xylene, but the distribution of positional isomers among the aromatic products has not been fully analyzed.¹⁸⁶

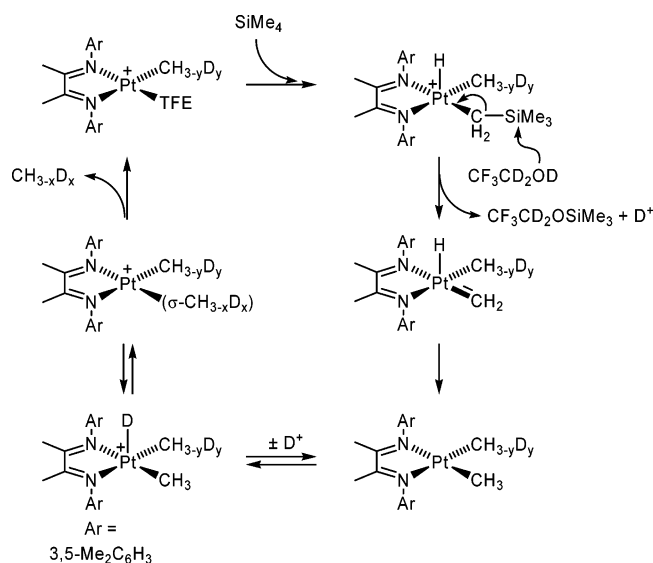
Considering the numerous examples that have been discussed, it is clear that the distribution of aromatic positional selectivities as well as the aromatic vs benzylic selectivities in the observed C–H activation products is influenced by many factors. It is important to establish whether observed product distributions reflect an intrinsic kinetic preference of the metal toward a specific C–H bond, or an overall thermodynamic preference in the C–H activated product, or a kinetic preference of a product-determining step that occurs after the initial C–H activation. An intimate knowledge of the underlying reaction mechanisms is obviously important if selectivities in these and other systems, including the aqueous Shilov system, are to be understood and used in the design of new catalyst systems with tunable selectivities.

6.7. Catalytic C–H Activation and Functionalization at Cationic Pt(II) N_2 Complexes

An unusual case of catalytic alkane C–H activation and functionalization was recently reported by Bercaw.¹⁸⁹ The (diimine) $Pt(Me)(TFE)^+$ complex in Scheme 54 was generated from (diimine) $PtMe_2$ by protonolysis with $H(OEt_2)_2BAR_F$ or $B(C_6F_5)_3$ in TFE- d_3 . Addition of excess (36 equiv) Me_4Si initiated a catalytic reaction that under very mild conditions produced the silyl ether $CF_3CD_2OSiMe_3$ and methane isotopomers $CH_{4-x}D_x$ (75% conversion after 18 h, 26 °C). More than 75% of the Pt complex remained, although H/D exchange into the Pt– CH_3 group was evidenced by Pt– CH_2D and Pt– CHD_2 signals in the 1H NMR spectrum. Clearly, the formation of strong Si–O and C–H bonds at the expense of weaker H–O and Si–C bonds provides the driving force for the catalysis. It was proposed that rate-limiting C–H activation of $SiMe_4$ was followed by rapid solvolysis (Scheme 54).

The mechanism of the fast step was probed by stoichiometric protonation reactions. Dissolution of (diimine) $Pt(CH_2SiMe_3)_2$ in TFE- $d_3/B(C_6F_5)_3$ produced 2 equiv of $CF_3CD_2OSiMe_3$ (unlabeled in the Si–Me groups) as well as (diimine) $Pt(Me)(TFE)^+$ (Pt–Me partially D labeled) and methane (partially D labeled). In THF- d_3 containing TFE- d_3 the same

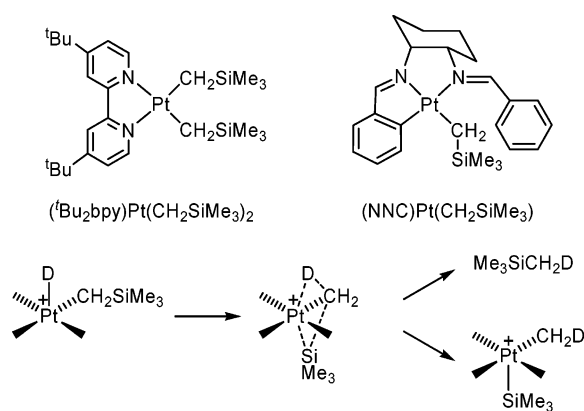
Scheme 55



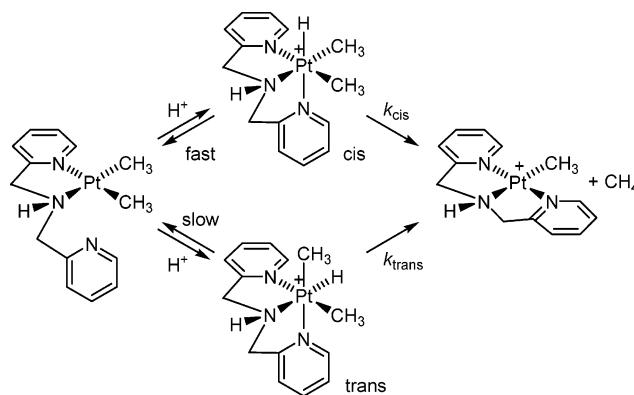
products were obtained except that the Pt product was the THF adduct (diimine)Pt(Me)(THF)⁺. The THF adduct, unlike the TFE analogue, did not produce the silyl ether from SiMe₄. Both equivalents of silyl ether therefore must arise from protonolysis of (diimine)Pt(CH₂SiMe₃)₂. No SiMe₄ was formed by protonolysis of (diimine)Pt(CH₂SiMe₃)₂. The observations were considered to be most consistent with the mechanism in Scheme 55. The rate-limiting C–H activation is followed by a rapid nucleophilic attack by TFE at the silyl group. This generates an unusual neutral five-coordinate (diimine)Pt(IV) hydrido-methyl methylidene complex. Subsequent α-H migration from Pt to methylene accesses the neutral (diimine)PtMe₂ complex which, under the acidic conditions, is known to undergo H/D exchange with the medium into the methyl groups before associative release of methane by TFE. The (diimine)Pt(Me)-(TFE)⁺ resting state of the catalyst is then produced. Mechanistic alternatives involving β-Me migration from the activated silane to Pt was discounted because D label should then be seen at the silyl ether. Furthermore, α-silyl migration to Pt was discounted. If it were to occur after reductive coupling, Me₄Si would be an expected byproduct. If it were to occur before reductive coupling, an unlikely Pt(VI) intermediate would result.

Puddephatt investigated the mechanism further by protonation of the complexes in Scheme 56.¹³⁴ Protonation by HX (X = Cl, Br) in moist solvents generated Me₃SiOH and methane (85–90%) as well as some Me₄Si (10–15%). In a solvent mixture containing CD₃OD, (NNC)Pt(CH₂SiMe₃) produced Me₃SiOCD₃ and CH₂D₂ (85–90%) as well as Me₃SiCH₂D (10–15%) along with (NNC)PtX. The labeling in methane and Me₄Si indicates that the C–H reductive couplings must be irreversible. (^tBu₂bpy)Pt(CH₂SiMe₃)₂ furnished Me₃SiOCD₃ and all isotopomers CH_nD_{4-n} (90%) as well as Me₃SiCH₂D (10%), indicative of irreversible C–H coupling, along with (^tBu₂bpy)Pt(X)(CD_nH_{3-n}). Monitoring the protonation of (^tBu₂bpy)Pt(X)(CH₂SiMe₃)₂ by ¹H NMR at –30 °C revealed the presence of (^tBu₂bpy)PtMe₂(X)(SiMe₃), a product of α-silyl migration to Pt. It was proposed

Scheme 56



Scheme 57



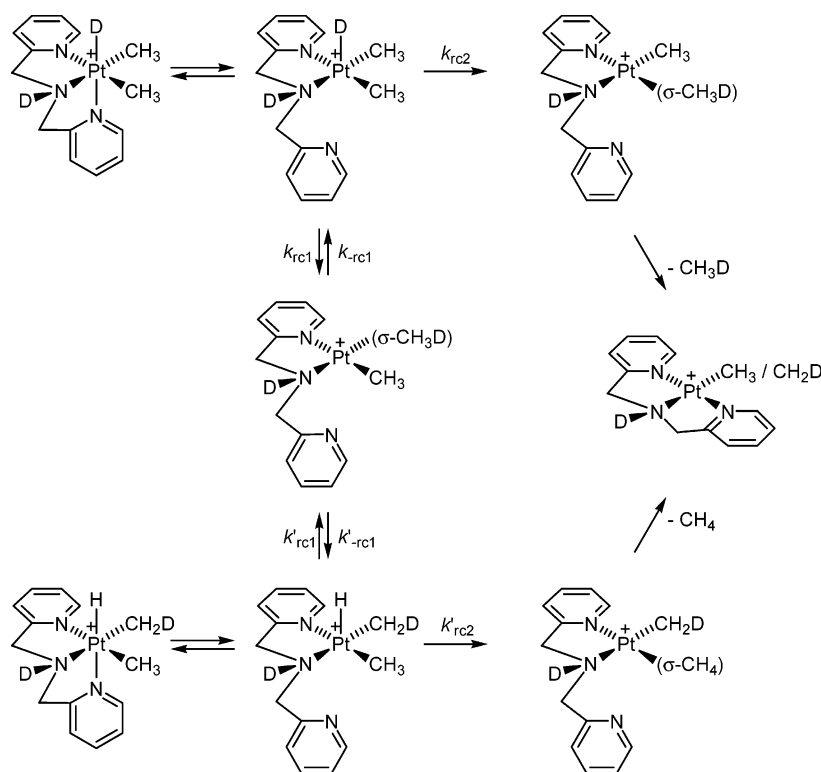
that the observations were consistent with a concerted migration of D to C and of Si to Pt (Scheme 56, bottom). This appears to be in accord with the deduction above¹⁸⁹ that α-Si migration does not occur before or after reductive coupling. The partitioning into Me₄Si and Me₃SiY products might be caused by the conformation of the CH₂SiMe₃ group when the hydride migration to carbon begins.¹³⁴ However, it is not obvious that the same mechanism should operate in all these systems. In addition to the variations in substrate structures, there are significant differences in solvent acidity, basicity, and nucleophilicity (H₂O and MeOH vs CF₃CH₂OH).

6.8. Reactions at Pt Complexes with Neutral Acyclic N₃ Ligands

There are a number of interesting cases in which chelating N-donor Pt(II) alkyls have been protonated to give stable Pt(IV) alkyl hydrides where the stabilization is caused by intramolecular coordination of a pendant sidearm of the ligand system, resembling the function of the methoxy group²³⁸ in Scheme 43.

The bis(2-pyridylmethyl)amine system is an early example of this approach. Protonation with HCl or HBF₄ in CD₂Cl₂ gave the cis (hydride vs amine) hydrido-dimethyl complex, which equilibrated to a mixture with the trans isomer.²⁶⁶ It was later demonstrated²⁶⁷ that the cis–trans interconversion is caused by reversible protonation, as indicated in Scheme 57, rather than via pyridine dissociation and site exchange in the resulting five-coordinate species. The cis and trans isomers both eliminate methane.

Scheme 58



The kinetics of the elimination was done in CD₂Cl₂ for the cis isomer alone and for the cis/trans mixture under base-free conditions where the two do not interconvert as well as under equilibrium conditions.²⁶⁷ The cis isomer ($\Delta H^\ddagger = 104 \pm 3 \text{ kJ mol}^{-1}$, $\Delta S^\ddagger = 28 \pm 10 \text{ J K}^{-1} \text{ mol}^{-1}$, $\Delta V^\ddagger = 6.2 \pm 0.3 \text{ cm}^3 \text{ mol}^{-1}$) reacted more than 1 order of magnitude faster than the trans isomer ($\Delta H^\ddagger = 133 \pm 5 \text{ kJ mol}^{-1}$, $\Delta S^\ddagger = 101 \pm 17 \text{ J K}^{-1} \text{ mol}^{-1}$, $\Delta V^\ddagger = 8 \pm 1 \text{ cm}^3 \text{ mol}^{-1}$). A major reason for this is the greater trans influence of a hydride relative to a methyl ligand; the hydride in the cis isomer causes labilization of the trans pyridine to access a reactive five-coordinate species more readily than what is possible from the trans isomer.²⁶⁷ The measured volumes of activation are considered to be too small for the pyridine dissociation (expected ca. $20 \text{ cm}^3 \text{ mol}^{-1}$)²⁴⁹ to be rate limiting.

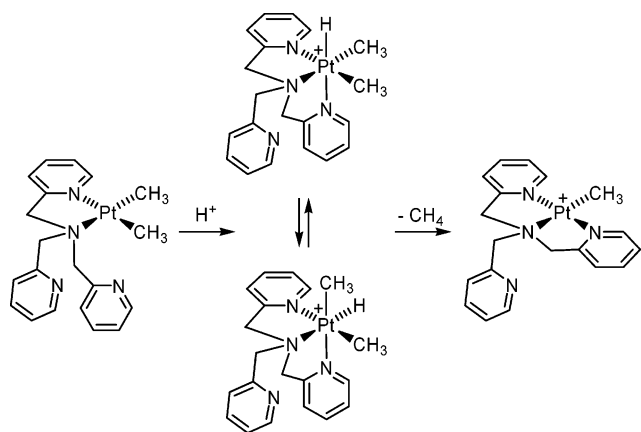
Treatment of the dimethyl complex with DCl under conditions that would allow reversible Pt–D formation during the methane elimination produced CH₄, CH₃D, and (with time) CH₂D₂. Interestingly, D was incorporated specifically in the Pt–Me group trans to the amine in the cis Pt(IV) isomer.²⁶⁶ These observations were better understood after experiments on the cis isomer under conditions of *irreversible* deuteride formation with TfOD in acetone-*d*₃.²⁶⁷ The experiments demonstrated that D scrambling occurred selectively into the methyl trans to amine (Pt–CH₂D but not Pt–CHD₂ was seen). Considerable amounts of D were incorporated into the Pt(II) methyl product, and CH₄ and CH₃D were seen but not CH₂D₂. The rate of H/D scrambling was ca. 1.6 times faster than the methane elimination with k^H/k^D close to unity. These observations are rationalized with Scheme 58, where two H/D reductive coupling pathways are available from the five-coordinate intermediate. One is reversible (k_{rc1} , k_{-rc1}) and leads

to scrambling but not methane loss, and the other is irreversible (k_{rc2}), somewhat slower, and leads to methane loss. The greater trans influence amine ligand weakens the trans Pt–C bond, facilitating the C–H reductive coupling of the trans methyl relative to the cis methyl, causing $k_{rc1} > k_{rc2}$. However, the trans σ -methane complex has the wrong geometry to readily form the Pt(II) product, while the cis σ -methane isomer has the correct geometry. The pyridine is conveniently located for an intramolecular associative displacement of methane by a nucleophilic attack at platinum. The low volumes of activation are accounted for since the preequilibrium pyridine dissociation (large positive ΔV^\ddagger) is followed by a rate-limiting reductive coupling for which ΔV^\ddagger should be negative.

Under conditions of reversible protonation, the pendant pyridine group in the σ -methane intermediate might assist deprotonation from the σ -methane ligand followed by reprotonation at the other face of the metal, thus driving the slow multiple D incorporation.²⁶⁶ The principle of microscopic reversibility then requires that pyridine protonation must also be available for the introduction of a proton to Pt in the first place, so that pyridine effectively acts as a “proton shuttle” between the reaction medium and the metal.

The Pt(II) dimethyl complex of tris(2-pyridylmethyl)amine in Scheme 59 is fluxional at ambient temperature as the free and coordinated pyridine moieties undergo exchange by ¹H NMR. Protonation with CF₃CO₂H, HOTf, or HBF₄ in acetone results in rapidly equilibrating Pt(IV) hydride isomers.²⁶⁸ The rapid exchange is in contrast to the behavior of the bis(2-pyridylmethane) analogues (Scheme 57) and is probably facilitated by proton transfer, the pendant pyridine ring acting as a “shuttle”. Methane was

Scheme 59



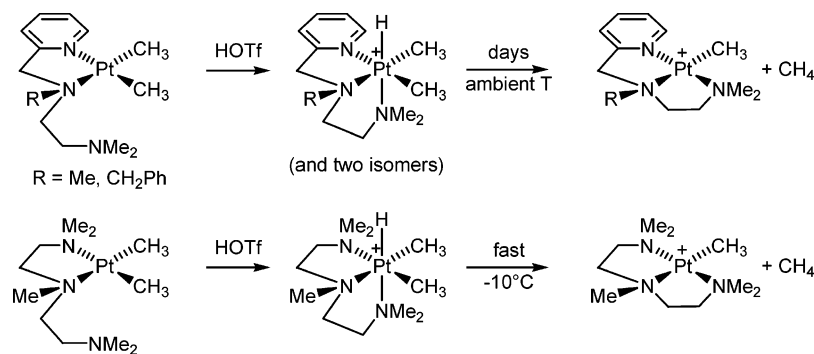
eliminated during 1 day at ambient temperature. DOTf produced CH₃D and gave no D incorporation into Pt–methyl groups. Reductive C–H coupling is apparently irreversible, although the tris(2-pyridylmethyl)amine Pt(IV) hydride has a thermal stability comparable to that of the bis(2-pyridylmethyl)amine analogue. The irreversibility may be caused by the ability of the pendant pyridine moiety to effect an intramolecular, associative methane displacement.

The protonation chemistry of the neutral N₃ ligand systems in Scheme 60 has also been investigated.²⁶⁹ The behavior of these systems largely parallels that of the bis(2-pyridylmethyl)amine in Scheme 58. The stability of the Pt(IV) hydrides appears to correlate

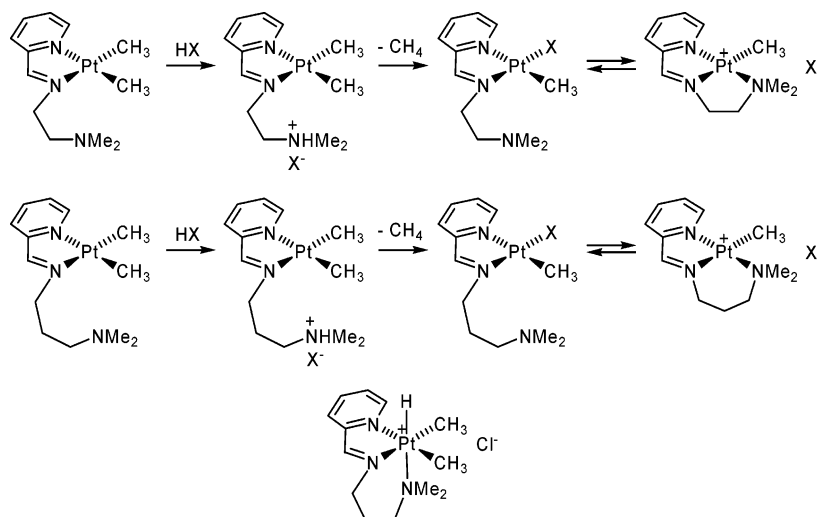
with the tendency of the ligands to form strong *fac*-tridentate binding to Pt(IV). Treatment with DOTf under reversible conditions (CD₃OD solvent) led to multiple D incorporation into the methane produced as well as the Pt–Me group of the products. The remaining methyl group in the products underwent protonolysis with excess HOTf; when DOTf was used, only CH₃D was produced, so σ -methane complex formation is not reversible. It is not known whether these reactions proceed via dicationic Pt(IV) hydrides.

The iminopyridyl ligand systems in Scheme 61 are less flexible than the amine analogues because of the geometrical constraints of the C=N bond.²⁷⁰ Indeed, the two-carbon chain (top) did not yield a *fac*-chelate in the oxidative addition of CH₃I but rather the Pt(IV) iodide (κ^2 -N₃)PtMe₃I. The three-carbon chain yielded solvent-dependent mixtures of (κ^2 -N₃)PtMe₃I and (κ^3 -N₃)PtMe₃. This difference in ability to form *fac*-N₃ chelates also has consequences for the protonation chemistry. Addition of 1 equiv of HX (X = Cl, CF₃CO₂, TfO) led to initial protonation at the basic amino group rather than at Pt. The N-protonated complexes slowly eliminated methane, presumably via proton transfer from N to Pt (intermediates were not observed) to give a counteranion and chain-length-dependent product mixture of neutral (κ^2 -N₃)Pt(Me)(X) and cationic (κ^3 -N₃)PtMe⁺ complexes in which the κ^3 -N₃ ligand has a mer coordination mode. The neutral complexes were kinetically favored; rearrangement to the cationic species presumably occurred by intramolecular associative attack by

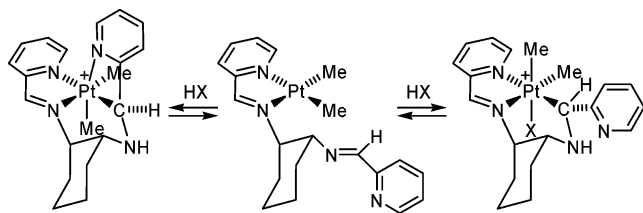
Scheme 60



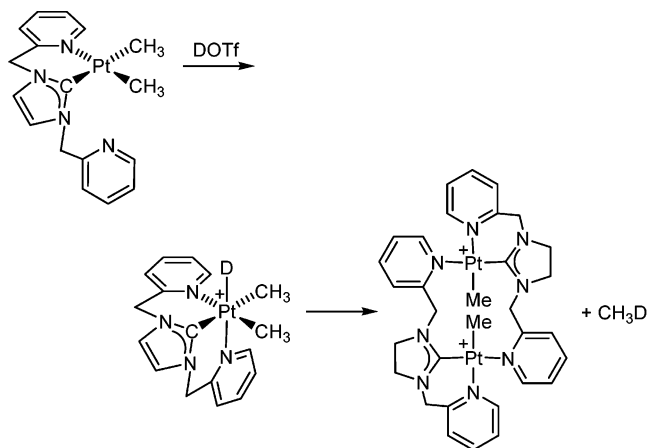
Scheme 61



Scheme 62



Scheme 63

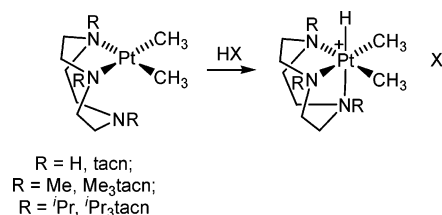


the dimethylamino group at an axial site of Pt. The cationic complex was preferred and formed faster for the poorer X ligands (OTf, CF_3CO_2) and large ring size (three-carbon chain, bottom). Protonation of the dimethyl complexes with 2 equiv of HX led to immediate loss of methane and produced mixtures of the cationic-at-Pt ($\kappa^3\text{-N}_3$)PtMe⁺ and the N-protonated form of ($\kappa^2\text{-N}_3$)Pt(Me)(X). Pt(IV) hydrides are presumed intermediates in all these reactions but could only be observed at low temperatures for X = Cl with the three-carbon chain in the ligand. This hydride (Scheme 61, bottom) eliminated methane at -30°C . DOTf in $\text{CD}_2\text{Cl}_2/\text{CD}_3\text{OD}$ (which facilitates reversible proton transfer, see previous examples) produced only CH_3D and no incorporation of D into Pt–methyl groups, and therefore, C–D reductive coupling is irreversible.

Interestingly, closely related complexes that bear a pendant iminopyridine, rather than an amine, substituent undergo stereoselective formation of aminoalkyl platinum complexes upon treatment with HX (Scheme 62).²⁷¹ Protonation occurs at imine-N, and the incipient iminium cation underwent electrophilic attack at Pt. The two products arise from trapping by the pyridine moiety or by X. Intramolecular axial trapping Pt(IV) hydrides by the pendant imine or pyridine groups was not observed, although evidence was presented that the proposed initial protonation at the imine had to be reversible.

The bis(2-pyridylmethyl)-substituted *N,N*-heterocyclic carbene^{172,173} system in Scheme 63 exhibits chemistry similar to that of the N_3 donors described already. Protonation provided the Pt(IV) hydrido carbene complex, which eliminated methane within 7 h already at -60°C .²⁷² The elimination was irreversible with no hint of D/ CH_3 isotope exchange when DOTf was used under the conditions that led to multiple D incorporation in the bis(2-pyridyl-

Scheme 64



methyl)amine system in Scheme 58. The strong trans influence carbene ligand should cause a significant trans Pt–CH₃ bond weakening that facilitates the reductive coupling and the ensuing methane elimination. It was suggested that the methane elimination occurs from the position trans to the carbene. This is consistent with the stereochemistry of the dinuclear product, proposed to arise from dimerization of the formally three-coordinate mononuclear precursor.

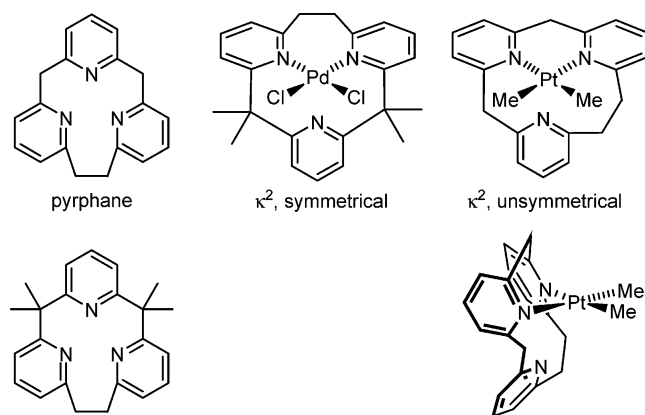
6.9. Reactions at Neutral Cyclic N₃ Ligands

The neutral triazacyclononane (tacn) molecule has a strong tendency to act as a *fac*-binding tridentate ligand.²⁷³ The ligand is bidentate chelating in ($\kappa^2\text{-tacn}$)PtMe₂, and reaction with HOTf (Scheme 64) leads to the thermally robust ($\kappa^3\text{-tacn}$)PtMe₂H⁺OTf[−], characterized crystallographically.²⁷⁴ This Pt(IV) alkyl hydride decomposes at 197°C (thermogravimetric analysis) and is stable for at least 2 h at 155°C . The ligand is clearly conferring an unusual stability to the molecule without the presence of excessive steric bulk. H/D exchange into the hydride and N–H sites but not into the Pt–CH₃ groups was seen in acetone-*d*₆ and methanol-*d*₄. This process is considered to be mediated by bases. The precursor ($\kappa^2\text{-tacn}$)PtMe₂ is itself a strong base, providing ($\kappa^3\text{-tacn}$)PtMe₂D⁺CD₃O[−] in methanol-*d*₄. The exceptional electron richness of ($\kappa^2\text{-tacn}$)PtMe₂ is underscored by the ease by which it undergoes rapid oxidation by air to give ($\kappa^3\text{-tacn}$)PtMe₂(OH)⁺ or ($\kappa^3\text{-tacn}$)PtMe₂(OH)₂²⁺ depending on the reaction conditions. These oxidations do *not* proceed via the intermediacy of ($\kappa^2\text{-tacn}$)PtMe₂H⁺ since this compound reacts only very slowly with O₂. The Me₃tacn and ⁱPr₃tacn ligands furnish Pt(IV) hydrides with analogous stabilities and reaction chemistry;^{275,276} the p*K*_a of ($\kappa^3\text{-}^i\text{Pr}_3\text{tacn}$)PtMe₂H⁺ has been estimated to be greater than 15 in methanol.

Vedernikov et al. used computational approaches to explore how the reactivity of square-planar d⁸ complexes toward C–H oxidative addition is affected by geometrical distortions. For example, distorting the geometry from square planar in the direction of a seesaw structure favors the oxidative addition. This is reminiscent of the effect of bending the structure of (PR₃)₂Pt⁰ away from linearity (see section 5.3). The computational results have served as a basis for the design of novel ligands that are tuned to optimize the reactivity of the C–H activating systems.^{277,278}

The [2.1.1]-(2,6)-pyridinophane (pyrphane) ligand system in Scheme 65 is a promising constrained-geometry system that confers a reactivity to Pt that is uniquely different from the tacn ligands above. The pyrphane geometry allows κ^2 coordination at a square-planar metal center, but due to geometrical con-

Scheme 65



straints, the pendant N donor is forced to be in close proximity to an axial site at the square plane. Filled-filled repulsions arise between the occupied d_{z^2} orbital on Pt and the N lone pair or ring π electrons of this pyridine ring.²⁷⁹ The ligand system is slightly oversized for an optimal fac κ^3 bonding mode in an octahedral environment, rendering κ^3 Pt(IV) species reactive by facilitating a κ^3 to κ^2 “slip” that accesses the necessary five-coordinate species.

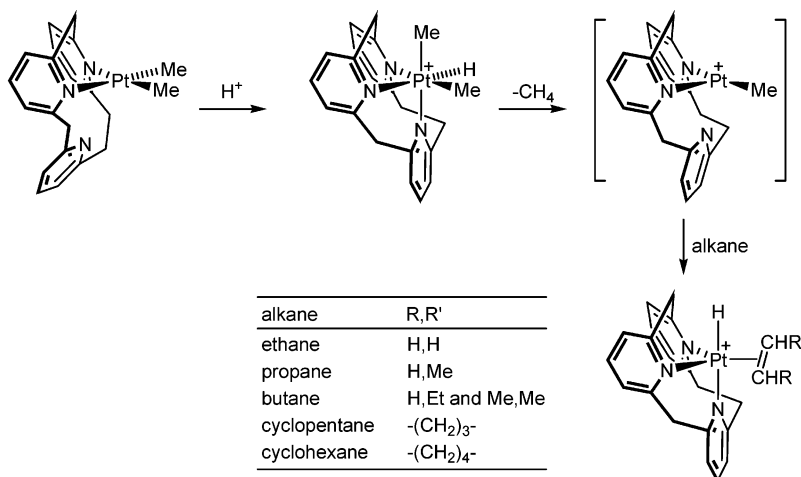
The PdCl₂ moiety binds in the κ^2 -symmetrical mode to the tetramethyl-substituted pyridinophane in Scheme 65, whereas PdCl₂ and PtMe₂ bind in the κ^2 -unsymmetrical mode to the unsubstituted pyrphane. The latter molecules are fluxional; for PtMe₂, the two ethylene-linked pyridine rings undergo site exchange with concurrent exchange of the two nonequivalent methyl sites.

According to DFT calculations²⁸⁰ the cationic Pt(IV) hydride (κ^3 -pyrphane)PtMe₂H⁺ (top center, Scheme 66) should allow kinetically facile ($\Delta G^\ddagger = 67$ kJ mol⁻¹) and thermodynamically only slightly uphill ($\Delta G^\circ = 46$ kJ mol⁻¹) elimination of methane to give the transient three-coordinate (κ^2 -pyrphane)PtMe⁺. The uncoordinated N in this species is located at a nonbonding distance, slightly more than 3 Å removed from Pt, according to DFT calculations.²⁸¹ Due to the constraints of the ligand system it cannot form the 16-electron square-planar and less reactive (κ^3 -pyrphane)PtMe⁺ cation. The Pt center is intermolecularly accessible for reactions that can be aided by

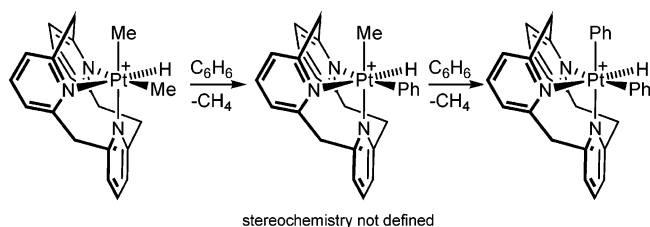
interactions with the nearby uncoordinated N atom. Accordingly, the unsymmetrical (κ^2 -pyrphane)PtMe₂ complex undergoes protonation at Pt with HOTf (anion exchange with NaBAR_F can be done) in CH₂-Cl₂ to give C_s -symmetric (κ^3 -pyrphane)PtMe₂H⁺X⁻ (X = OTf, BAR_F). Both salts eliminate methane to give a transient that reacts at the same rate, hence likely via the same rate-determining steps, with ethane, propane, *n*-butane, cyclopentane, and cyclohexane to give (κ^3 -pyrphane)Pt(alkene)H⁺ complexes in high yields (Scheme 66). Two diastereomers formed from propane (ca. 1:1), *n*-butane furnished two diastereotopic 1-butene complexes (81% combined), one *cis*-2-butene complex (5%), and two *trans*-2-butene complexes (14%). Heating at 100 °C led to decomposition of the 2-butene complexes and liberation of the 1-butenes, whereas the 1-butene complexes persisted in the same ratio as initially produced. No isomerization of the butene complexes occurred even at 100 °C, and the product ratio apparently reflects a kinetic selectivity for butane dehydrogenation.²⁸⁰ Only one cyclopentene and one cyclohexene product formed. The dehydrogenation presumably occurs by R–H oxidative addition, methane elimination, and β -elimination. It is not clear whether the 14-electron “T-shaped” species are truly involved (necessitating dissociative methane elimination) or whether methane is displaced by inter- or intramolecularly assisted associative mechanisms. It is interesting that in these C–H activation reactions it is the Pt(IV) hydride that is the reactant and the Pt(II) species that are intermediates, whereas the converse is true for all other C–H activating systems discussed thus far in section 6.

Benzene reacts with (κ^3 -pyrphane)PtMe₂H⁺BAR_F⁻ by a double benzene activation/methane elimination sequence to furnish the Pt(IV) diphenyl hydride (κ^3 -pyrphane)PtPh₂H⁺ (Scheme 67) via (κ^3 -pyrphane)Pt(Me)(Ph)(H)⁺. When (κ^3 -pyrphane)PtMe₂H⁺ reacts with C₆D₆ instead of C₆H₆, all isotopomers CH_{4-n}D_n of methane are detected by ¹H NMR. Thus, the C–H reductive coupling must be reversible, and Pt(II) intermediates with σ -methane and σ -benzene or π -benzene ligands are suggested.²⁸¹ An interesting experiment demonstrated unusual selectivity issues. When (κ^3 -pyrphane)PtPh₂H⁺BAR_F⁻ (and its equilib-

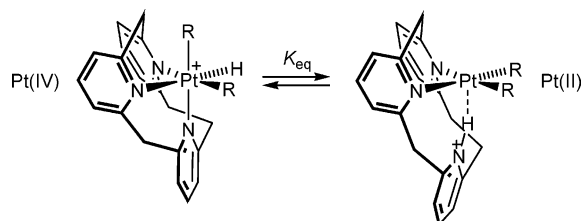
Scheme 66



Scheme 67



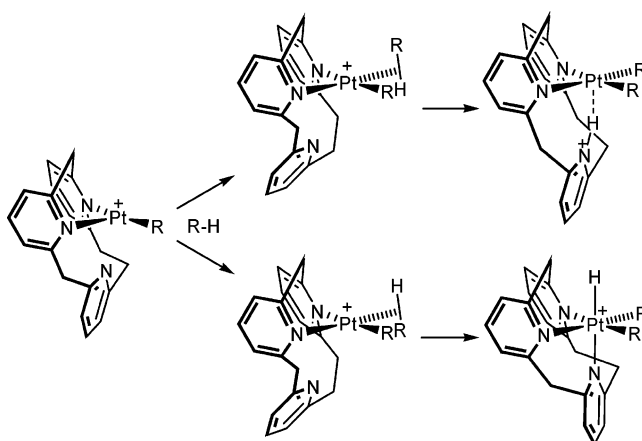
Scheme 68



rium tautomer, see below) was treated with cyclopentane in CD_2Cl_2 , the Pt(II) hydrido cyclopentene complex already depicted in Scheme 66 was formed during 3 days at 25 °C along with 2 equiv of benzene. Benzene activation at the Pt alkyl moiety therefore must be reversible; furthermore, the thermodynamic selectivity for alkane activation over arene activation is caused by the stability of the Pt(II) hydrido alkene complex. When $(\kappa^3\text{-pyrphane})PtMe_2H^+BAR_F^-$ is reacted with a 1.6:1 molar ratio of benzene and ethane, the diphenyl hydrido complex (and its tautomer) is quantitatively formed within 8 h at ambient temperature. During the next 4 days the Pt(II) hydrido ethene complex appeared to reach 10%. The kinetic preference appears to be in favor of benzene activation; however, the intrinsic reactivity of (pyrphane)-PtMe⁺ toward benzene and ethane may be masked by deactivation involving π -benzene complex formation.²⁸¹

Interestingly, the Pt(IV) diphenyl hydride is in equilibrium (NMR) with its Pt(II) diphenyl NH tautomer²⁸¹ in which the N–H bond is engaged in hydrogen bonding^{282–284} to Pt (Scheme 68). The ¹H NMR spectrum of the NH tautomer shows a characteristic low-field shift of N–H at δ 17.32 with $J_{Pt-H} = 86$ Hz. The equilibrium ratio of the two, Pt(IV) (left) to Pt(II) (right), was 1:9 at ambient temperature for R = Ph. The equilibrium shifted completely in favor of the N-protonated Pt(II) tautomer for R = C₆F₅ (prepared by C–H activation of pentafluorobenzene with $(\kappa^3\text{-pyrphane})PtMe_2H^+$).²⁸⁵ The Pt(IV) tautomer was undetected during the reaction and after prolonged heating at 80 °C, suggesting that the Pt(II) form is thermodynamically preferred. One might expect that the electron-withdrawing C₆F₅ has a stronger preference for the lower oxidation state and neutral Pt metal center than does C₆H₅. Accordingly, replacement of the phenyl groups with R = Me, a better donor, shifts the equilibrium in the opposite direction. At ambient temperature only the Pt(IV) form is seen. However, protonation of $(\kappa^2\text{-pyrphane})PtMe_2$ with HOTf in the presence of NaBAR_F in CD₂Cl₂ at –80 °C furnished 8% of the Pt(II) form and 4% symmetrical Pt(IV) and 88% unsymmetrical Pt(IV) tautomers; above –45 °C the mixture rapidly

Scheme 69

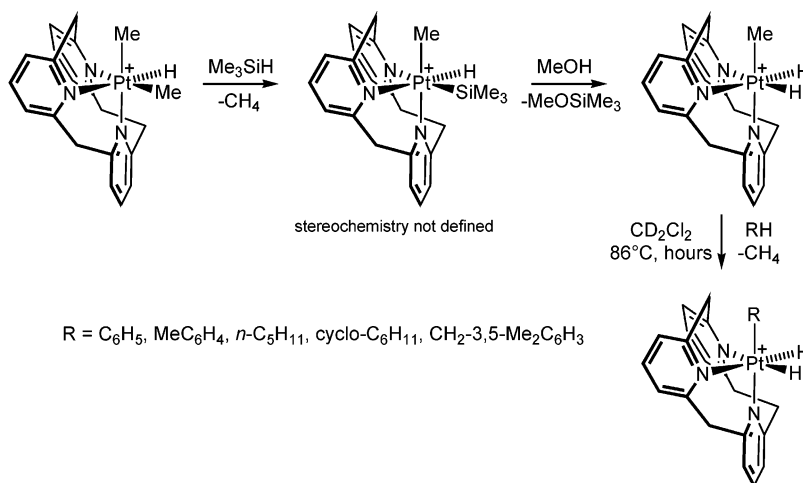


isomerized to the thermodynamically preferred symmetrical Pt(IV) tautomer.²⁸⁵

These findings have important implications regarding the mechanisms of hydrocarbon C–H activation. It is conceivable that at a given metal center alternative C–H activation mechanisms may operate dependent on the orientation of R–H relative to the pendant N group. When the proton is directed toward N, the C–H bond cleavage may be assisted by the N atom (Scheme 69, top). This represents an intramolecularly assisted electrophilic mechanism for the C–H activation. On the other hand, when the proton is oriented in the opposite direction, an oxidative addition mechanism may result, assisted by a lowering of the transition-state energy by the binding at Pt of the third pyridine N (bottom).²⁸⁵ When the Pt(II) and Pt(IV) tautomers are generated by protonation of $(\kappa^2\text{-pyrphane})PtR_2$, it is possible that two reaction channels operate—one in which protonation takes place at N (with subsequent transfer to the same side of the metal) and one that takes place directly at the metal, from the opposite side. It still remains to be unambiguously demonstrated if these parallel pathways for proton transfer are actually operative.

The $(\kappa^3\text{-pyrphane})PtMe_2H^+$ system cleaved two hydrocarbon C–H bonds, facilitated by the elimination of two molecules of methane. Starting with the methyl dihydride complex instead of the dimethyl hydride, single alkane C–H activation was possible,²⁸⁶ facilitated by methane elimination being kinetically and thermodynamically favored over H₂ elimination according to DFT calculations. The unsymmetrical air- and water-stable Pt(IV) methyl dihydride was prepared by an interesting Si–H activation/desilylation procedure (Scheme 70). This reaction is also interesting from a mechanistic viewpoint as it convincingly demonstrates that oxidative addition occurs at a cationic, electron-poor Pt(II) species. Reactions of $(\kappa^3\text{-pyrphane})PtH_2Me^+BAR_F^-$ with hydrocarbons in sealed tubes at 86 °C (1:1 hydrocarbon:CD₂Cl₂) led to products of single C–H bond activation and methane elimination. Benzene and cyclohexane gave the corresponding phenyl and cyclohexyl complexes. Interesting selectivity issues were addressed: *n*-pentane proceeded with selectivity for the terminal C–H bond. Toluene resulted in

Scheme 70



exclusive aromatic C–H activation (statistical 2:1 meta:para ratio; ortho not detected). Mesitylene, sterically encumbered to disfavor aromatic activation, yielded exclusive benzylic activation.

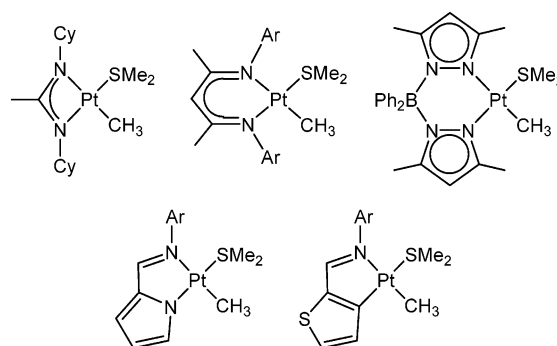
Reactions of (κ^3 -pyrphane)PtH₂Me⁺ with *n*-pentane and cyclohexane (Scheme 70) did *not* proceed to the Pt(II) hydrido alkene complexes, analogous to the reactions depicted in Scheme 66, but stopped after one C–H activation and methane elimination for the reasons given above. The alkane activation reactions were shown to be reversible. The Pt(IV) cyclohexyl complex reacted with *n*-pentane to give the Pt(IV) 1-pentyl complex and cyclohexane and vice versa. This demonstrated that primary and secondary C–H bond activation products could interchange during 3 h under the C–H bond activation conditions and strongly suggests that the preference for primary C–H bond activation in *n*-pentane is a thermodynamic preference. This does not rule out that the kinetic preference might also be for the same C–H bond.

7. Reactions at Pt Complexes with Anionic Donor Ligands

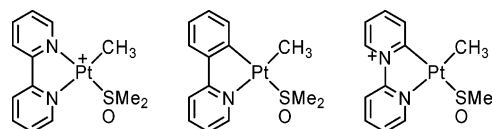
7.1. Anionic vs Neutral Ligands

The Shilov mechanism (Scheme 3) requires an oxidation of Pt(II) alkyl to Pt(IV) alkyl complexes. Experimental evidence has suggested that the cationic Pt complexes, based on neutral diimine and other N₂ ligands, are not very susceptible to oxidation.²⁸⁷ The presumption that *anionic* ligands would give *neutral* Pt(II) alkyls that should be more prone to oxidation has inspired efforts recently to explore the C–H activation chemistry of Pt complexes with a number of anionic ligands, mostly N donors. This led to the development of chemistry based on the anionic hydridotris(pyrazolyl)borate and diketiminate ligand systems. Recently, Bercaw and co-workers estimated the relative ease of oxidation of a range of complexes (Scheme 71) that bear anionic *N,N*- and *N,C*-chelating ligands.²⁸⁸ The relative ease of oxidation from Pt(II) L₂Pt(SMe₂)Me to Pt(IV) L₂PtI₂(SMe₂)Me was established by competition reactions with I₂ and measurements of equilibrium constants between pairs of Pt(II) methyl complexes and their corre-

Scheme 71



Scheme 72



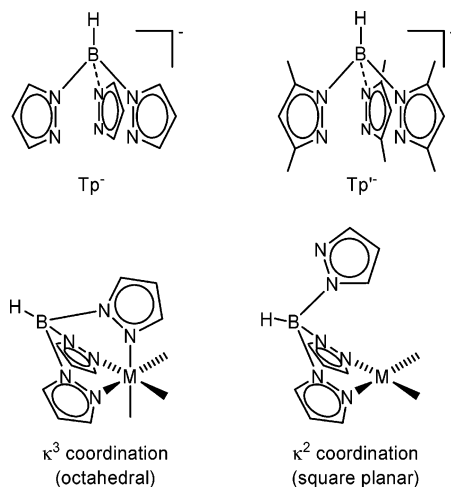
sponding Pt(IV) methyl diiodides. This is an interesting approach²⁸⁷ for quantifying the redox properties of complexes that frequently exhibit rather ill-defined responses during electrochemical oxidations.²⁸⁹ Initial results from C–H activation of benzene at some of these species have appeared²⁹⁰ and will be discussed at the end of this section.

Cyclometalated κ^2 -(C,X) heteroaromatic complexes are ubiquitous to Pt(II) chemistry (see references cited in ref 35). These anionic ligands that occupy two *cis* coordination sites are essentially unexplored as supporting ligands in C–H activation chemistry. Recently, Bercaw and co-workers²⁹¹ compared the substitution kinetics of substituted members of the Pt(II) complexes in Scheme 72. Substitution rates increased dramatically from left to right, and this creates interesting possibilities for C–H activation chemistry.

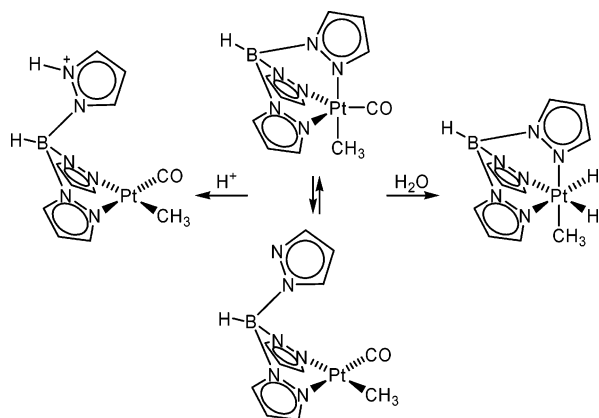
7.2. Reactions at Tp Complexes of Pt (Tp = Hydridotris(pyrazolyl)borate)

Hydridotris(pyrazolyl)borate (Tp) ligands are in widespread use in organometallic chemistry.^{292,293} With its constrained geometry, the Tp system is frequently coined an “octahedral enforcer ligand”, being perfectly suited for facial coordination at three

Scheme 73



Scheme 74

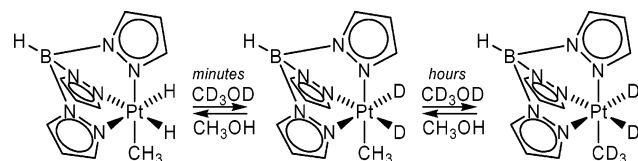


corners of an octahedron. This discussion will be mostly concerned with the parent Tp and the substituted hydridotrakis(3,5-dimethylpyrazolyl)borate analogue, Tp'. Although the κ^3 coordination mode is most commonly found and obviously applicable to d^6 Pt(IV) octahedral complexes, the κ^2 mode is also encountered and is particularly relevant to d^8 Pt(II) square-planar complexes (Scheme 73). Pt(IV) hydride and alkyl complexes that bear these ligands are well known, i.e., the thermally very stable trimethyl complexes TpPtMe₃²⁹⁴ and Tp'PtMe₃^{295,296} and the trihydride Tp'PtH₃.²⁹⁷ There appear to be no reports of thermal elimination of ethane from the trimethyl species or of H₂ from the trihydride. This contrasts the many reports of C–H elimination from mixed hydridoalkyl and aryl complexes, as will now be discussed. Parts of this chemistry have been recently reviewed.²⁹⁸

7.2.1. TpPtMeH₂ and Tp'PtMeH₂

The air- and moisture-stable dihydridomethyl complex TpPtMeH₂ has been obtained from reaction of TpPt(CO)Me with water.²⁹⁹ TpPt(CO)Me exists as rapidly interconverting pentacoordinated κ^3 and tetraordinated square-planar κ^2 forms in solution (Scheme 74);³⁰⁰ in the solid state the square-planar κ^2 form is assumed.^{139,301} Protonation of TpPt(CO)Me results in cleavage of a Pt–N bond to give the κ^2 structure that contains the N-protonated ligand (HTp). It is not known whether ligand protonation

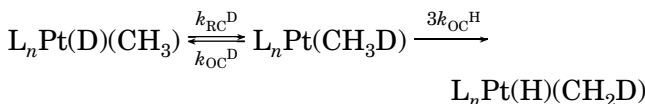
Scheme 75



occurs before or after “slippage” from a κ^3 to κ^2 coordination mode. Nevertheless, the facile κ^3/κ^2 interconversion of the Tp ligand system at Pt is important in the following chemistry.

TpPtMeH₂ has been reported by Keinan and co-workers to be stable toward elimination of methane even at 70 °C. However, heating at 55–70 °C in CD₃-OD leads to complete exchange of D for H into the hydride (<5 min) and methyl (hours) sites (Scheme 75).³⁰² (ansa-Tungstencene hydridomethyl complexes that undergo exchange without methane loss at even higher temperatures have been reported.^{57,74}) The exchange into Pt–H is straightforwardly explained by rapid, reversible proton transfer at Pt. The exchange into Pt–CH₃ implies a σ -methane intermediate for which the barrier toward methane dissociation is much greater than the barrier for the exchange (Figure 1 in section 1).

An inverse kinetic isotope effect $k^H/k^D = 0.76$ was observed for incorporation of D into the methyl site at 55 °C. It was argued that in past observations of inverse isotope effects in alkane eliminations the kinetic data reflected the overall rate of alkane elimination (including the reductive coupling and dissociation steps, see Scheme 7). The claim was made that the measured rate constant for TpPtMeH₂ and hence the inverse isotope effect must be associated with the H₃C–H(D) reductive coupling elementary step. This interpretation has been convincingly refuted by Parkin⁵⁷ and Jones⁵⁶ (see section 2.6 for background). The original Keinan analysis³⁰² was based on the premises that the scrambling reaction is (i) irreversible, which is clearly not the case, and (ii) one-step, which also is clearly not the case since the exchange results from C–D reductive coupling followed by C–H oxidative cleavage. This complicates the kinetics, as is readily seen when one considers that the σ -methane complex is a high-energy intermediate for which the steady-state approximation may be safely applied.³⁰³ The resulting k_{obs} in the rate law is a composite rate constant that involves the rate constants for the three elementary steps k_{RC}^D , k_{OC}^D , and k_{OC}^H



$$\begin{aligned} \text{Rate} &= \frac{d[\text{L}_n\text{Pt}(\text{H})(\text{CH}_2\text{D})]}{dt} = k_{\text{obs}}^D [\text{L}_n\text{Pt}(\text{D})(\text{CH}_3)] \\ &= \frac{3k_{\text{RC}}^D k_{\text{OC}}^H}{k_{\text{OC}}^D + 3k_{\text{OC}}^H} [\text{L}_n\text{Pt}(\text{D})(\text{CH}_3)] \end{aligned}$$

The factor 3 is included before k_{OC}^H to reflect the fact that the σ -methane complex has three C–H bonds that may be oxidatively cleaved but only one C–D bond.⁵⁷ A similar treatment applies to the exchange

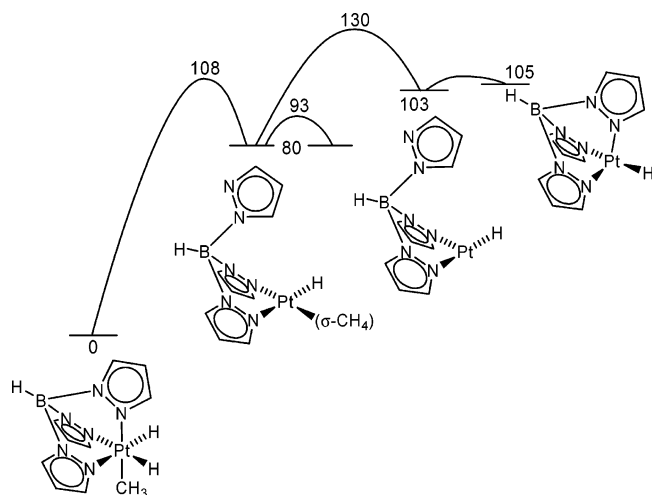


Figure 12. Energy diagram (kJ/mol) for reductive coupling of methane and methane dissociation, based on DFT-calculated data.

of $\text{TpPt}(\text{CD}_3)_2$ in MeOH. The resulting kinetic isotope effect will depend on $k_{\text{RC}}^{\text{H}}/k_{\text{RC}}^{\text{D}}$ as well as $k_{\text{OC}}^{\text{H}}/k_{\text{OC}}^{\text{D}}$, i.e., the observed isotope effect cannot simply express the isotope effect on the reductive coupling event alone.

In a subsequent addendum³⁰⁴ Keinan gives a modified expression for the isotope effect that clearly invalidates the original idea that the measured $k^{\text{H}}/k^{\text{D}}$ was that for the reductive coupling. Nevertheless, the claim is still made that “the observed isotope effect could represent the initial reductive-coupling step in the σ -methane intermediate”. Parkin analyzed the underlying assumptions and concluded that “it is evident that the experiment purported to determine an inverse isotope effect of 0.76 for the reductive coupling of TpPtMeX_2 ($\text{X} = \text{H}, \text{D}$) is erroneous and that the system does not provide the claimed unprecedented opportunity to study the initial step of reductive coupling in alkyl hydride compounds”. Thus, to date there are no unambiguous reports of inverse H/D isotope effects for proven one-step C–H reductive cleavage or elimination reactions.

The slow exchange and elimination from TpPtMeH_2 contrasts the rapid processes that are clearly involved at much lower temperatures in the cationic Pt hydridoalkyl and hydridoaryl systems that have been discussed already. The relative propensity for methane elimination vs H/ CH_3 scrambling in TpPtMeH_2 has been investigated by DFT calculations (Figure 12).³⁰⁵ The calculations indicated barriers of 130 kJ/mol for methane loss and 108 kJ/mol for H/ CH_3 scrambling. The difference, $\Delta\Delta G^\ddagger_{298} = 22$ kJ/mol, is consistent with the experimentally observed

complete exchange without methane loss. The barrier for “rotation” of the σ - CH_4 ligand was 13 kJ/mol. Methane rotation, which is a prerequisite for the scrambling, is therefore rapid compared to the oxidative cleavage. The reluctance toward methane dissociation is attributed to the instability of the product TpPtH for which two isomers of very similar energies were possible according to calculations: the three-coordinate κ^2 and a four-coordinate κ^3 form with a distorted seesaw geometry. The overall unfavorable energy of the reaction is imposed by the geometrical constraints of the Tp ligand, which cannot support the preferred square-planar geometry of the Pt(II) product. In comparison, the tris-ammonia complex $(\text{NH}_3)_3\text{Pt}(\text{Me})\text{H}_2^+$ undergoes a more favorable methane loss since the square-planar geometry of the product $(\text{NH}_3)_3\text{PtH}^+$ can be readily accessed.

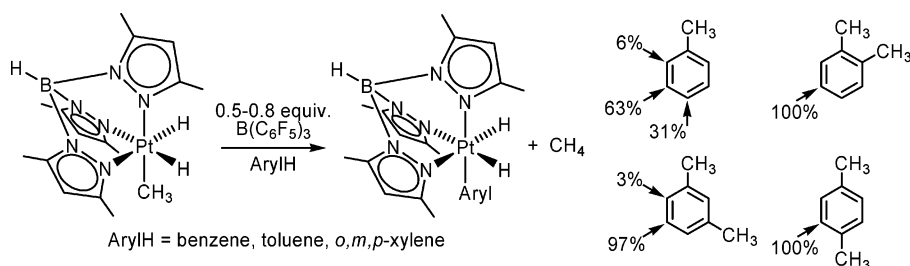
Treatment of $\text{Tp}'\text{PtMeH}_2$ with $\text{H}(\text{OEt}_2)_2\text{BAR}_F$ in CD_2Cl_2 at -78 °C led to protonation at a pz' -N with concomitant sidearm decomplexation and elimination of methane and provided the solvento complex $(\kappa^2\text{-HTp}')\text{Pt}(\text{H})(\text{Solv})^+\text{BAR}_F^-$ where Solv is probably ether and $\text{HTp}' = \text{N-protonated Tp}'$.³⁰⁶ No D incorporation into methane was detected when $\text{D}(\text{OEt}_2)_2\text{BAR}_F$ was used. Protonation of $\text{Tp}'\text{PtMeD}_2$ with $\text{H}(\text{OEt}_2)_2\text{BAR}_F$ furnished both CH_2D_2 and CH_3D by ^1H NMR, suggesting reversible formation of a σ -methane complex prior to methane loss. The data are consistent with protonation exclusively at N and H/D exchange between Pt–H and Pt– CH_3 but not with the medium. Analogous behavior is seen for $\text{Tp}'\text{PtMe}_2\text{H}$ (see section 7.2.2).

Aromatic C–H activation was observed when $\text{Tp}'\text{PtMeH}_2$ was treated with substoichiometric amounts of $\text{B}(\text{C}_6\text{F}_5)_3$ in benzene, toluene, and xylenes (Scheme 76).³⁰⁷ Toluene gave ca. 94% meta- and para-activated products (2:1 ratio) and 6% ortho. Single isomer products were observed for *o*-xylene and *p*-xylene; *m*-xylene gave mostly the 3,5-dimethylxylyl isomer with trace amounts of the 2,4-dimethylxylyl complex. Steric factors appear to direct the reactions. Benzylic activation was not reported for any of these reactions, contrasting the behavior of sterically hindered (diimine)Pt complexes (see section 6.6). The role of $\text{B}(\text{C}_6\text{F}_5)_3$, which worked in substoichiometric quantities, has not been assessed. Borane-assisted pz' dissociation (analogous to pz' -N protonation), methyl anion abstraction, or reactions with the acid $\text{H}(\text{HOB}(\text{C}_6\text{F}_5)_3)$ arising from the borane and adventitious water must be considered.

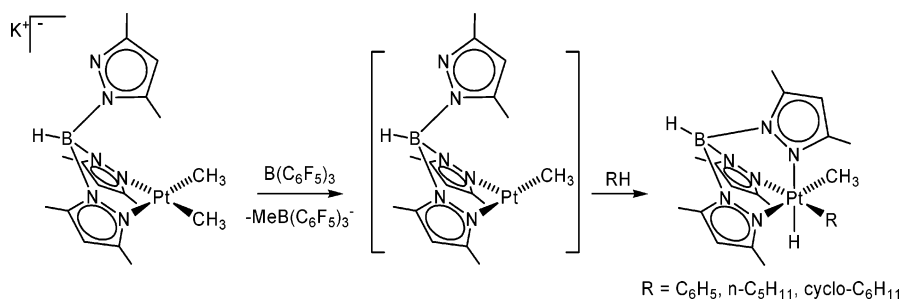
7.2.2. TpPtMe_2H and $\text{Tp}'\text{PtMe}_2\text{H}$

Canty reported the preparation of $\kappa^3\text{-TpPtMe}_2\text{H}$ by protonation of $[\kappa^2\text{-TpPtMe}_2]^- \text{K}^+$ with phenol.³⁰⁸ Model

Scheme 76



Scheme 77



system calculations suggested that protonation was favored at Pt rather than at pyrazole N by 92 kJ/mol, and no local energy minimum was identified for the five-coordinate dimethyl hydride complex. The preferred protonation at Pt contrasts with the behavior of TpPt(Me)(CO) (see above), which was protonated at pz-N. Thermal decomposition of TpPtMe₂H in toluene gave methane and Pt metal within 10 min at 150 °C. TpPtMe₂H was stable in acidic solution but reacted in basic aqueous acetone to reform (κ^2 -Tp)PtMe₂⁻ and, more slowly, the oxidation product (κ^3 -Tp)PtMe₂(OH).

Tp'PtMe₂H and Tp'PtPh₂H were obtained by protonation of [Tp'PtR₂]⁻K⁺ with HCl.³⁰⁹ Tp'PtPh₂H did not decompose nor did it incorporate toluene after 15 h in toluene at reflux. The dimethyl hydride Tp'PtMe₂H, characterized by X-ray crystallography, was also robust with respect to methane elimination in solution or as a solid. Thermogravimetric analysis (TGA) of Tp'PtPh₂H indicated decomposition at *T* > 230 °C by a process that did not correspond to simple benzene elimination. Tp'PtMe₂H decomposed at ca. 190 °C. The thermal robustness of these species was attributed to (1) the reluctance to form the required five-coordinate intermediate and (2) the inaccessible square-planar geometry in the resulting Tp'PtX residue.

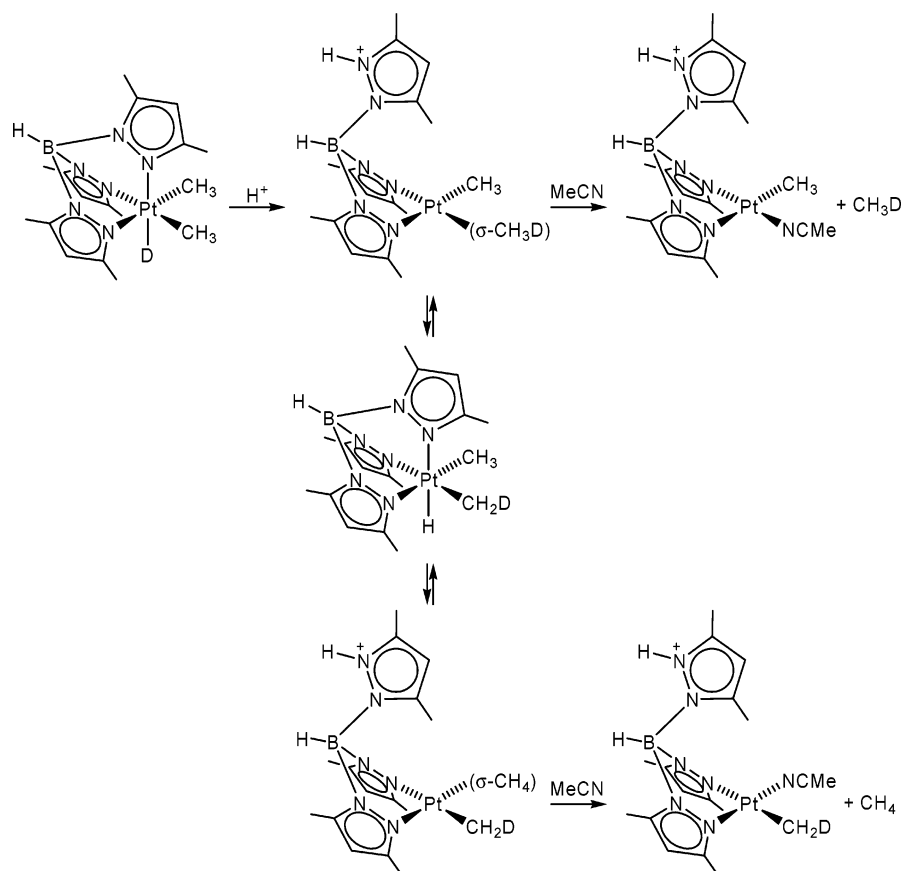
The reluctance of Tp'PtR₂H species to undergo RH extrusion suggested that hydrocarbon addition might be observed at (κ^2 -Tp')PtR₂ precursors after appropriate activation. Coordination of a pendant pz'-N should contribute favorably to the overall thermodynamics. Thus, Wick and Goldberg³¹⁰ found that methyl anion abstraction from [κ^2 -Tp'PtMe₂]⁻K⁺ with the highly electrophilic borane reagent B(C₆F₅)₃ MeB(C₆F₅)₃⁻ was seen by ¹¹B NMR generated a transient intermediate "Tp'PtMe" that reacted with a range of hydrocarbons according to Scheme 77. Reaction with C₆D₆ produced Tp'PtMe(D)(C₆D₅). Reaction with pentane occurred selectively at the terminal carbon. The proposed mechanism involved the formation of the reactive three-coordinate Tp'PtMe, oxidative addition (presumably via a σ -RH complex) to give five-coordinate κ^2 -Tp'Pt(Me)(R)(H), and intramolecular trapping by the pendant sidearm of the Tp' ligand to give the stable Pt(IV) octahedral product. This sequence is in accord with the principle of microscopic reversibility—reductive elimination of RH from the product would proceed dissociatively, as discussed in section 7.2.1.

Electrophilic activation of Tp'PtMe₂H might also constitute a means for activating the Pt(IV) system

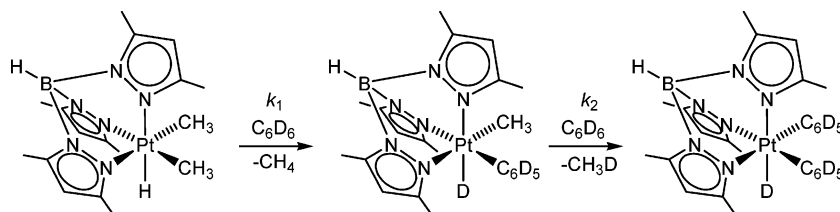
since formal abstraction of H⁻ or Me⁻ would generate a five-coordinate species. Protonation of Tp'PtMe₂H with H(OEt₂)₂BAR_F in CD₂Cl₂ at -78 °C led to formation of methane and (κ^2 -HTp')Pt(Me)(ClCD₂-Cl)⁺BAR_F⁻.³¹¹ The CD₂Cl₂ ligand was quantitatively displaced by MeCN and other two-electron donors. Interestingly, treatment of Tp'PtMe₂H with D(OEt₂)₂BAR_F also produced CH₄; no D was incorporated into methane or the remaining Pt–Me group. A broad resonance was observed in the ²H NMR spectrum, indicative of deuteration at pz'-N. Furthermore, Tp'PtMe₂D reacted with H(OEt₂)₂BAR_F to give a ca. 1:1 ratio of CH₃D and CH₄ as well as Pt–CH₃ and Pt–CH₂D signals. The results establish that protonation occurs exclusively at a pz'-N rather than at Pt, Pt–Me, or Pt–H sites. It was surmised that protonation occurred after pz' decoordination, although this was not verified by experiment. The H/D scrambling between D and CH₃ implies reversible coupling to give Pt σ -methane intermediates (Scheme 78). The greater than statistical amount of CH₃D indicates incomplete scrambling, i.e., methane dissociation and reductive coupling occur at similar rates.

Thermolysis of Tp'PtMe₂H in C₆D₆ at 110 °C resulted in two successive methane elimination/benzene addition reactions (Scheme 79).³¹² The kinetics were quite well described by two successive unimolecular reactions, although small systematic deviations were observed. Some CH₂D₂ was formed after an induction period, and H incorporation into the Pt–D sites of the products and D incorporation into Pt–phenyl were also seen. The H/D scrambling and the kinetics were reconciled with rapid exchange between the hydride and methyl positions and slower exchange between the hydride and phenyl positions in the Tp'Pt(Me)(Ph)H intermediate. Accordingly, thermolysis of Tp'Pt(CD₃)₂D in C₆D₆ resulted in improved fit of the kinetic data. Inverse kinetic isotope effects were observed for both steps: $k^H/k^D = 0.81 \pm 0.03$ for k_1 and $\leq 0.78 \pm 0.03$ for k_2 . The kinetic data (90–130 °C) yielded $\Delta H_1^\ddagger = 147 \pm 5$ kJ mol⁻¹ and $\Delta S_1^\ddagger = 54 \pm 13$ J K⁻¹ mol⁻¹ (step 1) and $\Delta H_2^\ddagger = 142 \pm 4$ kJ mol⁻¹ and $\Delta S_2^\ddagger = 46 \pm 13$ J K⁻¹ mol⁻¹ (step 2). Each step is believed to occur by sidearm pz' dissociation, so the data reflect the energetics of methane reductive elimination and pz' sidearm dissociation. Nearly identical activation parameters were found in toluene, which gave primarily meta and para activated products. Thermolysis in C₆F₆/CD₃CN led to (κ^2 -Tp')Pt(Me)(NCCD₃) at a rate that was insensitive to changes in [CD₃CN] (0.56–4.9 M); k_{obs} -

Scheme 78



Scheme 79



(110 °C) was very close to that in C₆D₆. Finally, the observed thermolysis rate in cyclohexane was also close to that in C₆D₆ even in the presence of PPh₃; cyclohexane—evidence of cyclohexane C–H activation—was the major organic product. Thus, the rate of methane elimination is essentially solvent independent. The rate-limiting step for these reactions is believed to be decoordination of a pz' ring and reductive C–H coupling to yield a (κ^2 -Tp')Pt(CH₃)(σ -CH₄) intermediate that leads to the products by oxidative addition (hydrocarbon solvents) or methane substitution (acetonitrile).

Evidence for the (κ^2 -Tp')Pt(CH₃)(σ -CH₄) intermediate was obtained through H/D scrambling in Tp'Pt-(CH₃)₂D at temperatures well below those required for methane elimination. This behavior is entirely analogous to that of TpPtMeH₂, described in section 7.2.1. The rate of scrambling was monitored at 46–66 °C and resulted in $\Delta H_{\text{scr}}^\ddagger = 109 \pm 4 \text{ kJ mol}^{-1}$ and $\Delta S_{\text{scr}}^\ddagger = 4 \pm 13 \text{ J K}^{-1} \text{ mol}^{-1}$. The difference in activation enthalpies for methane reductive elimination (147 kJ mol⁻¹) and reductive coupling (109 kJ mol⁻¹) provides a *minimum* binding enthalpy for methane in the Pt-(σ -CH₄) intermediate of 38 kJ

mol⁻¹ provided that formation of the Pt-(σ -CH₄) adduct from Tp'PtMe and CH₄ is almost barrierless (Figure 13). If the activation barrier toward oxidative cleavage is very low, this value should be close to the true value. If the oxidative cleavage barrier is significant, then the binding energy will be correspondingly higher. The calculated barrier for the reductive cleavage in the TpPtMeH₂ system (Figure 12) is ca. 28 kJ mol⁻¹; the combined data suggest that σ -methane intermediates might be sufficiently stable to be detected spectroscopically if generated by suitable methods.

The rate-limiting step in these reactions is methane elimination. One interesting question is whether methane loss occurs associatively or dissociatively (Scheme 80). The independence of the overall reaction rate on the identity of the solvent (benzene, toluene, cyclohexane, acetonitrile/C₆F₆) suggests that the solvent does not assist the elimination on the microscopic level, and therefore, a dissociative process was favored.³¹² The substantially positive ΔS^\ddagger of 54 J K⁻¹ mol⁻¹ also supports this conclusion. However, the data do not rule out substitution that is assisted by the pendant pz' group, i.e., an intramolecular as-

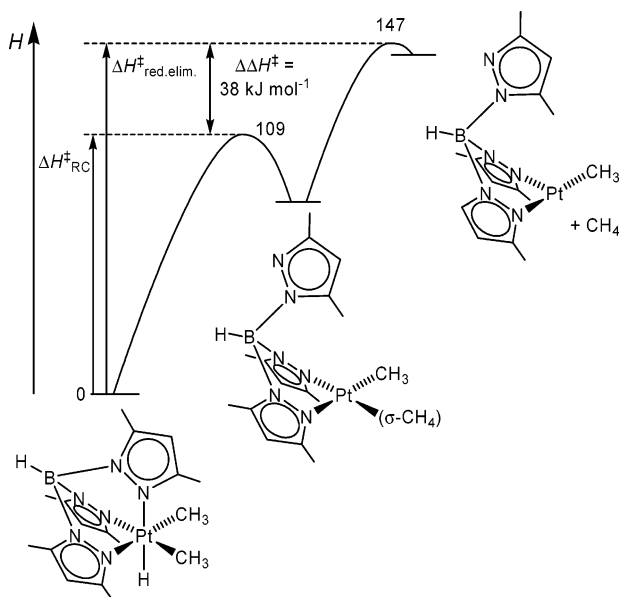
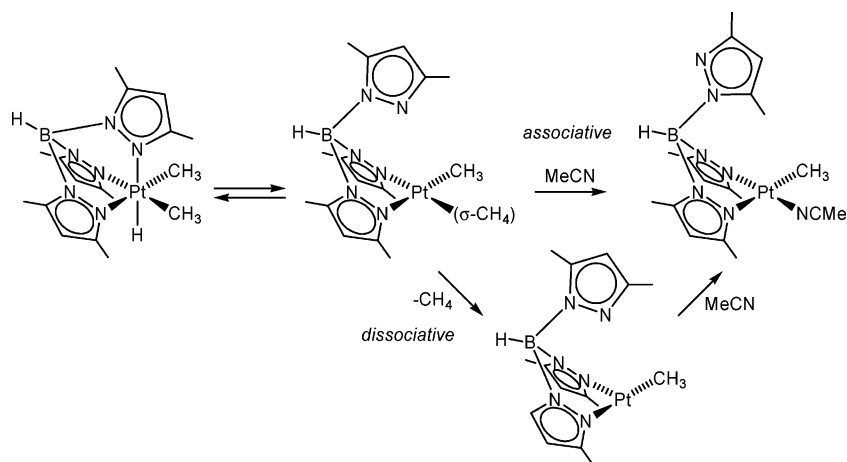


Figure 13. Energy diagram (kJ/mol) based on experimental data for reductive coupling and reductive elimination of methane from $\text{Tp}'\text{PtMe}_2\text{H}$ in benzene.

sociative substitution or interchange displacement of methane. Some support for the interchange mechanism was provided by the DFT calculations on TpPtMe_2H (Figure 12).³⁰⁵ A true dissociative behavior is at odds with the commonly observed associative substitution behavior of square-planar Pt(II) complexes. However, the Tp systems are neutral and hence less electrophilic at Pt, so a switch to dissociative behavior as seen for numerous neutral Pt complexes with strong donors trans to the leaving group^{63,313–315} might be anticipated. It has also been reported that arene displacement from a neutral Ir(I) complex occurs dissociatively.³¹⁶

In an interesting case of simultaneous Si–H activation and C–H elimination, $\text{Tp}'\text{PtMe}_2\text{H}$ reacts with Et_3SiH solvent at reflux (108 °C) to give modest yields of $\text{Tp}'\text{Pt}(\text{SiEt}_3)\text{H}_2$,²⁹⁷ which underwent subsequent methanolysis to $\text{Tp}'\text{PtH}_3$. The proposed pathway for the dihydride formation, supported by the observation of MeSiEt_3 , is shown in Scheme 81. It is reasonable, but not addressed by the authors, that κ^3/κ^2 Tp interconversions are involved in the transformations.

Scheme 80



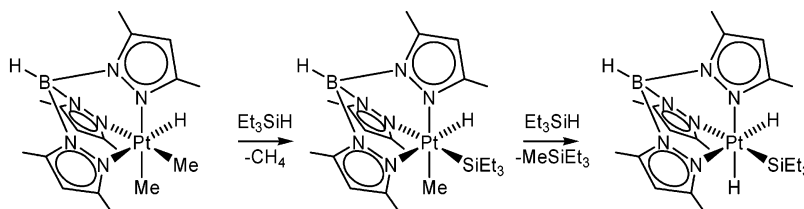
Interestingly, N-protonation of $\text{Tp}'\text{Pt}(\text{SiEt}_3)\text{H}_2$ furnished the five-coordinate Pt(IV) complex $(\kappa^2\text{-HTp}')\text{-Pt}(\text{SiEt}_3)\text{H}_2^+$ (Scheme 82). This and analogous species are also available by protonation of $\text{Tp}'\text{PtMe}_2\text{H}$ in the presence of HSiR_3 ($\text{R}_3 = \text{Et}_3, \text{Ph}_3, \text{Ph}_2\text{H}$).³¹⁷ Although the hydrides at Pt were not located in the X-ray structure, the bond angles at Si were near tetrahedral with no deformations that would indicate an η^2 -(Si,H) silane σ -complex. The products constitute rare³¹⁸ cases of five-coordinate Pt(IV) complexes. The unusual structures are likely stabilized by the combined effects of a strongly trans-labilizing silyl group, the steric bulk of the HTp' and silyl ligands, the large weakly interacting BAR_F^- anion, and the fact that although the complexes are positively charged the charge does not reside at Pt. Another example of a crystallographically characterized five-coordinate Pt(IV) complex bearing a diketimate ligand (see section 7.4) appeared in the same issue of the *Journal of the American Chemical Society*.³¹⁹

7.2.3. $\text{Tp}'\text{Pt}(\text{Ar})\text{H}_2$

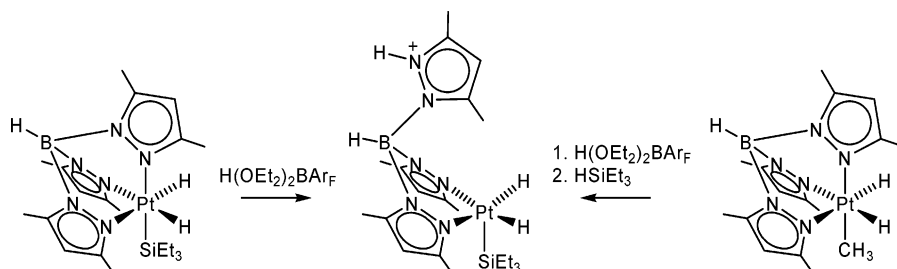
Protonation of $\text{Tp}'\text{Pt}(\text{Ph})\text{H}_2$ with $\text{H}(\text{OEt}_2)_2\text{BAR}_F$ in CD_2Cl_2 at -78 °C induced reductive C–H coupling to yield the chiral, square-planar Pt(II) η^2 -benzene complex $(\kappa^2\text{-HTp}')\text{Pt}(\eta^2\text{-C}_6\text{H}_6)(\text{H})^+\text{BAR}_F^-$, characterized by X-ray crystallography.⁸⁷ Analogous η^2 -arene complexes of toluene and *p*-xylene (X-ray) were prepared (Scheme 83).⁸⁶ The arene ligands were relatively strongly bonded—no exchange of added C_6D_6 for coordinated benzene occurred in **A**, even after 2 days at -30 °C. Slow, irreversible loss of arene to provide a dicationic hydride-bridged Pt dimer³⁰⁶ occurred at ca. 0 °C for **A**, **B**, and **C**.^{86,87}

The NMR spectra of these species exhibited interesting dynamic features. The spectra of the η^2 -benzene complex **A** indicated that the Pt was rapidly migrating around the benzene ring, even at -130 °C.⁸⁶ At -21 °C the ^1H NMR spectrum exhibited broadened $\eta^2\text{-C}_6\text{H}_6$ and Pt–H resonances, indicating H exchange between these groups. Spin-saturation transfer was observed from -74 to -22 °C and provided kinetic data $\Delta H^\ddagger = 49 \pm 2$ kJ mol $^{-1}$ and $\Delta S^\ddagger = -16 \pm 8$ J mol $^{-1}$ K $^{-1}$. It is likely that the Pt–H/ C_6H_6 exchange occurs via rapid, reversible oxidative cleavage of a C–H bond of coordinated benzene to

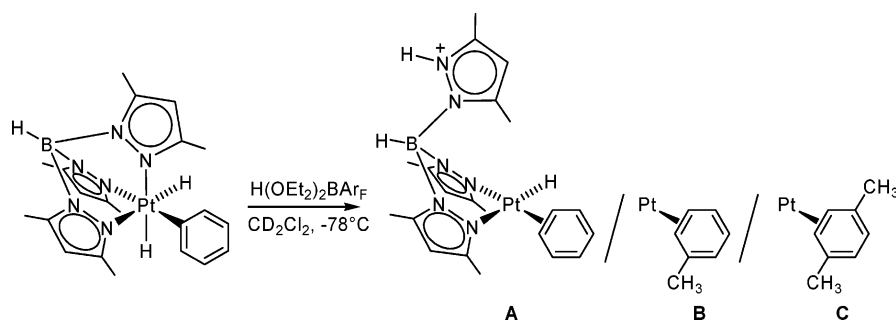
Scheme 81



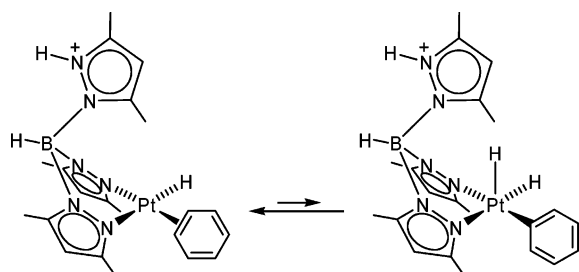
Scheme 82



Scheme 83



Scheme 84



furnish a Pt(IV) phenyl dihydride complex in which scrambling of the two hydrides must occur (Scheme 84). The involvement of η^2 -arene complexes as intermediates in arene C–H activation was discussed in section 2.4. The H/D kinetic isotope effect for the exchange process was 3.0 at $-14\text{ }^\circ\text{C}$ by comparison of the exchange rate of **A** (^1H NMR line broadening) with that of the Pt–D/C₆D₆ analogue **A-d₇** (^2H NMR spin saturation transfer). The large and normal kinetic isotope effect is consistent with considerable C–H(D) bond cleavage in the rate-limiting transition state.

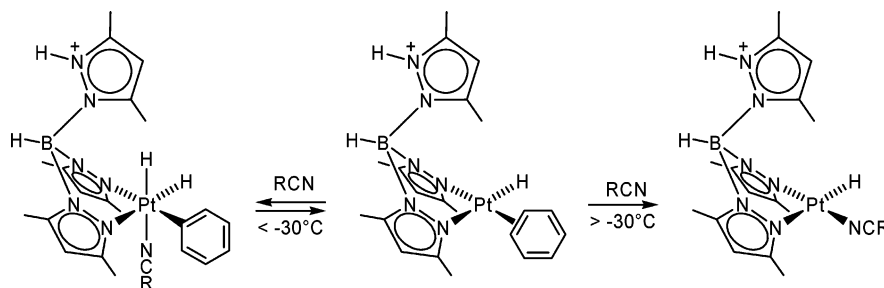
The toluene adduct **B** in Scheme 83 gave rise to five separate aromatic signals in the ^1H NMR spectrum at $-80\text{ }^\circ\text{C}$. This is expected because of the chirality of the complex and will persist even with rapid migration of Pt around one face of the aromatic ring. The two *m*-H resonances underwent coalescence ($\Delta G^\ddagger = 57\text{ kJ mol}^{-1}$) as did the two *o*-H resonances while the *p*-resonance remained unchanged at -12

$^\circ\text{C}$. This symmetrization was rationalized in terms of relatively rapid rotation around a Pt–aryl σ bond in a *p*-tolyl intermediate arising from oxidative cleavage of the para C–H bond in **B**. Spin-saturation transfer was observed from Pt–H into the para and two meta (to a different extent into each) hydrogens of the toluene ligand but not to the ortho or benzylic C–H bonds. The estimated barriers ($\Delta G^\ddagger = 55\text{--}57\text{ kJ mol}^{-1}$) were believed to reflect a slight kinetic preference for para activation. In comparison, a kinetic preference for para relative to meta and benzyl (4:2:3 ratio) activation of toluene was seen at the Tp⁺Rh(CNCH₂^tBu) moiety at ambient temperature; the thermodynamic ratio ($100\text{ }^\circ\text{C}$) was a statistical 2:1 meta-to-para ratio.²⁶²

The *p*-xylene complex **C** in Scheme 83 exhibited distinct NMR resonances for each arene-H, each arene-CH₃, and each arene-C at $-90\text{ }^\circ\text{C}$. The migration of Pt around the arene ring must therefore be slow. At temperatures above $-40\text{ }^\circ\text{C}$ the two aryl-CH₃ groups were averaged and two arene-H signals were observed. The behavior is consistent with rapid Pt migration around the ring ($\Delta G^\ddagger = 39\text{ kJ mol}^{-1}$) but not with a face-flipping process.⁸⁶ Line broadening of the arene-H and Pt–H resonances at $-1\text{ }^\circ\text{C}$ indicated reversible C–H oxidative cleavage akin to Scheme 84 with a barrier $\Delta G^\ddagger = 60\text{ kJ/mol}$.

Although the putative five-coordinate intermediates in these C–H oxidative cleavage reactions have not been directly observed, additional evidence for their existence has been recently provided.²⁵² When

Scheme 85



the π -benzene complex was generated at low temperature and nitriles RCN (R = Me, t -Bu, p -X-C₆H₄) were subsequently added, the ensuing reaction was not a simple substitution of nitrile for benzene but rather trapping of the Pt(IV) phenyl dihydride as its hexacoordinate nitrile adduct (Scheme 85). Temperature-dependent equilibria between the Pt(II) and the Pt(IV) species were observed and quantified from -80 to -30 °C. The equilibria were exothermic ($\Delta H^\circ = -17$ to -21 kJ mol⁻¹), and a plot of $\log K_{\text{eq}}$ vs σ_p for a series of aromatic nitriles gave a Hammett ρ value of -1.8 , i.e., Pt(IV) is favored by more electron-rich nitriles. Accordingly, slightly greater K_{eq} values were observed for alkyl nitriles than benzonitriles. The activation barrier for the interconversion between Pt(II) π -benzene and Pt(IV) hydridophenyl MeCN adduct was determined by spin-saturation transfer from the Pt(II) π -benzene ligand to Pt(IV)–H at -43 °C. The reaction coordinate diagram in Figure 14 was constructed on the basis of these data and those established for the oxidative cleavage, described above.

At temperatures above -30 °C the Pt(II)/Pt(IV) equilibrium was perturbed by irreversible displacement of η^2 -benzene by nitrile to provide Pt(II) nitrile adducts (Scheme 85). The energetics of this process have not been reported nor is it not known whether

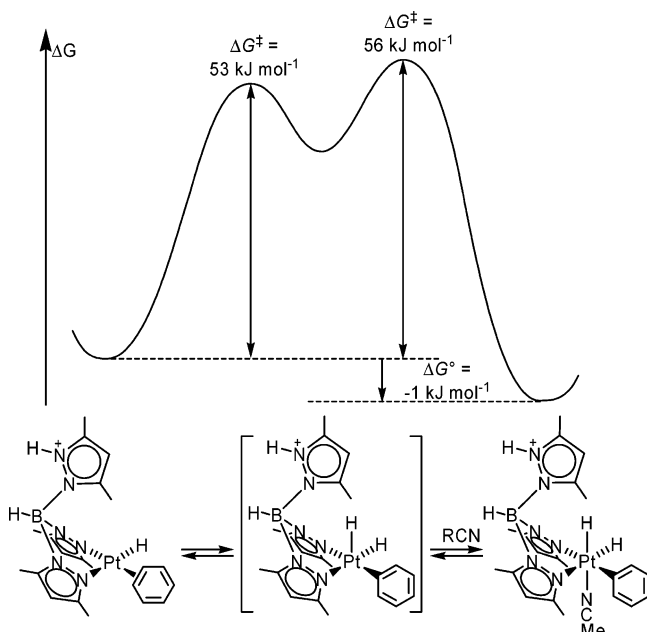


Figure 14. Reaction coordinate diagram for the equilibrium between Pt(II) hydrido π -benzene and Pt(IV) dihydrido phenyl complexes in acetonitrile.

the displacement of benzene by nitrile occurs associatively or dissociatively, so it is not clear whether these reactions may lead to estimates of Pt–(π -arene) bond energies in the way that Pt–(σ -methane) bond energies were estimated for the Tp’PtMe₂H system. It is interesting that reversible trapping occurs for the five-coordinate Pt(IV) species here, in contrast with the irreversible trapping that was observed at low temperatures for the cationic diimine complexes in section 6.1. A possible reason is that nitrile bonding at the neutral Pt(IV) center in the Tp’ system is weaker than at the positively charged Pt center in the diimine systems.

7.2.4. Tp’PtAr₂H

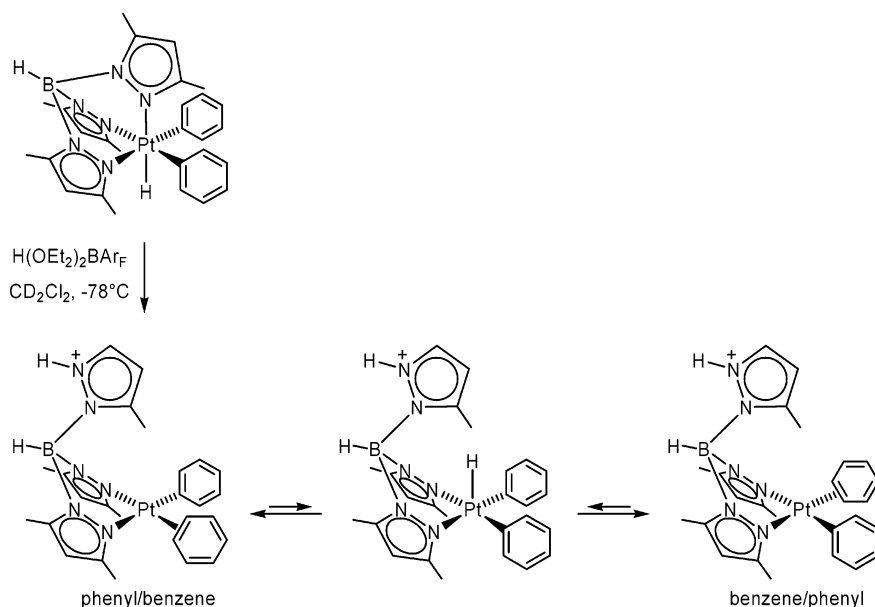
Canty³⁰⁸ reported that an acid as strong as acetic acid was required for protonation of [κ^2 -TpPt(p -Tol)₂]⁻K⁺ to provide κ^3 -TpPt(p -Tol)₂H. The ditolyl complex decomposed in nitrobenzene-*d*₅ to give toluene and trace amounts of ditolyls along with “TpPtMe oligomer”,³²⁰ i.e., Pt metal was not deposited during the thermolysis.

Protonation of Tp’PtPh₂H occurred at a pz’ N atom and provided the chiral (κ^2 -HTp’)Pt(Ph)(η^2 -C₆H₆)⁺ (Scheme 86).⁸⁶ The benzene ligand was considerably more weakly bonded than in (κ^2 -HTp’)Pt(H)(η^2 -C₆H₆)⁺ (Scheme 83), slowly dissociating to form a solvento complex even at -90 °C and in less than 24 h at -30 °C. A dynamic process caused averaging of the two Pt-bonded pz’ groups by ¹H NMR at $T_c = -17$ °C. Spin-saturation transfer was observed between the Pt–(C₆H₆) and Pt–C₆H₅ resonances. In analogy with the complexes above, an oxidative cleavage of a benzene C–H bond is proposed to explain this behavior (Scheme 86). The activation barrier was estimated at $\Delta G^\ddagger = 54$ kJ mol⁻¹, and a H/D kinetic isotope effect of 4.7 was measured by comparison of the Pt(C₆H₆)(C₆H₅) and Pt(C₆D₆)(C₆D₅) complexes at -32 °C. By analogy with the Pt hydride π -benzene complex described above, the Pt phenyl π -benzene complex undergoes reversible trapping as its Pt(IV) hydridodiphenyl isomer by nitriles at temperatures below -30 °C.²⁵²

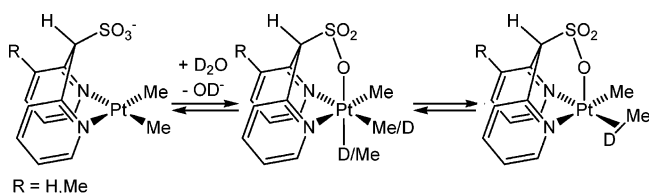
7.3. Reactions at a fac-Chelating Sulfonated Di(pyridyl) System

Vedernikov and co-workers recently³²¹ described the use of a novel sulfonated di(pyridyl) ligand system (L) that can act as a κ^2 (N,N) or κ^3 (N,N,O) donor toward Pt (Scheme 87). The potassium salt K(κ^2 -L)-PtMe₂ exists as equilibrating endo (shown) and exo

Scheme 86



Scheme 87



(not shown) isomers in methanol; the pendant sulfonate group gains stabilization by hydrogen bonding to the solvent, and the κ^2 coordination mode is favored. Reversible H/D exchange into the Pt–Me groups was observed in methanol- d_4 and mixtures with D_2O , implying facile ($\Delta G^\ddagger = 95 \text{ kJ mol}^{-1}$) and reversible protonation and reductive C–H coupling without methane elimination. The Pt(IV) hydrido-dimethyl complex ($\kappa^3\text{-L}$)PtMe₂H was isolated by extraction with dichloromethane or protonation with HOTf and was crystallographically characterized; the κ^3 coordination mode is favored in less polar media. Hydrolysis of K($\kappa^2\text{-L}$)PtMe₂ in D_2O furnished methane and K($\kappa^2\text{-L}$)Pt(Me)(OD), whereas hydrolysis of the isolated Pt(IV) hydride produced ($\kappa^2\text{-L}$)Pt(Me)(H₂O). The latter did not undergo methyl exchange with $^{13}\text{CH}_4$ after 1 week at ambient temperature in water. Although ($\kappa^3\text{-L}$)PtMe₂H decomposed during attempted reactions with benzene in dichloromethane for R = H (see Scheme 87), the benzene C–H activation product ($\kappa^3\text{-L}$)Pt(Me)(Ph)(H) was obtained for R = Me. Even more impressive, with R = Me, ($\kappa^3\text{-L}$)PtMe₂H reacted with $^{13}\text{CH}_4$ (2 atm) in CH_2Cl_2 to give the ^{13}C isotopomer with 10% enrichment after 30 h. This work established interesting ties between nonaqueous and aqueous Shilov-type chemistry.

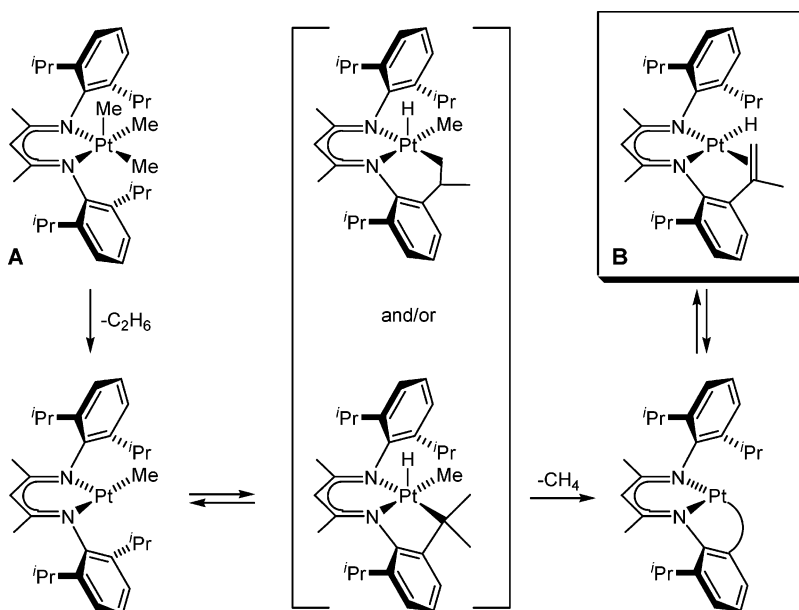
7.4. Reactions at Pt Diketimate Complexes

Diketimates (also termed “nacnac” ligands because of their relation to the acetylacetonate or “acac” systems) have gained tremendous popularity in or-

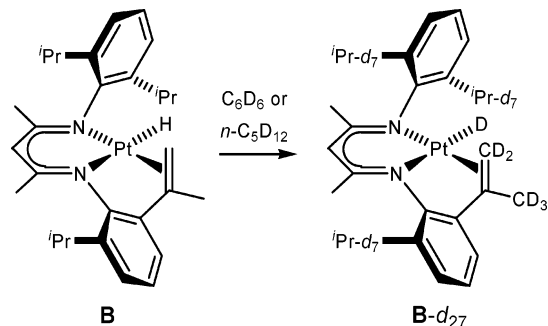
ganometallic chemistry during recent years³²² and are a most promising ligand type in the context of Pt-mediated C–H activation. Goldberg and co-workers reported recently³¹⁹ the preparation of (nacnac)-PtMe₃ complex **A** depicted in Scheme 88 from [PtMe₃(OTf)₄ and K(nacnac). This complex constitutes a rare example³¹⁸ (see also section 7.2.2) of an isolable, five-coordinate Pt(IV) complex. The X-ray structure established a square-pyramidal structure with one methyl group occupying the apical position. The ^1H and ^{13}C NMR spectra demonstrated a highly fluxional molecule in solution, as the Pt–Me groups give one signal, and the “up” and “down” isopropyl groups at the aryl substituents also appear identical, without signs of line broadening at temperatures down to at least -50°C .

Thermolysis of **A** in C_6H_6 at 150°C led to elimination of ethane and methane and yielded Pt hydrido alkene **B**. The product is derived from dehydrogenation of a ligand isopropyl group, believed to occur according to Scheme 88.³²³ Consistent with this, thermolysis in C_6D_6 led to very little (<5%) D incorporation into the methane. However, using C_6D_6 all methine and methyl hydrogens in all isopropyl groups of **B** had been exchanged with D. Furthermore, complete H/D exchange into the isopropyl groups was seen when **B** was heated in C_6D_6 at 85°C . Even more remarkable, H/D exchange into the isopropyl groups of **B** was seen even upon heating in pentane- d_{12} (Scheme 89). When **B**- d_{27} was heated in pentane- h_{12} , deuteration of pentane into the primary positions was favored over the secondary ones by a statistically corrected factor of 6. It is believed that these reactions occur by initial reversal of the β -elimination that completed the formation of **B**. The C–H activation of benzene and pentane by **B** is therefore initiated by generation of a vacant coordination site for hydrocarbon binding by initial alkene insertion into an M–H bond. Intermolecular alkane dehydrogenation to give a (nacnac)Pt(H)(alkene) product was considered. However, such species were not seen, presumably because the intramolecular

Scheme 88



Scheme 89



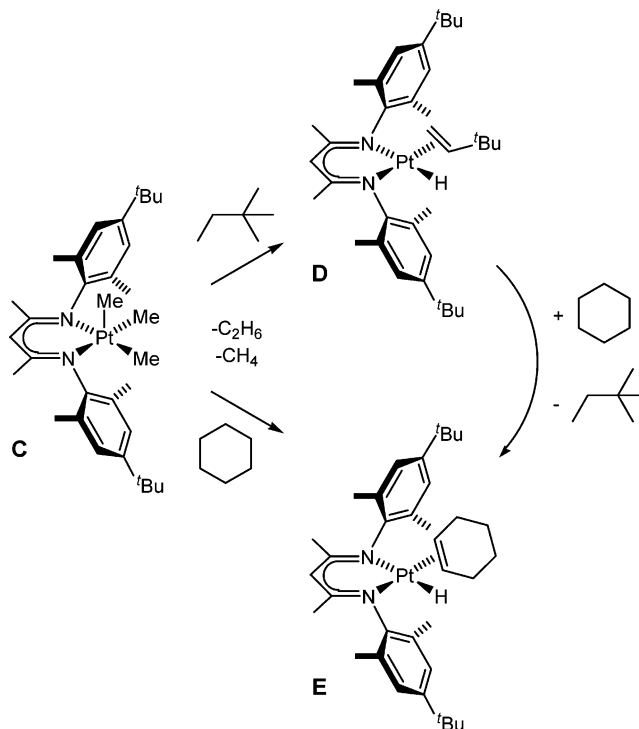
alkene binding in **B** is favored over binding of an external alkene.

This preference can be averted by choosing the substituents at the aryl group of the nacnac ligand such that the β -elimination and intramolecular alkene coordination are suppressed. Thus, the nacnac–Pt complex **C** was explored in some detail (Scheme 90).³²⁴ Indeed, intermolecular alkane dehydrogenation was seen when **C** was heated in 2,2-dimethylbutane or cyclohexane, resulting in the hydrido alkene complexes **D** and **E**. Furthermore, stoichiometric transfer dehydrogenation was successfully achieved when **D** was treated with cyclohexane. Catalytic transfer dehydrogenation^{325–327} of cyclohexane using 3,3-dimethylbutene is thermodynamically feasible yet was not observed in these systems. One possible explanation for this is that a catalytic process requires substitution of 3,3-dimethylbutene for cyclohexene in **E**. This reaction is inhibited by the steric bulk of the ligand system and of the alkene since associative alkene substitution is anticipated.³²⁸ Nevertheless, it appears that catalytic transfer dehydrogenation might soon be achievable using Pt(II) catalysts.

7.5. Reactions at a N_3 Pincer Amido Pt Complex

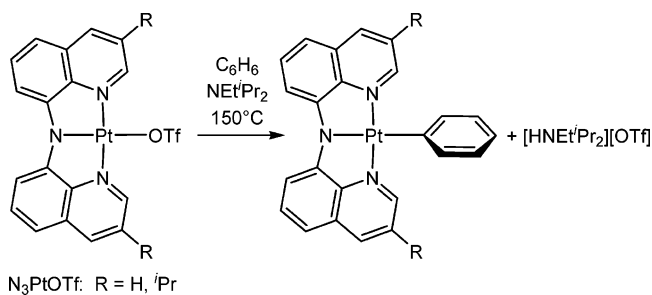
Contrasting the intensely studied TpPt complexes, there appears to be only one other example of C–H

Scheme 90

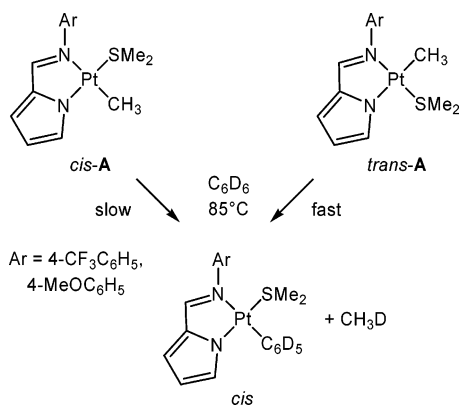


activation chemistry described at anionic N_3 ligand systems. Harkins and Peters³²⁹ found that the “pincer”³³⁰ ligand system in Scheme 91³³¹ undergoes base-promoted activation of benzene. Interestingly, it is not methane (or another hydrocarbon) that is the byproduct of the C–H activation but rather protons. In this respect the chemistry is a highly relevant mimic of the Shilov system. The N_3PtOTf complex was unreactive toward benzene over 36 h at 150 °C, but with 1 equiv of NEt^iPr_2 base added C–H activation occurred according to Scheme 91 already at 100 °C. The system did not catalyze scrambling of protons from added $HNEt^iPr_2 + TfO^-$ into C_6D_6 , although addition of triflic acid converted the N_3PtPh product back to N_3PtOTf .

Scheme 91



Scheme 92



The reaction rate was independent of the base concentration, and no C–H activation occurred in the presence of a more hindered base 2,6-di-*tert*-butylpyridine. The analogous N_3PtCl complex did not react with benzene whether NEt^iPr_2 was present or not. Consistent with these findings the favored mechanism was initial associative displacement of triflate by benzene, oxidative addition of a C–H bond in precoordinated benzene, and proton transfer from the resulting Pt(IV) phenyl hydride to the base. Alternative deprotonation from the Pt–benzene intermediate as well as a concerted mechanism, both of which would constitute *electrophilic* mechanisms, were also considered.

7.6. Reactions at 2-(*N*-Arylimino)pyrrolide Pt Complexes

The *cis* and *trans* aminopyrrolide complexes in Scheme 92 (Ar = 4-CF₃C₆H₅ or 4-MeOC₆H₅) undergo benzene C–H activation upon heating at 85 °C.²⁹⁰ The reactions have half-lives of ca. 1 and 4 h for the *trans* and 3 and 14 days for the *cis* isomers. This dramatic stereoelectronic effect was attributed to a rate-limiting associative substitution of benzene for Me₂S; the *trans* complex would have the imine π -acceptor in an equatorial position and the pyrrolide donor in an axial position in the trigonal-bipyramidal intermediate. This structure is stabilized relative to the opposite conformation with a π -acceptor axial and σ -donor equatorial.³³² Interestingly, treatment of a series of iminopyrroles with $[PtMe_2(\mu-SMe_2)]_2$, which in principle might give the Pt(II) reactants **A** in Scheme 92, provided evidence that reactions with the solvent C₆D₆ proceeded considerably faster than the direct reactions between **A** and C₆D₆. A likely explanation for this is that a methyl group in $[PtMe_2(\mu-$

SMe₂)]₂ undergoes protonolysis by the acidic pyrrole-N proton to give a Pt–pyrrolide intermediate. This intermediate then is responsible for benzene C–H activation *before* chelation occurs by imine coordination.

Undoubtedly, further exploration of Pt systems with anionic “spectator” ligands, including an already existing array of cyclometalated systems (see section 7.1), is poised to give rise to a fascinating part of the developing C–H activation chemistry of Pt in the future.

8. Examples of Applications in Synthesis

Despite the efforts to understand Pt-mediated C–H activation reactions, comparatively few examples exist where such reactions have been used as part of a synthetic strategy (excluding, of course, oxidation of simple hydrocarbons). A challenge when attempting to achieve selective synthetic transformations in organic synthesis is the presence of various functional groups. The considerable tolerance toward several functional groups is a desirable feature of Pt(II)/Pt(IV)-mediated C–H activation chemistry. The original Garnett/Shilov chemistry was performed in aqueous acidic solutions in the presence of air. The selected examples that will be discussed in the following will demonstrate tolerance toward functional groups including carboxylic acids, amines, and alcohols. Coordination of Pt to these functional groups during the course of the reaction may have a profound effect on the regioselectivity and reactivity of the reactions. The unique reactivity of Pt toward otherwise unreactive C–H bonds is another reason to focus on synthetic transformations. This review has largely focused on hydrocarbon C–H activation by oxidative cleavage, electrophilic substitution, and σ -bond metathesis. Selected, but not exhaustive, examples of synthetic transformations that might adhere to such mechanisms are presented here. The discussion is limited to reactions where Pt is removed or liberated from the organic product after the C–H activation and functionalization as will be the case for catalytic reactions.

Early work on the aqueous Pt(II)/Pt(IV) system in the Bercaw group showed remarkable selectivities in hydroxylation reactions.³³³ Subjecting ethanol to catalytic amounts of PtCl₄²⁻ with PtCl₆²⁻ as the oxidant at 120 °C (sealed NMR tubes) produced ca. 5% ethylene glycol, 2% 2-chloroethanol, 5% glycolic acid, and products that are derived from oxidation at C1 of ethanol. Remarkably, oxidation of ¹²CH₃-¹³CH₂OH yielded glycolic acid that was nearly equally labeled at C1 and C2, demonstrating that the acid arises primarily from oxidation of ethylene glycol rather than from hydroxylation of acetic acid. The product and label distribution demonstrated that approximately equal amounts of products are derived from initial reactions at the methyl and hydroxymethyl groups of ethanol. For 1-propanol the selectivity was even higher, with 48% 1,3-propanediol and 30% 3-chloro-1-propanol arising from methyl oxidation at 25% conversion. The reaction appears to be quite sensitive to reaction conditions with highly variable selectivity.¹⁴⁹ Good selectivities in hydroxy-

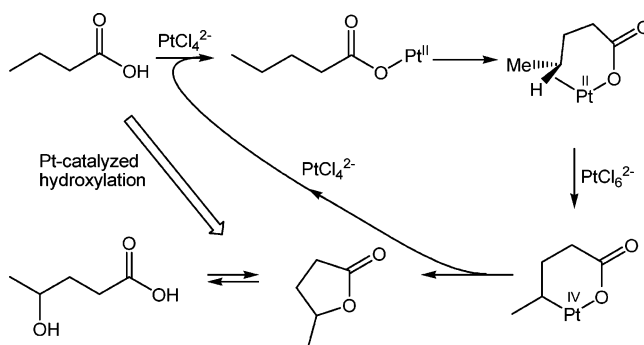
lation reactions have also been reported by Sen and co-workers.^{334,335} Lowering the temperature combined with increased reaction time and absence of light improved the selectivity. Thus, subjecting ethanol to stoichiometric amounts of PtCl_4^{2-} and PtCl_6^{2-} at 86 °C for 6 days yielded ethylene glycol as the major product at 50% conversion. Trace amounts of hydroxyacetaldehyde and/or chloroacetaldehyde were usually formed also. When 1-propanol was subjected to substoichiometric amounts of PtCl_4^{2-} and PtCl_6^{2-} at 115 °C for 24 h, 1,3-propanediol was the major product. No details were given on the amounts of byproducts formed. Catalytic hydroxylation of alcohols has recently been further investigated by Thorn and co-workers.³³⁶ Treatment of 1-propanol with PtCl_4 as the Pt(IV) oxidizing component and catalytic amounts of $\text{Pt}^{\text{II}}\text{Cl}_4^{2-}$ yielded 1,3-propanediol and 1,2-propanediol in addition to acetic acid. The initial rates using $\text{Pt}^{\text{IV}}\text{Cl}_4$ rather than $\text{Pt}^{\text{IV}}\text{Cl}_6^{2-}$ are higher, the amounts of chlorinated products formed in the initial stages of the reaction are lower, and the system is more stable with respect to deposition of metallic Pt. Even though these reactions are not synthetically useful yet, the examples exhibit important selectivity patterns and functional group tolerance. *p*-Toluenesulfonic acid is oxidized cleanly at the methyl position, giving the corresponding alcohol and aldehyde; no carboxylic acid is formed.^{122,149} The first step is faster than the second by a factor of about 1.5. No oxidation is observed in the aromatic positions. This gives the following rather unusual order of reactivity: $-\text{CH}_3 > -\text{CH}_2\text{OH} > \text{aryl-H} \gg -\text{CHO}$. On the other hand, sodium *p*-ethylbenzene sulfonate was oxidized at comparable rates at the α and β positions and also at the aromatic ring, underlining the nonradical nature of the reactions.

Kański and Kańska explored the deuteration of a number of substituted aromatic carboxylic acids with K_2PtCl_4 in $\text{D}_2\text{O}/\text{DCI}/\text{CH}_3\text{COOD}$.³³⁷ Generally, 4–5% D incorporation is observed within 1–4 days at 130 °C. The rate of D incorporation in a particular position depends largely on the substituents. To a large extent, D is not incorporated into the ortho position to the carboxylic acid groups.

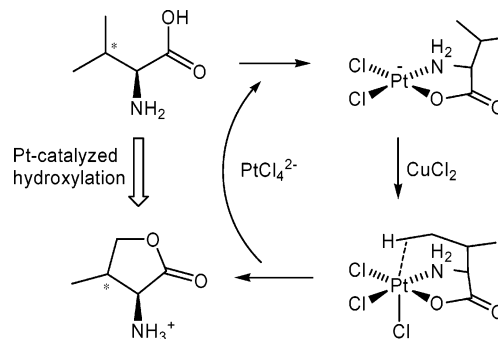
Kao and Sen studied Pt-catalyzed oxidation of remote C–H bonds in carboxylic acids.³³⁸ Using $\text{K}_2\text{PtCl}_4/\text{K}_2\text{PtCl}_6$ in D_2O under an O_2 atmosphere at 80–90 °C, the reactions are catalytic with respect to Pt(II). A preferential attack at the γ position yields the lactone in equilibrium with the corresponding hydroxycarboxylic acid. This regioselectivity is explained in terms of a chelate giving rise to strain-free six-membered metallacycles (Scheme 93). Further support for this mechanism is provided by the observation of β -lactones from C3 and C4 carboxylic acids. No equilibrium is observed between β -hydroxycarboxylic acid and the corresponding lactone due to the strain of a four-membered ring, but it is plausible that the acids are kinetic products formed by reductive elimination from five-membered metallacycles.

Sames and co-workers reported that catalytic functionalization of α -amino acids was possible using catalytic amounts of K_2PtCl_4 with CuCl_2 acting as a stoichiometric oxidant (Scheme 94).³³⁹ This chemistry

Scheme 93



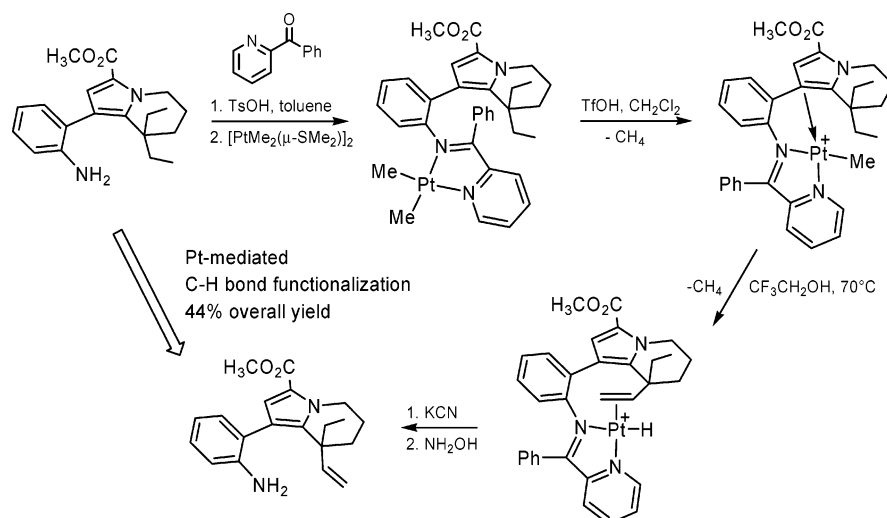
Scheme 94



elegantly combines know-how from the field of Pt(II) coordination chemistry related to cisplatin (used in treatment of cancer³⁴⁰) with the desirable functional group tolerance of Pt(II)/Pt(IV). Hydroxylation of either *n*-butylamine or *n*-pentanoic acid with the same system gave a slight preference for hydroxylation in the δ over the γ position (3:2). The regioselectivity of reactions with α -amino acids, however, suggests a chelate mechanism involving coordination of both the amino group and the hydroxyl group. The chelate structure then favors C–H bond activation and hydroxylation in the γ position. The resistance of the cyclic α -amino acid proline toward oxidation under similar conditions provides further support for the chelate-directed mechanism since the cyclic nature of proline prevents an intramolecular approach of the metal toward the C–H bonds.

One particularly elegant example of Pt-mediated C–H activation used in organic synthesis is the recent total synthesis of rhazinilam by Sames and co-workers.^{341,342} A key step in the synthetic strategy is based on the proximity of an aromatic amino group to the ethyl groups in the aniline derivative at top left in Scheme 95. The aniline was converted to the Schiff base by condensation with 2-benzoylpyridine, and the Schiff base was attached to Pt by treatment with $[\text{Me}_2\text{Pt}(\mu\text{-SMe}_2)]_2$. The resulting Pt dimethyl complex was treated with TfOH to liberate methane and provided a cationic species with an unusual η^1 coordination of the pyrrole ring. The lability of this bond facilitated the regio- and stereoselective oxidative addition of a methylene C–H bond of the proximal ethyl group. Liberation of a second methane and β -hydride elimination yielded the platinum alkene hydride. Platinum was removed by treatment with aqueous KCN, and the Schiff base was hydro-

Scheme 95



lyzed to give rhazinilam. The enantioselective synthesis of (–)-rhazinilam was achieved with 96% ee by asymmetric C–H bond activation using a chiral oxazolonyl ketone auxiliary instead of the Schiff base in Scheme 95.³⁴²

9. Summary and Outlook

As illustrated in this review, Pt has much to offer in the realm of C–H activation. The strong Pt–H and Pt–C bonds that can be formed in a C–H activation reaction undoubtedly contribute to the success of Pt. Hydrocarbon activation, the first step in the Shilov cycle in Scheme 3, is probably the most intensely explored and best understood of the three steps. The C–H activation step, with its vast array of interesting mechanistic and selectivity issues, will undoubtedly continue to fascinate chemists for years to come.

Examples have been presented that C–H activation can occur at electron-rich and electron-poor Pt complexes. Reactions occur at complexes that have cationic, neutral, and anionic metal centers with Pt in formal oxidation states 0, +2, and +4. Pt complexes are capable of reacting by diverse mechanisms, including oxidative addition and electrophilic substitution. It is well understood that relatively electron-rich metal centers show a propensity for oxidative addition reactivity whereas electron-deficient metal centers prefer to react by electrophilic activation. However, the distinction is far from clear cut, and in many cases the mechanisms are ambiguous at best. The C–H activation mechanism is determined not only by the nature of the metal center but also is strongly dependent on the reaction conditions. After all, the electrophilic mechanism involves a proton transfer from an activated hydrocarbon, and this proton transfer clearly will be strongly affected by the nature of the medium.

Most of the efforts of the past decade have been inspired by the Shilov chemistry with the ultimate goal of producing oxidized products R–X where X is an electronegative group such as OH. Other recent developments that have been described show great promise for Pt complexes also as potential catalysts for alkane dehydrogenation reactions to form alkenes.

The first mode of functionalization has mostly been investigated at relatively electron-deficient Pt complexes and the second one at electron-rich complexes. However, there is no reason to believe that this distinction should limit our efforts in future research. The last example in section 8, which deals with functionalization by dehydrogenation of an alkyl group in a sophisticated organic molecule, was performed at a relatively electron-deficient cationic Pt center.

All C–H activation reactions that have been described here are believed to proceed by the same initial step, namely, coordination of a hydrocarbon substrate at Pt to form a σ -alkane or π -arene complex. The barrier toward forming this complex always constitutes a significant part of the overall barrier for C–H activation, and in fact, this step is often seen to be the rate-limiting step. Once the σ or π complex has been formed, C–H bond cleavage is quite facile, as evidenced by the numerous instances of H/D scrambling reactions. Paradoxically, the alkane (or arene) C–H σ complexes of Pt that have been so firmly entrenched in our mechanistic thinking have never been directly observed by NMR spectroscopy much less structurally characterized. Combined evidence from experiments and calculations strongly suggests that the σ -alkane complexes may be kinetically and thermodynamically sufficiently stable with respect to alkane loss that they may be directly observable if generated under mild conditions.

Future progress in the Pt approach to alkane functionalization, from a fundamental research as well as a commercial point of view, will depend on further exploration of novel, reactive, and yet robust ligand systems. There are already indications that *N*-heterocyclic carbene systems and κ^2 -(C,X)-cyclo-metallated systems, which have hitherto been underutilized, may offer great opportunities for future investigations.

There is still a long and challenging path ahead of us that leads from the fundamental research described in this review to commercially successful processes for hydrocarbon functionalization. The rapid progress that has been made during the past decade or so lends us reason to hope that ongoing

research in this pivotal field of chemistry and catalysis will one day allow us to utilize the hydrocarbons that Nature has provided in more direct, efficient, and environmentally benign ways.

10. Abbreviations

acac	acetylacetonato
Ar	aryl
BAr _F [−]	(3,5-(CF ₃) ₂ C ₆ H ₃) ₄ B [−]
bpy	2,2′-bipyridyl
bpym	bipyrimidine
Bu	butyl
Cp	cyclopentadienyl
Cy	cyclohexyl
depe	1,2-bis(dicyclohexylphosphino)ethane, Cy ₂ -PCH ₂ CH ₂ PCy ₂
depe	1,2-bis(diethylphosphino)ethane, Et ₂ PCH ₂ -CH ₂ PEt ₂
dfep	1,2-bis(diperfluoroethylphosphino)ethane, (C ₂ F ₅) ₂ PCH ₂ CH ₂ P(C ₂ F ₅) ₂
DFT	density functional theory
diimine	Ar–N=CR–CR=N–Ar (R = H, Me)
dmpe	1,2-bis(dimethylphosphino)ethane, Me ₂ PCH ₂ -CH ₂ PMe ₂
dppbz	1,2-bis(diphenylphosphino)benzene, Ph ₂ P-(C ₆ H ₄)PPh ₂
dppe	1,2-bis(diphenylphosphino)ethane, Ph ₂ PCH ₂ -CH ₂ PPh ₂
dppf	diphenylphosphiniferrocene, Ph ₂ P(C ₅ H ₄ FeCp)
dppp	1,3-bis(diphenylphosphino)propane, Ph ₂ PCH ₂ -CH ₂ CH ₂ PPh ₂
dtbpm	bis(di- <i>tert</i> -butylphosphino)methane, ^t Bu ₂ PCH ₂ -P ^t Bu ₂
eda	ethylenediamine
EIE	equilibrium isotope effect
Et	ethyl
EXSY	exchange spectroscopy
HOTf	triflic acid, CF ₃ SO ₃ H
HTp	N-protonated Tp
HTp′	N-protonated Tp′
ⁱ Pr ₃ tacn	1,4,7-tri(isopropyl)-1,4,7-triazacyclononane
KIE	kinetic isotope effect
L	ligand
Me	methyl
Me ₃ tacn	1,4,7-trimethyl-1,4,7-triazacyclononane
MeCN	acetonitrile
MeOH	methanol
N′–N′	diimine, with Ar = 2,6-Me ₂ C ₆ H ₃ and R = Me
nacnac	diketiminato
N ^{Cl} –N ^{Cl}	diimine, with Ar = 2,6-Cl ₂ C ₆ H ₃ and R = Me
NCN	pincer-type NCN ligand, 2,6-C ₆ H ₃ (CH ₂ NMe ₂) ₂
N ^f –N ^f	diimine, with Ar = 3,5-(CF ₃) ₂ C ₆ H ₃ and R = Me
N ^h –N ^h	HN=CH–CH=NH
OAc	acetate
OC	oxidative cleavage
OTf [−]	triflate, CF ₃ SO ₃ [−]
PCP	pincer-type P–C–P ligand
Ph	phenyl
phen	1,10-phenanthroline
pyrphane	[2.1.1]-(2,6)-pyridinophane
pz	pyrazolyl
pz′	3,5-dimethylpyrazolyl
RC	reductive coupling
Solv	solvent
tacn	1,4,7-triazacyclononane
^t Bu	<i>tert</i> -butyl
^t Bu ₂ bpy	4,4′-di- <i>tert</i> -butyl-2,2′-bipyridyl
TfE	trifluoroethanol
tmeda	tetramethylethylenediamine

Tol	tolyl
Tp	hydridotris(pyrazolyl)borate
Tp′	hydridotris(3,5-dimethylpyrazolyl)borate

11. Acknowledgment

We thank the Norwegian Research Council (NFR) and the U.S.–Norway Fulbright Foundation for generous stipends to M.L.

12. References

- Labinger, J. A.; Bercaw, J. E. *Nature* **2002**, *417*, 507.
- Periana, R. A.; Bhalla, G.; Tenn, W. J.; Young, K. J. H.; Liu, X. Y.; Mironov, O.; Jones, C.; Ziatdinov, V. R. *J. Mol. Catal. A* **2004**, *220*, 7.
- Labinger, J. A. *J. Mol. Catal. A* **2004**, *220*, 27.
- Arakawa, H.; Aresta, M.; Armor, J. N.; Barteau, M. A.; Beckman, E. J.; Bell, A. T.; Bercaw, J. E.; Creutz, C.; Dinjus, E.; Dixon, D. A.; Domen, K.; DuBois, D. L.; Eckert, J.; Fujita, E.; Gibson, D. H.; Goddard, W. A., III; Goodman, D. W.; Keller, J.; Kubas, G. J.; Kung, H. H.; Lyons, J. E.; Manzer, L. E.; Marks, T. J.; Morokuma, K.; Nicholas, K. M.; Periana, R.; Que, L.; Rostrup-Nielson, J.; Sachtler, W. M. H.; Schmidt, L. D.; Sen, A.; Somorjai, G. A.; Stair, P. C.; Stults, B. R.; Tumas, W. *Chem. Rev.* **2001**, *101*, 953.
- Lowry, T. H.; Richardson, K. S. *Mechanism and Theory in Organic Chemistry*, 3rd ed.; Benjamin-Cummings Publishing Co.: New York, 1987.
- Berkowitz, J.; Ellison, G. B.; Gutman, D. *J. Phys. Chem.* **1994**, *98*, 2744.
- Nolan, S. P.; Hoff, C. D.; Stoutland, P. O.; Newman, L. J.; Buchanan, J. M.; Bergman, R. G.; Yang, G. K.; Peters, K. S. *J. Am. Chem. Soc.* **1987**, *109*, 3143.
- Simoes, J. A. M.; Beauchamp, J. L. *Chem. Rev.* **1990**, *90*, 629.
- Takhin, G. A.; Skinner, H. A.; Zaki, A. A. *J. Chem. Soc., Dalton Trans.* **1984**, 371.
- Miedaner, A.; Raebiger, J. W.; Curtis, C. J.; Miller, S. M.; DuBois, D. L. *Organometallics* **2004**, *23*, 2670.
- Mortimer, C. T. *Rev. Inorg. Chem.* **1984**, *6*, 233.
- Roy, S.; Puddephatt, R. J.; Scott, J. D. *J. Chem. Soc., Dalton Trans.* **1989**, 2121.
- Goldberg, K. I.; Yan, J.; Breitung, E. M. *J. Am. Chem. Soc.* **1995**, *117*, 6889.
- Janowicz, A. H.; Bergman, R. G. *J. Am. Chem. Soc.* **1982**, *104*, 352.
- Hoyano, J. K.; Graham, W. A. G. *J. Am. Chem. Soc.* **1982**, *104*, 3723.
- Jones, W. D.; Feher, F. J. *Organometallics* **1983**, *2*, 562.
- Arndtsen, B. A.; Bergman, R. G.; Mobley, T. A.; Peterson, T. H. *Acc. Chem. Res.* **1995**, *28*, 154.
- Shilov, A. E.; Shul'pin, G. B. *Chem. Rev.* **1997**, *97*, 2879.
- Crabtree, R. H. *J. Chem. Soc., Dalton Trans.* **2001**, 2437.
- Fekl, U.; Goldberg, K. I. *Adv. Inorg. Chem.* **2003**, *54*, 259.
- Stahl, S. S.; Labinger, J. A.; Bercaw, J. E. *Angew. Chem., Int. Ed.* **1998**, *37*, 2181.
- Jones, W. D. *Top. Organomet. Chem.* **1999**, *3*, 9.
- Crabtree, R. H. *J. Organomet. Chem.* **2004**, *689*, 4083.
- Leitch, L. C. *Can. J. Chem.-Rev. Can. Chim.* **1954**, *32*, 813.
- Brown, W. G.; Garnett, J. L. *J. Am. Chem. Soc.* **1958**, *80*, 5272.
- Garnett, J. L.; Sollich, W. A. *J. Catal.* **1963**, *2*, 350.
- Garnett, J. L.; Hodges, R. J. *J. Am. Chem. Soc.* **1967**, *89*, 4546.
- Garnett, J. L.; Hodges, R. J.; Sollich-Baumgartner, W. A. *Osn. Predvideniya Katal. Deistviya, Tr. Mezhdunar. Kongr. Katal.*, *4th* **1970**, *1*, 62.
- Goldshleger, N. F.; Tyabin, M. B.; Shilov, A. E.; Shteinman, A. A. *Zh. Fiz. Khim.* **1969**, *43*, 2174; *Russ. J. Phys. Chem.* **1969**, *43*, 1222 (english translation).
- Lin, M.; Shen, C.; Garcia-Zayas, E. A.; Sen, A. *J. Am. Chem. Soc.* **2001**, *123*, 1000.
- Luinstra, G. A.; Wang, L.; Stahl, S. S.; Labinger, J. A.; Bercaw, J. E. *J. Organomet. Chem.* **1995**, *504*, 75.
- Smythe, N. A.; Williams, B. S.; Goldberg, K. I. *Abstracts of Papers*, 226th National Meeting of the American Chemical Society, New York, Sept 7–11, 2003, American Chemical Society: Washington, DC, 2003; INOR-075.
- Koszinowski, K.; Schroeder, D.; Schwarz, H. *Organometallics* **2004**, *23*, 1132.
- Koszinowski, K.; Schroeder, D.; Schwarz, H. *J. Phys. Chem. A* **2003**, *107*, 4999.
- Wong-Foy, A. G.; Henling, L. M.; Day, M.; Labinger, J. A.; Bercaw, J. E. *J. Mol. Catal. A* **2002**, *189*, 3.
- Blum, S. A.; Tan, K. L.; Bergman, R. G. *J. Org. Chem.* **2003**, *68*, 4127.
- Jones, W. D.; Feher, F. J. *Acc. Chem. Res.* **1989**, *22*, 91.

- (38) Watson, P. L.; Parshall, G. W. *Acc. Chem. Res.* **1985**, *18*, 51.
- (39) Hill, C. L. *Activation and Functionalization of Alkanes*; John Wiley and Sons: New York, 1989.
- (40) Fendrick, C. M.; Marks, T. J. *J. Am. Chem. Soc.* **1986**, *108*, 425.
- (41) Thompson, M. E.; Baxter, S. M.; Bulls, A. R.; Burger, B. J.; Nolan, M. C.; Santarsiero, B. D.; Schaefer, W. P.; Bercaw, J. E. *J. Am. Chem. Soc.* **1987**, *109*, 203.
- (42) Webster, C. E.; Fan, Y.; Hall, M. B.; Kunz, D.; Hartwig, J. F. *J. Am. Chem. Soc.* **2003**, *125*, 858.
- (43) Waltz, K. M.; Hartwig, J. F. *Science* **1997**, *277*, 211.
- (44) Waltz, K. M.; Hartwig, J. F. *J. Am. Chem. Soc.* **2000**, *122*, 11358.
- (45) Kubas, G. J. *Acc. Chem. Res.* **1988**, *21*, 120.
- (46) Kubas, G. J. *J. Organomet. Chem.* **2001**, *635*, 37.
- (47) Crabtree, R. H. *Acc. Chem. Res.* **1990**, *23*, 95.
- (48) Crabtree, R. H. *Angew. Chem., Int. Ed. Engl.* **1993**, *32*, 789.
- (49) Jessop, P. G.; Morris, R. H. *Coord. Chem. Rev.* **1992**, *121*, 155.
- (50) Heinekey, D. M.; Oldham, W. J. *Chem. Rev.* **1993**, *93*, 913.
- (51) Arndtsen, B. A.; Bergman, R. G. *Science* **1995**, *270*, 1970.
- (52) Golden, J. T.; Andersen, R. A.; Bergman, R. G. *J. Am. Chem. Soc.* **2001**, *123*, 5837.
- (53) Tellers, D. M.; Yung, C. M.; Arndtsen, B. A.; Adamson, D. R.; Bergman, R. G. *J. Am. Chem. Soc.* **2002**, *124*, 1400.
- (54) Klei, S. R.; Golden, J. T.; Burger, P.; Bergman, R. G. *J. Mol. Catal. A* **2002**, *189*, 79.
- (55) Su, M.-D.; Chu, S.-Y. *J. Am. Chem. Soc.* **1997**, *119*, 5373.
- (56) Jones, W. D. *Acc. Chem. Res.* **2003**, *36*, 140.
- (57) Churchill, D. G.; Janak, K. E.; Wittenberg, J. S.; Parkin, G. J. *Am. Chem. Soc.* **2003**, *125*, 1403.
- (58) Lincoln, S. F.; Merbach, A. E. *Adv. Inorg. Chem.* **1995**, *42*, 1.
- (59) Langford, C. H.; Gray, H. B. *Ligand Substitution Processes*; Benjamin: New York, 1965.
- (60) Basolo, F.; Gray, H. B.; Pearson, R. G. *J. Am. Chem. Soc.* **1960**, *82*, 4200.
- (61) Basolo, F.; Pearson, R. G. *Mechanisms of Inorganic Reactions*; John Wiley and Sons: New York, 1967.
- (62) Atwood, J. D. *Inorganic and Organometallic Reaction Mechanisms*; VCH: New York, 1997.
- (63) Plutino, M. R.; Scolaro, L. M.; Albinati, A.; Romeo, R. *J. Am. Chem. Soc.* **2004**, *126*, 6470.
- (64) Krogh-Jespersen, K.; Czerw, M.; Goldman, A. S. *ACS Symp. Ser.* **2004**, *885*, 216.
- (65) Krogh-Jespersen, K.; Czerw, M.; Summa, N.; Renkema, K. B.; Achord, P. D.; Goldman, A. S. *J. Am. Chem. Soc.* **2002**, *124*, 11404.
- (66) Hodges, R. J.; Garnett, J. L. *J. Phys. Chem.* **1968**, *72*, 1673.
- (67) Tyabin, M. B.; Shilov, A. E.; Shteinman, A. A. *Dokl. Akad. Nauk* **1971**, *198*, 380.
- (68) Hodges, R. J.; Webster, D. E.; Wells, P. B. *J. Chem. Soc., Chem. Commun.* **1971**, 462.
- (69) Makhaev, V. D. *Russ. Chem. Rev.* **2003**, *72*, 257.
- (70) Schneider, J. J. *Angew. Chem., Int. Ed. Engl.* **1996**, *35*, 1068.
- (71) Crabtree, R. H. *Chem. Rev.* **1995**, *95*, 987.
- (72) Hall, C.; Perutz, R. N. *Chem. Rev.* **1996**, *96*, 3125.
- (73) Gould, G. L.; Heinekey, D. M. *J. Am. Chem. Soc.* **1989**, *111*, 5502.
- (74) Chernega, A. N.; Cook, J.; Green, M. L. H.; Labella, L.; Simpson, S. J. *J. Chem. Soc., Dalton Trans.* **1997**, 3225.
- (75) Gross, C. L.; Girolami, G. S. *J. Am. Chem. Soc.* **1998**, *120*, 6605.
- (76) Flood, T. C.; Janak, K. E.; Iimura, M.; Zhen, H. *J. Am. Chem. Soc.* **2000**, *122*, 6783.
- (77) Wang, C.; Ziller, J. W.; Flood, T. C. *J. Am. Chem. Soc.* **1995**, *117*, 1647.
- (78) Wick, D. D.; Reynolds, K. A.; Jones, W. D. *J. Am. Chem. Soc.* **1999**, *121*, 3974.
- (79) Northcutt, T. O.; Wick, D. D.; Vetter, A. J.; Jones, W. D. *J. Am. Chem. Soc.* **2001**, *123*, 7257.
- (80) Buchanan, J. M.; Stryker, J. M.; Bergman, R. G. *J. Am. Chem. Soc.* **1986**, *108*, 1537.
- (81) Periana, R. A.; Bergman, R. G. *J. Am. Chem. Soc.* **1986**, *108*, 7332.
- (82) Bullock, R. M.; Headford, C. E. L.; Hennessy, K. M.; Kegley, S. E.; Norton, J. R. *J. Am. Chem. Soc.* **1989**, *111*, 3897.
- (83) Parkin, G.; Bercaw, J. E. *Organometallics* **1989**, *8*, 1172.
- (84) Stahl, S. S.; Labinger, J. A.; Bercaw, J. E. *J. Am. Chem. Soc.* **1996**, *118*, 5961.
- (85) Mobley, T. A.; Schade, C.; Bergman, R. G. *J. Am. Chem. Soc.* **1995**, *117*, 7822.
- (86) Norris, C. M.; Reinartz, S.; White, P. S.; Templeton, J. L. *Organometallics* **2002**, *21*, 5649.
- (87) Reinartz, S.; White, P. S.; Brookhart, M.; Templeton, J. L. *J. Am. Chem. Soc.* **2001**, *123*, 12724.
- (88) Geftakis, S.; Ball, G. E. *J. Am. Chem. Soc.* **1998**, *120*, 9953.
- (89) Evans, D. R.; Drovetskaya, T.; Bau, R.; Reed, C. A.; Boyd, P. D. *W. J. Am. Chem. Soc.* **1997**, *119*, 3633.
- (90) Castro-Rodriguez, I.; Nakai, H.; Gantzel, P.; Zakharov, L. N.; Rheingold, A. L.; Meyer, K. J. *J. Am. Chem. Soc.* **2003**, *125*, 15734.
- (91) McGrady, G. S.; Guiler, G. *Chem. Soc. Rev.* **2003**, *32*, 383.
- (92) Schubert, U. *Adv. Organomet. Chem.* **1990**, *30*, 151.
- (93) Brookhart, M.; Green, M. L. H.; Wong, L. L. *Prog. Inorg. Chem.* **1988**, *36*, 1.
- (94) Sweet, J. R.; Graham, W. A. G. *J. Am. Chem. Soc.* **1983**, *105*, 305.
- (95) Sweet, J. R.; Graham, W. A. G. *Organometallics* **1983**, *2*, 135.
- (96) Jones, W. D.; Dong, L. *J. Am. Chem. Soc.* **1989**, *111*, 8722.
- (97) Cordone, R.; Taube, H. *J. Am. Chem. Soc.* **1987**, *109*, 8101.
- (98) Jones, W. D.; Feher, F. J. *J. Am. Chem. Soc.* **1986**, *108*, 4814.
- (99) Chin, R. M.; Dong, L.; Duckett, S. B.; Jones, W. D. *Organometallics* **1992**, *11*, 871.
- (100) Vigalok, A.; Uzan, O.; Shimon, L. J. W.; Ben-David, Y.; Martin, J. M. L.; Milstein, D. *J. Am. Chem. Soc.* **1998**, *120*, 12539.
- (101) Peterson, T. H.; Golden, J. T.; Bergman, R. G. *J. Am. Chem. Soc.* **2001**, *123*, 455.
- (102) Krumper, J. R.; Gerisch, M.; Magistrato, A.; Rothlisberger, U.; Bergman, R. G.; Tilley, T. D. *J. Am. Chem. Soc.* **2004**, *126*, 12492.
- (103) Johansson, L.; Tilset, M.; Labinger, J. A.; Bercaw, J. E. *J. Am. Chem. Soc.* **2000**, *122*, 10846.
- (104) Bullock, R. M.; Bender, B. R. *Encyclopedia of Catalysis*; Wiley-Interscience: Hoboken, NJ, 2002.
- (105) Bullock, R. M. *Transition Metal Hydrides*; VCH: New York, 1992; pp 263.
- (106) Melander, L. C. S.; Saunders, W. *Reaction Rates of Isotopic Molecules*; Wiley: New York, 1980.
- (107) Melander, L. *Acta Chem. Scand.* **1971**, *25*, 3821.
- (108) Bigeleisen, J. *Pure Appl. Chem.* **1964**, *8*, 217.
- (109) Janak, K. E.; Churchill, D. G.; Parkin, G. *Chem. Commun.* **2003**, 22.
- (110) Janak, K. E.; Parkin, G. *J. Am. Chem. Soc.* **2003**, *125*, 6889.
- (111) Shilov, A. E.; Shul'pin, G. B. *Activation and catalytic reactions of saturated hydrocarbons in the presence of metal complexes*; Kluwer Academic: Dordrecht, 1999.
- (112) Garnett, J. L.; Hodges, R. J.; Kenyon, R. S.; Long, M. A. *J. Chem. Soc., Perkin Trans. 2* **1979**, 885.
- (113) Garnett, J. L.; West, J. C. *Austr. J. Chem.* **1974**, *27*, 129.
- (114) Hodges, R. J.; Webster, D. E.; Wells, P. B. *J. Chem. Soc. A* **1971**, 3230.
- (115) Hodges, R. J.; Webster, D. E.; Wells, P. B. *J. Chem. Soc., Dalton Trans.* **1972**, 2571.
- (116) Hodges, R. J.; Webster, D. E.; Wells, P. B. *J. Chem. Soc., Dalton Trans.* **1972**, 2577.
- (117) Ginstrup, O.; Leden, I. *Acta Chem. Scand.* **1967**, *21*, 2689.
- (118) Dunham, S. O.; Larsen, R. D.; Abbott, E. H. *Inorg. Chem.* **1991**, *30*, 4328.
- (119) Gerdes, G.; Chen, P. *Organometallics* **2004**, *23*, 3031.
- (120) Es'kova, V. V.; Shilov, A. E.; Shteinman, A. A. *Kinet. Katal.* **1972**, *13*, 534.
- (121) Rudakov, E. S. *Zh. Fiz. Khim.* **1987**, *61*, 289.
- (122) Labinger, J. A.; Herring, A. M.; Bercaw, J. E. *Adv. Chem. Ser.* **1992**, *230*, 221.
- (123) Goldshleger, N. F.; Shteinman, A. A. *React. Kinet. Catal. Lett.* **1977**, *6*, 43.
- (124) Repka, L. F.; Shteinman, A. A. *Kinet. Katal.* **1974**, *15*, 805.
- (125) Goldshleger, N. F.; Shteinman, A. A.; Shilov, A. E.; Eskova, V. V. *Zh. Fiz. Khim.* **1972**, *46*, 1353.
- (126) Garnett, J. L.; Kenyon, R. S. *J. Chem. Soc., Chem. Commun.* **1971**, 1227.
- (127) Davis, K. P.; Garnett, J. L. *J. Phys. Chem.* **1971**, *75*, 1175.
- (128) Hodges, R. J.; Garnett, J. L. *J. Catal.* **1969**, *13*, 83.
- (129) Hodges, R. J.; Garnett, J. L. *J. Phys. Chem.* **1969**, *73*, 1525.
- (130) Anderson, J. R.; Kembal, C. *Adv. Catal.* **1957**, *9*, 51.
- (131) Rudakov, E. S.; Shteinman, A. A. *Kinet. Katal.* **1973**, *14*, 1346.
- (132) Jennings, P. W.; Johnson, L. L. *Chem. Rev.* **1994**, *94*, 2241.
- (133) Shestakov, A. F. *Kinet. Catal.* **1990**, *31*, 511.
- (134) Ong, C. M.; Burchell, T. J.; Puddephatt, R. J. *Organometallics* **2004**, *23*, 1493.
- (135) Kushch, L. A.; Lavrushko, V. V.; Misharin, Y. S.; Moravskii, A. P.; Shilov, A. E. *Nouv. J. Chim.* **1983**, *7*, 729.
- (136) Zamashchikov, V. V.; Popov, V. G.; Rudakov, E. S.; Mitchenko, S. A. *Dokl. Akad. Nauk* **1993**, *333*, 34.
- (137) Zamashchikov, V. V.; Popov, V. G.; Rudakov, E. S. *Kinet. Catal.* **1994**, *35*, 339.
- (138) Belluco, U.; Croatto, U.; Uguagliati, P.; Pietropaolo, R. *Inorg. Chem.* **1967**, *6*, 718.
- (139) Goldshleger, N. F.; Lavrushko, V. V.; Khrush, A. P.; Shteinman, A. A. *Bull. Acad. Sci. USSR, Chem. Sci.* **1976**, *25*, 2031.
- (140) Goldshleger, N. F.; Shteinman, A. A.; Moiseev, I. I.; Khidekel, M. L. *Dokl. Akad. Nauk* **1972**, *206*, 106.
- (141) Zamashchikov, V. V.; Rudakov, E. S.; Mitchenko, S. A.; Litvinenko, S. L. *Teor. Eksp. Khim.* **1982**, *18*, 510.
- (142) Zamashchikov, V. V.; Mitchenko, S. A. *Kinet. Katal.* **1983**, *24*, 254.
- (143) Zamashchikov, V. V.; Rudakov, E. S.; Garkusha-Bozhko, V. S.; Mitchenko, S. A.; Litvinenko, S. L.; Chuprina, V. S. *Koord. Khim.* **1986**, *12*, 822.
- (144) Luinstra, G. A.; Labinger, J. A.; Bercaw, J. E. *J. Am. Chem. Soc.* **1993**, *115*, 3004.
- (145) Zamashchikov, V. V.; Kitaigorodskii, A. N.; Litvinenko, S. L.; Rudakov, E. S.; Uzhik, O. N.; Shilov, A. E. *Izv. Akad. Nauk SSSR, Ser. Khim.* **1985**, 1730.

- (146) Zamashchikov, V. V.; Litvinenko, S. L.; Shologon, V. I. *Kinet. Katal.* **1987**, *28*, 1059.
- (147) Luinstra, G. A.; Wang, L.; Stahl, S. S.; Labinger, J. A.; Bercaw, J. E. *Organometallics* **1994**, *13*, 755.
- (148) Wang, L.; Stahl, S. S.; Labinger, J. A.; Bercaw, J. E. *J. Mol. Catal. A* **1997**, *116*, 269.
- (149) Labinger, J. A.; Herring, A. M.; Lyon, D. K.; Luinstra, G. A.; Bercaw, J. E.; Horvath, I. T.; Eller, K. *Organometallics* **1993**, *12*, 895.
- (150) Chinn, M. S.; Heinekey, D. M. *J. Am. Chem. Soc.* **1987**, *109*, 5865.
- (151) Broderick, W. E.; Kanamori, K.; Willett, R. D.; Legg, J. I. *Inorg. Chem.* **1991**, *30*, 3875.
- (152) Mustafin, A. I.; Rudakov, E. S.; Shilov, A. E.; Shteinman, A. A. *Kinet. Catal.* **1975**, *16*, 1015.
- (153) Mustafin, A. I.; Shteinman, A. A. *React. Kinet. Catal. Lett.* **1977**, *6*, 153.
- (154) Dedieu, A. *Chem. Rev.* **2000**, *100*, 543.
- (155) Siegbahn, P. E. M.; Crabtree, R. H. *J. Am. Chem. Soc.* **1996**, *118*, 4442.
- (156) Siegbahn, P. E. M. *J. Phys. Chem.* **1995**, *99*, 12723.
- (157) Mylvaganam, K.; Bacskay, G. B.; Hush, N. S. *J. Am. Chem. Soc.* **2000**, *122*, 2041.
- (158) Shulpin, G. B.; Shilov, A. E.; Kitaigorodskii, A. N.; Krevor, J. V. *Z. J. Organomet. Chem.* **1980**, *201*, 319.
- (159) Shulpin, G. B. *J. Organomet. Chem.* **1981**, *212*, 267.
- (160) Shulpin, G. B.; Kitaigorodskii, A. N. *J. Organomet. Chem.* **1981**, *212*, 275.
- (161) Shulpin, G. B.; Nizova, G. V.; Nikitaev, A. T. *J. Organomet. Chem.* **1984**, *276*, 115.
- (162) Shulpin, G. B.; Nizova, G. V.; Shilov, A. E. *J. Chem. Soc., Chem. Commun.* **1983**, 671.
- (163) Serdobov, M. V.; Nizova, G. V.; Shulpin, G. B. *J. Organomet. Chem.* **1984**, *265*, C12.
- (164) Periana, R. A.; Taube, D. J.; Gamble, S.; Taube, H.; Satoh, T.; Fujii, H. *Science* **1998**, *280*, 560.
- (165) Wolf, D. *Angew. Chem., Int. Ed. Engl.* **1998**, *37*, 3351.
- (166) Seidel, S.; Seppelt, K. *Inorg. Chem.* **2003**, *42*, 3846.
- (167) Kua, J.; Xu, X.; Periana, R. A.; Goddard, W. A., III *Organometallics* **2002**, *21*, 511.
- (168) Gilbert, T. M.; Hristov, I.; Ziegler, T. *Organometallics* **2001**, *20*, 1183.
- (169) Xu, X.; Kua, J.; Periana, R. A.; Goddard, W. A., III *Organometallics* **2003**, *22*, 2057.
- (170) Muehlhofer, M.; Strassner, T.; Herrmann, W. A. *Angew. Chem., Int. Ed.* **2002**, *41*, 1745.
- (171) Maletz, G.; Schmidt, F.; Reimer, A.; Strassner, T.; Muehlhofer, M.; Mihaliós, D.; Herrmann, W. DE Patent 10151660,2001, 2003, 10-20030508.
- (172) Herrmann, W. A. *Angew. Chem., Int. Ed.* **2002**, *41*, 1290.
- (173) Arduengo, A. J., III *Acc. Chem. Res.* **1999**, *32*, 913.
- (174) Brown, M. P.; Puddephatt, R. J.; Upton, C. E. E. *J. Chem. Soc., Dalton Trans.* **1974**, 2457.
- (175) Goldberg, K. I.; Yan, J. Y.; Winter, E. L. *J. Am. Chem. Soc.* **1994**, *116*, 1573.
- (176) Williams, B. S.; Holland, A. W.; Goldberg, K. I. *J. Am. Chem. Soc.* **1999**, *121*, 252.
- (177) Williams, B. S.; Goldberg, K. I. *J. Am. Chem. Soc.* **2001**, *123*, 2576.
- (178) Crumpton, D. M.; Goldberg, K. I. *J. Am. Chem. Soc.* **2000**, *122*, 962.
- (179) Crumpton-Bregel, D. M.; Goldberg, K. I. *J. Am. Chem. Soc.* **2003**, *125*, 9442.
- (180) Abis, L.; Sen, A.; Halpern, J. *J. Am. Chem. Soc.* **1978**, *100*, 2915.
- (181) Michelin, R. A.; Faglia, S.; Uguagliati, P. *Inorg. Chem.* **1983**, *22*, 1831.
- (182) Hackett, M.; Ibers, J. A.; Whitesides, G. M. *J. Am. Chem. Soc.* **1988**, *110*, 1436.
- (183) Bartlett, K. L.; Goldberg, K. I.; Borden, W. T. *J. Am. Chem. Soc.* **2000**, *122*, 1456.
- (184) Bartlett, K. L.; Goldberg, K. I.; Borden, W. T. *Organometallics* **2001**, *20*, 2669.
- (185) Hackett, M.; Whitesides, G. M. *J. Am. Chem. Soc.* **1988**, *110*, 1449.
- (186) Heyduk, A. F.; Driver, T. G.; Labinger, J. A.; Bercaw, J. E. *J. Am. Chem. Soc.* **2004**, *126*, 15034.
- (187) Hofmann, P.; Heiss, H.; Muller, G. Z. *Naturforsch., B* **1987**, *42*, 395.
- (188) Hofmann, P.; Heiss, H.; Neiteler, P.; Muller, G.; Lachmann, J. *Angew. Chem., Int. Ed. Engl.* **1990**, *29*, 880.
- (189) Heyduk, A. F.; Labinger, J. A.; Bercaw, J. E. *J. Am. Chem. Soc.* **2003**, *125*, 6366.
- (190) Somorjai, G. A. *Chemistry in Two Dimensions*; Cornell University: Ithaca, NY, 1981.
- (191) Somorjai, G. A. *Acc. Chem. Res.* **1976**, *9*, 392.
- (192) Lebrilla, C. B.; Maier, W. F. *J. Am. Chem. Soc.* **1986**, *108*, 1606.
- (193) Duin, M. A.; Clement, N. D.; Cavell, K. J.; Elsevier, C. J. *Chem. Commun.* **2003**, 400.
- (194) Alder, R. W.; Allen, P. R.; Williams, S. J. *J. Chem. Soc., Chem. Commun.* **1995**, 1267.
- (195) Amyes, T. L.; Diver, S. T.; Richard, J. P.; Rivas, F. M.; Toth, K. *J. Am. Chem. Soc.* **2004**, *126*, 4366.
- (196) Kim, Y. J.; Streitwieser, A. *J. Am. Chem. Soc.* **2002**, *124*, 5757.
- (197) Alibrandi, G.; Minniti, D.; Romeo, R.; Uguagliati, P.; Calligaro, L.; Belluco, U.; Crociani, B. *Inorg. Chim. Acta* **1985**, *100*, 107.
- (198) Belluco, U.; Giustiniani, M.; Graziani, M. *J. Am. Chem. Soc.* **1967**, *89*, 6494.
- (199) Alibrandi, G.; Minniti, D.; Romeo, R.; Uguagliati, P.; Calligaro, L.; Belluco, U. *Inorg. Chim. Acta* **1986**, *112*, L15.
- (200) Romeo, R.; Minniti, D.; Lanza, S.; Uguagliati, P.; Belluco, U. *Inorg. Chem.* **1978**, *17*, 2813.
- (201) Jawad, J. K.; Puddephatt, R. J.; Stalteri, M. A. *Inorg. Chem.* **1982**, *21*, 332.
- (202) Holtkamp, M. W.; Labinger, J. A.; Bercaw, J. E. *Inorg. Chim. Acta* **1997**, *265*, 117.
- (203) Stahl, S. S.; Labinger, J. A.; Bercaw, J. E. *Inorg. Chem.* **1998**, *37*, 2422.
- (204) Kimmich, B. F. M.; Bullock, R. M. *Organometallics* **2002**, *21*, 1504.
- (205) Gusev, D. G.; Notheis, J. U.; Rambo, J. R.; Hauger, B. E.; Eisenstein, O.; Caulton, K. G. *J. Am. Chem. Soc.* **1994**, *116*, 7409.
- (206) Butts, M. D.; Scott, B. L.; Kubas, G. J. *J. Am. Chem. Soc.* **1996**, *118*, 11831.
- (207) Gerdes, G.; Chen, P. *Organometallics* **2003**, *22*, 2217.
- (208) Appelt, A.; Ariaratnam, V.; Willis, A. C.; Wild, S. B. *Tetrahedron: Asymmetry* **1990**, *1*, 9.
- (209) Bennett, B. L.; Birnbaum, J.; Roddick, D. M. *Polyhedron* **1995**, *14*, 187.
- (210) Bennett, B. L.; Hoerter, J. M.; Houllis, J. F.; Roddick, D. M. *Organometallics* **2000**, *19*, 615.
- (211) Kalberer, E. W.; Houllis, J. F.; Roddick, D. M. *Organometallics* **2004**, *23*, 4112.
- (212) Butikofer, J. L.; Hoerter, J. M.; Peters, R. G.; Roddick, D. M. *Organometallics* **2004**, *23*, 400.
- (213) Saillard, J. Y.; Hoffmann, R. *J. Am. Chem. Soc.* **1984**, *106*, 2006.
- (214) Hill, G. S.; Puddephatt, R. J. *Organometallics* **1998**, *17*, 1478.
- (215) Rendina, L. M.; Puddephatt, R. J. *Chem. Rev.* **1997**, *97*, 1735.
- (216) van Asselt, R.; Rijnberg, E.; Elsevier, C. J. *Organometallics* **1994**, *13*, 706.
- (217) Puddephatt, R. J. *Coord. Chem. Rev.* **2001**, *219–221*, 157.
- (218) Brainard, R. L.; Nutt, W. R.; Lee, T. R.; Whitesides, G. M. *Organometallics* **1988**, *7*, 2379.
- (219) Thorn, D. L. *Organometallics* **1998**, *17*, 348.
- (220) Konze, W. V.; Scott, B. L.; Kubas, G. J. *Chem. Commun.* **1999**, 1807.
- (221) Konze, W. V.; Scott, B. L.; Kubas, G. J. *J. Am. Chem. Soc.* **2002**, *124*, 12550.
- (222) Baratta, W.; Stoccoro, S.; Doppiu, A.; Herdtweck, E.; Zucca, A.; Rigo, P. *Angew. Chem., Int. Ed.* **2003**, *42*, 105.
- (223) Ingleson, M. J.; Mahon, M. F.; Weller, A. S. *Chem. Commun.* **2004**, 2398.
- (224) Thomas, J. C.; Peters, J. C. *J. Am. Chem. Soc.* **2001**, *123*, 5100.
- (225) Thomas, J. C.; Peters, J. C. *J. Am. Chem. Soc.* **2003**, *125*, 8870.
- (226) Crespo, M.; Puddephatt, R. J. *Organometallics* **1987**, *6*, 2548.
- (227) Hill, G. S.; Rendina, L. M.; Puddephatt, R. J. *Organometallics* **1995**, *14*, 4966.
- (228) De Felice, V.; De Renzi, A.; Panunzi, A.; Tesaro, D. *J. Organomet. Chem.* **1995**, *488*, C13.
- (229) Hill, G. S.; Puddephatt, R. J. *J. Am. Chem. Soc.* **1996**, *118*, 8745.
- (230) Hill, G. S.; Vittal, J. J.; Puddephatt, R. J. *Organometallics* **1997**, *16*, 1209.
- (231) Stahl, S. S.; Labinger, J. A.; Bercaw, J. E. *J. Am. Chem. Soc.* **1995**, *117*, 9371.
- (232) Johansson, L.; Tilset, M. *J. Am. Chem. Soc.* **2001**, *123*, 739.
- (233) Tilset, M.; Johansson, L.; Lersch, M.; Wik, B. *J. ACS Symp. Ser.* **2004**, *885*, 264.
- (234) Seeman, J. I. *Chem. Rev.* **1983**, *83*, 83.
- (235) Zhong, H. A.; Labinger, J. A.; Bercaw, J. E. *J. Am. Chem. Soc.* **2002**, *124*, 1378.
- (236) Wik, B. J.; Lersch, M.; Tilset, M. *J. Am. Chem. Soc.* **2002**, *124*, 12116.
- (237) Zhang, F.; Jennings, M. C.; Puddephatt, R. J. *Organometallics* **2004**, *23*, 1396.
- (238) Fang, X.; Scott, B. L.; Watkin, J. G.; Kubas, G. J. *Organometallics* **2000**, *19*, 4193.
- (239) Ong, C. M.; Jennings, M. C.; Puddephatt, R. J. *Can. J. Chem.* **2003**, *81*, 1196.
- (240) Holtkamp, M. W.; Labinger, J. A.; Bercaw, J. E. *J. Am. Chem. Soc.* **1997**, *119*, 848.
- (241) Holtkamp, M. W.; Henling, L. M.; Day, M. W.; Labinger, J. A.; Bercaw, J. E. *Inorg. Chim. Acta* **1998**, *270*, 467.
- (242) Johansson, L.; Ryan, O. B.; Tilset, M. *J. Am. Chem. Soc.* **1999**, *121*, 1974.
- (243) Heiberg, H.; Johansson, L.; Gropen, O.; Ryan, O. B.; Swang, O.; Tilset, M. *J. Am. Chem. Soc.* **2000**, *122*, 10831.
- (244) Heiberg, H.; Swang, O.; Ryan, O. B.; Gropen, O. *J. Phys. Chem. A* **1999**, *103*, 10004.

- (245) van Eldik, R.; Dücker-Benfer, C.; Thaler, F. *Adv. Inorg. Chem.* **2000**, *49*, 1–58.
- (246) van Eldik, R. *Studies in Inorganic Chemistry*; Elsevier: Amsterdam, 1986; Vol. 7 (Inorganic High-Pressure Chemistry: Kinetics and Mechanisms).
- (247) Procelewaska, J.; Zahl, A.; van Eldik, R.; Zhong, H. A.; Labinger, J. A.; Bercaw, J. E. *Inorg. Chem.* **2002**, *41*, 2808.
- (248) van Eldik, R.; Asano, T.; le Noble, W. J. *Chem. Rev.* **1989**, *89*, 549.
- (249) Drljaca, A.; Hubbard, C. D.; van Eldik, R.; Asano, T.; Basilevsky, M. V.; le Noble, W. J. *Chem. Rev.* **1998**, *98*, 2167.
- (250) Lersch, M.; Wik, B. J.; Tilset, M. Unpublished results.
- (251) Wik, B. J.; Lersch, M.; Tilset, M. Manuscript in preparation.
- (252) Norris, C. M.; Templeton, J. L. *Organometallics* **2004**, *23*, 3101.
- (253) Ackerman, L. J.; Sadighi, J. P.; Kurtz, D. M.; Labinger, J. A.; Bercaw, J. E. *Organometallics* **2003**, *22*, 3884.
- (254) Tellers, D. M.; Bergman, R. G. *J. Am. Chem. Soc.* **2000**, *122*, 954.
- (255) Labinger, J. A.; Bercaw, J. E.; Tilset, M. Submitted.
- (256) Song, D.; Wang, S. *Organometallics* **2003**, *22*, 2187.
- (257) Song, D.; Wang, S. *Comments Inorg. Chem.* **2004**, *25*, 1.
- (258) Song, D.; Sliwowski, K.; Pang, J.; Wang, S. *Organometallics* **2002**, *21*, 4978.
- (259) Johansson, L.; Ryan, O. B.; Rømming, C.; Tilset, M. *J. Am. Chem. Soc.* **2001**, *123*, 6579.
- (260) Zhang, X.; Kanzelberger, M.; Emge, T. J.; Goldman, A. S. *J. Am. Chem. Soc.* **2004**, *126*, 13192.
- (261) Jones, W. D.; Feher, F. J. *J. Am. Chem. Soc.* **1984**, *106*, 1650.
- (262) Jones, W. D.; Hessel, E. T. *J. Am. Chem. Soc.* **1993**, *115*, 554.
- (263) Burger, P.; Bergman, R. G. *J. Am. Chem. Soc.* **1993**, *115*, 10462.
- (264) Adams, C. S.; Legzdins, P.; Tran, E. *J. Am. Chem. Soc.* **2001**, *123*, 612.
- (265) We thank Jay Labinger for providing a preprint of this manuscript.
- (266) Jenkins, H. A.; Yap, G. P. A.; Puddephatt, R. J. *Organometallics* **1997**, *16*, 1946.
- (267) Fekl, U.; Zahl, A.; van Eldik, R. *Organometallics* **1999**, *18*, 4156.
- (268) Jenkins, H. A.; Klempner, M. J.; Prokopchuk, E. M.; Puddephatt, R. J. *Inorg. Chim. Acta* **2003**, *352*, 72.
- (269) Prokopchuk, E. M.; Puddephatt, R. J. *Organometallics* **2003**, *22*, 787.
- (270) Hinman, J. G.; Baar, C. R.; Jennings, M. C.; Puddephatt, R. J. *Organometallics* **2000**, *19*, 563.
- (271) Baar, C. R.; Carbray, L. P.; Jennings, M. C.; Puddephatt, R. J.; Vittal, J. J. *Organometallics* **2001**, *20*, 408.
- (272) Prokopchuk, E. M.; Puddephatt, R. J. *Organometallics* **2003**, *22*, 563.
- (273) Davies, M. S.; Hambley, T. W. *Inorg. Chem.* **1998**, *37*, 5408.
- (274) Prokopchuk, E. M.; Jenkins, H. A.; Puddephatt, R. J. *Organometallics* **1999**, *18*, 2861.
- (275) Prokopchuk, E. M.; Puddephatt, R. J. *Can. J. Chem.* **2003**, *81*, 476.
- (276) Sobanov, A. A.; Vedernikov, A. N.; Dyuker, G.; Solomonov, B. N. *Russ. J. Gen. Chem.* **2003**, *73*, 842.
- (277) Vedernikov, A. N.; Shamov, G. A.; Solomonov, B. N. *Russ. J. Gen. Chem.* **1997**, *67*, 1159.
- (278) Vedernikov, A. N.; Shamov, G. A.; Solomonov, B. N. *Russ. J. Gen. Chem.* **1999**, *69*, 1102.
- (279) Vedernikov, A. N.; Huffman, J. C.; Caulton, K. G. *Inorg. Chem.* **2002**, *41*, 6867.
- (280) Vedernikov, A. N.; Huffman, J. C.; Caulton, K. G. *New J. Chem.* **2003**, *27*, 665.
- (281) Vedernikov, A. N.; Caulton, K. G. *Chem. Commun.* **2003**, 358.
- (282) Crabtree, R. H. *Dalton Trans.* **2003**, 3985.
- (283) Brammer, L. *Dalton Trans.* **2003**, 3145.
- (284) Epstein, L. M.; Shubina, E. S. *Coord. Chem. Rev.* **2002**, *231*, 165.
- (285) Vedernikov, A. N.; Pink, M.; Caulton, K. G. *Inorg. Chem.* **2004**, *43*, 3642.
- (286) Vedernikov, A. N.; Caulton, K. G. *Angew. Chem., Int. Ed.* **2002**, *41*, 4102.
- (287) Scollard, J. D.; Day, M.; Labinger, J. A.; Bercaw, J. E. *Helv. Chim. Acta* **2001**, *84*, 3247.
- (288) Iverson, C. N.; Carter, C. A. G.; Scollard, J. D.; Pribisko, M. A.; John, K. D.; Scott, B. L.; Baker, R. T.; Bercaw, J. E.; Labinger, J. A. *ACS Symp. Ser.* **2004**, *885*, 319.
- (289) Johansson, L.; Ryan, O. B.; Rømming, C.; Tilset, M. *Organometallics* **1998**, *17*, 3957.
- (290) Iverson, C. N.; Carter, C. A. G.; Baker, R. T.; Scollard, J. D.; Labinger, J. A.; Bercaw, J. E. *J. Am. Chem. Soc.* **2003**, *125*, 12674.
- (291) Owen, J. S.; Labinger, J. A.; Bercaw, J. E. *J. Am. Chem. Soc.* **2004**, *126*, 8247.
- (292) Trofimenko, S. *Scorpionates. The Chemistry of Polybrazolyliborate Ligands*; Imperial College Press: London, 1999.
- (293) Sadimenko, A. P. *Adv. Heterocycl. Chem.* **2001**, *81*, 167.
- (294) King, R. B.; Bond, A. *J. Am. Chem. Soc.* **1974**, *96*, 1338.
- (295) Roth, S.; Ramamoorthy, V.; Sharp, P. R. *Inorg. Chem.* **1990**, *29*, 3345.
- (296) Fekl, U.; van Eldik, R.; Lovell, S.; Goldberg, K. I. *Organometallics* **2000**, *19*, 3535.
- (297) Reinartz, S.; White, P. S.; Brookhart, M.; Templeton, J. L. *Organometallics* **2000**, *19*, 3748.
- (298) Norris, C. M.; Templeton, J. L. *ACS Symp. Ser.* **2004**, *885*, 303.
- (299) Haskel, A.; Keinan, E. *Organometallics* **1999**, *18*, 4677.
- (300) Manzer, L. E.; Meakin, P. Z. *Inorg. Chem.* **1976**, *15*, 3117.
- (301) Rush, P. E.; Oliver, J. D. *J. Chem. Soc., Chem. Commun.* **1974**, 996.
- (302) Lo, H. C.; Haskel, A.; Kapon, M.; Keinan, E. *J. Am. Chem. Soc.* **2002**, *124*, 3226.
- (303) Lowry, T. H.; Richardson, K. S. *Mechanism and Theory in Organic Chemistry*, 3rd ed.; Benjamin-Cummings Publishing Co.: New York, 1987.
- (304) Lo, H. C.; Haskel, A.; Kapon, M.; Keinan, E. *J. Am. Chem. Soc.* **2002**, *124*, 12626.
- (305) Iron, M. A.; Lo, H. C.; Martin, J. M. L.; Keinan, E. *J. Am. Chem. Soc.* **2002**, *124*, 7041.
- (306) Reinartz, S.; Baik, M. H.; White, P. S.; Brookhart, M.; Templeton, J. L. *Inorg. Chem.* **2001**, *40*, 4726.
- (307) Reinartz, S.; White, P. S.; Brookhart, M.; Templeton, J. L. *Organometallics* **2001**, *20*, 1709.
- (308) Canty, A. J.; Dedieu, A.; Jin, H.; Milet, A.; Richmond, M. K. *Organometallics* **1996**, *15*, 2845.
- (309) O'Reilly, S. A.; White, P. S.; Templeton, J. L. *J. Am. Chem. Soc.* **1996**, *118*, 5684.
- (310) Wick, D. D.; Goldberg, K. I. *J. Am. Chem. Soc.* **1997**, *119*, 10235.
- (311) Reinartz, S.; White, P. S.; Brookhart, M.; Templeton, J. L. *Organometallics* **2000**, *19*, 3854.
- (312) Jensen, M. P.; Wick, D. D.; Reinartz, S.; White, P. S.; Templeton, J. L.; Goldberg, K. I. *J. Am. Chem. Soc.* **2003**, *125*, 8614–8624.
- (313) Alibrandi, G.; Sclaro, L. M.; Romeo, R. *Inorg. Chem.* **1991**, *30*, 4007.
- (314) Romeo, R. *Comments Inorg. Chem.* **1990**, *11*, 21.
- (315) Romeo, R.; Monsu Scolaro, L.; Plutino, M. R.; Fabrizi de Biani, F.; Bottari, G.; Romeo, A. *Inorg. Chim. Acta* **2003**, *350*, 143.
- (316) Kanzelberger, M.; Singh, B.; Czerw, M.; Krogh-Jespersen, K.; Goldman, A. S. *J. Am. Chem. Soc.* **2000**, *122*, 11017.
- (317) Reinartz, S.; White, P. S.; Brookhart, M.; Templeton, J. L. *J. Am. Chem. Soc.* **2001**, *123*, 6425.
- (318) Puddephatt, R. *J. Angew. Chem., Int. Ed.* **2002**, *41*, 261.
- (319) Fekl, U.; Kaminsky, W.; Goldberg, K. I. *J. Am. Chem. Soc.* **2001**, *123*, 6423.
- (320) Clark, H. C.; Manzer, L. E. *Inorg. Chem.* **1974**, *13*, 1291.
- (321) Vedernikov, A. N.; Fettingner, J. C.; Mohr, F. *J. Am. Chem. Soc.* **2004**, *126*, 11160.
- (322) Bourget-Merle, L.; Lappert, M. F.; Severn, J. R. *Chem. Rev.* **2002**, *102*, 3031.
- (323) Fekl, U.; Goldberg, K. I. *J. Am. Chem. Soc.* **2002**, *124*, 6804.
- (324) Fekl, U.; Kaminsky, W.; Goldberg, K. I. *J. Am. Chem. Soc.* **2003**, *125*, 15286.
- (325) Goldman, A. S.; Renkema, K. B.; Czerw, M.; Krogh-Jespersen, K. *ACS Symp. Ser.* **2004**, *885*, 198.
- (326) Jensen, C. M. *Chem. Commun.* **1999**, 2443.
- (327) Renkema, K. B.; Kissin, Y. V.; Goldman, A. S. *J. Am. Chem. Soc.* **2003**, *125*, 7770.
- (328) Saito, K.; Kashiwabara, K. *J. Organomet. Chem.* **1987**, *330*, 291.
- (329) Harkins, S. B.; Peters, J. C. *Organometallics* **2002**, *21*, 1753.
- (330) Albrecht, M.; van Koten, G. *Angew. Chem., Int. Ed.* **2001**, *40*, 3750.
- (331) Peters, J. C.; Harkins, S. B.; Brown, S. D.; Day, M. W. *Inorg. Chem.* **2001**, *40*, 5083.
- (332) Tobe, M. L.; Burgess, J. *Inorganic Reaction Mechanisms*; Addison-Wesley Longman: New York, 1999; pp 101–103.
- (333) Labinger, J. A.; Herring, A. M.; Bercaw, J. E. *J. Am. Chem. Soc.* **1990**, *112*, 5628.
- (334) Sen, A.; Benvenuto, M. A.; Lin, M.; Hutson, A. C.; Basicckes, N. *J. Am. Chem. Soc.* **1994**, *116*, 998.
- (335) Hutson, A. C.; Lin, M.; Basicckes, N.; Sen, A. *J. Organomet. Chem.* **1995**, *504*, 69.
- (336) DeVries, N.; Roe, D. C.; Thorn, D. L. *J. Mol. Catal. A* **2002**, *189*, 17.
- (337) Kanski, R.; Kanska, M. *J. Radioanal. Nucl. Chem.* **2003**, *257*, 385 and references therein.
- (338) Kao, L. C.; Sen, A. *J. Chem. Soc., Chem. Commun.* **1991**, 1242.
- (339) Dangel, B. D.; Johnson, J. A.; Sames, D. *J. Am. Chem. Soc.* **2001**, *123*, 8149.
- (340) See, for instance: *Cisplatin—Chemistry and Biochemistry of a Leading Anticancer Drug*; Lippert, B., Ed.; Verlag Helvetica Chimica Acta: Zürich, 1999 or the journal *Platinum-Based Drugs in Cancer Therapy* (Humana Press).
- (341) Johnson, J. A.; Sames, D. *J. Am. Chem. Soc.* **2000**, *122*, 6321.
- (342) Johnson, J. A.; Ning, L.; Sames, D. *J. Am. Chem. Soc.* **2002**, *124*, 6900.